CRANFIELD INSTITUTE OF TECHNOLOGY

COLLEGE OF AERONAUTICS

DEPARTMENT OF AIRCRAFT DESIGN

Ph D THESIS

A.SOUAHI

STRUCTURAL OPTIMIZATION OF AIRCRAFT LIFTING SURFACES TO SATISFY FLUTTER REQUIREMENTS

Supervisor: Pr. A.J.MORRIS

June 1986

بسم الله الرحمن الرحيم

In the Name of God, Most Gracious, Most Merciful

"...وما أوتيتم من العلم إلا قليلا"

"...and of knowledge you (man) have been given only a little."

قرآن كريم - سورة بني إسرائيل (17) آية 85

Surah 17 (Bani Isra-il), verse 85 of the holy Quran

DEDICATION

I acknowledge your Aid, O Lord of the eternity!

Were it not with your Love and Guidance,

This humble contribution would have never become a reality.

Please bless it with your Acceptance.

For I am dedicating it to You with genuine humility.

ACKNOWLEDGMENTS

As is always the case, any author of a piece of work must inevitably owe a debt of gratitude to all those who helped him, assisted him or even simply encouraged him in achieving his work.

For my part, I am firstly and mostly indebted to my mother who sacrificed part of her life and happiness just for us, her children. I am also indebted to my brother-in-law Abdelkrim, his wife and my sister Fatiha and to my brother Abdelhamid for their encouragement, enlightened moral support and constant financial help. I cannot, alas, thank my youngest but revered brother Mounir. Words cannot show my bitter anguish and deep sorrow for his recent and sudden death that happened shortly after his extremely brilliant success in the extremely selective environment of the French "Ecole Polytechnique". I must pay tribute to him for giving me an admirable example of faith, courage and perseverance and for imbibing me with his love and devotion to research. His devastating disappearance nearly unseated my reason and made life seem so hopeless and meaningless. If I recovered and continued finishing this work, it is to respect and cherish in my mind his permanent concern for me, my family and my studies even when he was facing death.

From the academic side, I have been fortunate to have Pr. A.J. Morris as a supervisor. I must record here that we have always been in agreement even in discussions involving

political matters. Many thanks are due to him for his competency, valued and expert advices, political opinion and sense of humor.

I am sincerely obliged to Dr. A.El-Zafrani (CIT), Dr. D.E.Davies (RAE), Herr O.Sensburg (MBB) and S.Clamp (doctoral candidate) for the assistance far beyond what I can expect.

Last but by no means least, I wish to express my appreciation to my wife Fadhila for her understanding and patience in addition to attending to the demands of a home and our quiet little daughter Wacima.

SUMMARY

The research reported in this thesis is concerned with the structural weight optimization of aircraft lifting surfaces when subjected to the satisfaction of flutter requirements.

The main text is intended primarily as an expository account on the work and as such it aims at introducing and defining the subject of research and presenting the results. Accordingly, the mathematics have been simplified to the utmost in the main text and heavy theoretical treatments are revealed in the appendices.

As the aim of this work is not directed at in-depth studies of the physical nature of flutter nor for a comprehensive treatment of structural optimization, the basic concepts of these two subjects are touched upon in the beginnings of chapters II and III respectively. We concluded these two chapters by clarifying the class of flutter, constraints and design variables for which the program we developed is designed. We endeavored to keep the problem to within certain practical boundaries without loosing too much of either its generality or its applicability to structures in realistic operational environments.

This work is illustrated with two structural examples of small and moderate sizes because of the limited capacity of the College of Aeronautics DEC VAX 11/750 mini-computer.

Nevertheless, all the techniques are derived with the view to being applied to large problems and for this reason attention is focused on the efficiency of such methods. In actual fact, firm emphasis on algorithmic efficiency is a prime necessity because of the prominent complexity and numerical costs of flutter synthesis. Hence, a sizable portion of the text converge to one single objective: efficiency and convergence of algorithms.

One aspect never applied to flutter synthesis but with probably potential fallouts on efficiency and accuracy of this type of problem is dual theory. The dual problem expressed herein is non-linear, as complicated as the primal problem and probably not easily adapted to a numerical maximization scheme. Duality may be, however, rewarding in that it can bound the structural mass with the evident feature of monitoring the convergence of the algorithm. As far as efficiency is concerned, it may permit certain approximations in the analysis to be made. When the latest stages of the computer runs are identified by dual bounding a more stringent analysis may be then activated to achieve accuracy.

CONTENTS

LIST OF SYMBOLS AND ABBREVIATIONS

LATIN SYMBOLS

a	speed of sound in the uniform flow far upstream of the lifting surface
A_j	total surface of all the membrane elements linked as the jth design variable
b	typical (reference) length of the lifting planform
[C]	structural damping matrix
C_j	redesign factor for jth design variable
D	determinant
[D]	hysteretic damping matrix
e_1	resizing exponent
e_2	resizing exponent
$(e_v)_j$	strain energy (or pseudo-strain-energy) density of jth design variable
(e_{av})	average of all $(e_v)_j$ of active design variables
(e_{avav})	average of $(e_v)_j$ that exceeds (e_{av})
E	Young modulus
E^N	N dimensional Euclidean space
[F]	flutter matrix
g	structural damping factor or more exactly artificial damping
J_a	set of indices representing the active design variables only
k	iteration counter
[K]	stiffness matrix

$[K_G]$ generalized stiffness matrix

$[K_r]$ reduced stiffness matrix

$[K_0]$ contributions of fixed structural items to the stiffness matrix

$[K_j]$ jth elemental stiffness matrix or changes in stiffness per unit length or area of the jth variable element

$[\bar{K}_j]$ same as $[K_j]$ but the terms in the x- and y-directions are deleted by simply removing complete lines and columns

L Lagrangian function

L(x,y,t) net aerodynamic pressure acting at time t at a point (x,y) on an element of the planform with area dxdy; aerodynamic loading distribution

l_j total length of all the bar elements linked as the jth design variable

$\ell_j(x,y;\nu,M_\infty)$ loading function corresponding to the jth harmonic oscillation

$L_j(x,y,t)$ aerodynamic loading in the jth harmonic oscillation

$\mathcal{L}$ Lagrangian function

m total mass of the structure

m_0 mass of fixed structural items

m_j mass per unit length (for bar elements) or per unit area (for quadrilateral or triangular elements) of jth variable element

[M] mass or inertia matrix

$[M_G]$ generalized inertia matrix

$[M_r]$ reduced mass matrix

$[M_0]$ contributions of fixed structural items to the inertia matrix

$[M_j]$ jth elemental inertia matrix or changes in inertia per unit length or area of the jth variable element

$[\bar{M}_j]$ same as $[M_j]$ but the terms in the x- and y-directions are deleted by simply removing complete lines and columns

M_∞ free-stream Mach number

n number of mode shapes considered; order of the system

N number of design variables

{P} load vector

q_i ith generalized coordinate

{q} vector of generalized coordinates (weighting vector or vector of modal amplitudes)

$\{\bar{q}\}$ vector of quantities or amplitudes defining the amount of harmonic constituent in {q}; aeroelastic eigenvector

$Q_i(t)$ generalized aerodynamic force in the ith mode of oscillation at time t; ith generalized aerodynamic force

{Q} vector of generalized aerodynamic forces

Q_{ij} generalized airforce coefficient

[Q] matrix of generalized airforce coefficients

[Q'] real part of [Q]

$\nu[Q"]$	imaginary part of [Q]
R	dissipation function (structural damping)
s	complex frequency
t	time
T	kinetic energy
[T]	transformation matrix
{U}	vector of nodal displacements
$\begin{Bmatrix}\{u\}\\{v}\end{Bmatrix}$	vector of nodal displacements in the x- and y-direction (not necessarily separated); in-plane displacements of the nodes of the structure
V	speed of the main airstream (flight velocity); it is in the positive x-direction
V_f	flutter speed
V_r	required speed
{w}	vector of nodal displacements in the z-direction; out-of-plane or transverse displacements of the nodes of the structure
W	work
x,y,z	rectangular cartesian coordinates stationary with respect to the mean position of the oscillating lifting surface
x_j	jth design variable
$\underline{x}_j$	jth minimum gauge constraints; minimum value imposed on jth design variable
$\overline{x}_j$	jth maximum gauge constraints; maximum value imposed on jth design variable
X	set of the primal points satisfying the constraints on the gauges or side constraints

{x} vector grouping all design variables

Z(X,Y,t) out-of-plane displacement of a point (X,Y) on the aerodynamic planform

GREEK SYMBOLS

δ_{ij} Kronecker delta

$\{\zeta\}$ full mode shape

$\{\zeta\}_i$ ith full mode shape

$\{\zeta\}_{m_i}$ shape of ith out-of-plane mode of oscillation of the structure (ith out-of-plane mode shape or ith master mode shape)

$\{\zeta\}_m$ out-of-plane mode shape of the structure (master mode shape)

$[\zeta_m]$ modal matrix whose columns are the out-of-plane mode shapes

$[\zeta_m^{(0)}]$ modal matrix whose columns are the master mode shapes of the original structure

$\{\zeta\}_s$ slave mode shape

$[\zeta]$ modal matrix whose columns are the full mode shapes

$[\zeta^{(0)}]$ modal matrix of the original structure; matrix whose columns are the full mode shapes of the original structure

$\{\lambda\}$ vector of Lagrangian multipliers

$\{\lambda^c\}$ adjoint aeroelastic eigenvector

Λ Lagrange multiplier

μ_j Lagrange multiplier associated with jth side constraint

ν { reduced frequency; Poisson's ratio

$\xi_i(X,Y)$ deflection of the aerodynamic planform at a point (X,Y) due to ith structural mode shape

π 3.1415926536...

Π_p potential (strain) energy

ρ material density

ρ_∞ air density in the uniform flow far upstream of the lifting planform

ρ_j density of the structural material of the jth variable element

ω circular frequency of harmonic oscillation

ω_N circular natural frequency

$(\omega_N)^2$ circular natural frequency squared or eigenvalue of the free vibration problem

$(\omega_{Ni})^2$ ith eigenvalue corresponding to ith out-of-plane mode shape

$[\omega_N^2]$ spectral matrix; diagonal matrix of the squared natural frequencies or eigenvalues; generalized stiffness matrix

Ω complex eigenvalue (aeroelastic eigenvalue)

MATHEMATICAL SYMBOLS

$\{\ \}$ vector (column matrix)

$[\ ]$ matrix

$[\ ]$ diagonal matrix

$[1]$ identity matrix; generalized inertia matrix

f	function
e	exponential function
$\Rightarrow$	implies
$\Leftrightarrow$	if and only if; equivalent to
$\forall$	for any; for all
$\in$	belongs to
:	such that
$\equiv$	identical to
$\lvert\ \rvert$	absolute value of a scalar
d	total derivative symbol (total differential)
∂	partial derivative symbol
δ	virtual operator
$\sum$	summation operator
$\int$	integral operator
$\iint_S$	integration extending over a surface
>	strictly greater
$\geq$	greater than or equal to
$\leq$	less than or equal to
>>	much greater
i	$\sqrt{-1}$
Re	real part of
Im	imaginary part of

GENERAL SYMBOLS

§	section(s)
%	percent

GRAPHIC SYMBOL

 pinned support (resists all forces but not moments)

FLOW CHART SYMBOLS

 terminator (start/end)

 decision (if)

 process

SUBSCRIPTS

f	pertaining to flutter
i	ith / imaginary
r	required / real
∞	free-stream condition

SUPERSCRIPTS

′	real part
″	imaginary part
c	complex conjugate
H	hermitian transpose
T	transpose of a vector or a matrix

OVERLAYS

−	amplitude / maximum imposed value
.	$\frac{\partial}{\partial t}$, time differentiation; $\dot{q}_i \equiv \frac{\partial q_i}{\partial t}$

"UNDERLAY"

— minimum imposed value

ABBREVIATIONS

Dept.	department
e.g	"exempli gratia", for example, for instance
Eq.	equation(s)
et al.	"et alii" meaning and other people
etc	"et cetera" meaning and the rest
Fig.	figure(s)
i.e	"id est", which is to say, in other words
mflops	million of floating-point operations per second
No	number(s)
pp.	pages
Ref.	reference(s)
viz.	"videlicet", namely
Vol.	volume(s)

ACRONYMS

AFFDL	Air Force Flight Dynamics Laboratory
AGARD	Advisory Group for Aerospace Research & development
AIAA	American Institute of Aeronautics and Astronautics
A.R.C.	Aeronautical Research Council
ASCE	American Society of Civil Engineers
C.P.	Current Papers
ASME	American Society of Mechanical Engineers
CDC	Control Data Corporation
CPU	Central Processing Unit

FSD	Fully-Stressed-Design
IBM	International Business Machines
KBES	Knowledge-Based Expert System
MBB	Messerschmitt-Bölkow-Blohm
MP	Mathematical Programming
NASA	National Aeronautics and Space Administration
NASTRAN	National Aeronautics and Space Administration Structural Analysis
OC	Optimality Criterion or Criteria
ONÉRA	Office National d' Études et de Recherches Aérospatiales
RAE	Royal Aircraft Establishment
R. & M.	Reports and Memoranda
SAE	Society of Automotive Engineers
TN	Technical Note
TR	Technical Report
UK	United Kingdom
USA	United States of America

CHAPTER I

PROLEGOMENA

Major features of today's digital computers are their abilities to handle massive amounts of information and to perform a huge number of routine instructions extremely fast. Yet these powerful capabilities are nonetheless considered to be inadequate and ought to be boosted even further in order to solve urgent and nagging scientific or engineering problems. Even Cray supercomputers that are sheer number-crunching machines can frustrate many engineers.

In parallel to the hardware revolutions, an impressive number of methods of design analysis and synthesis have been developed almost at the same pace. Improvement of the efficiency of these methods is continuously pursued even though we may shortly see a computer generation whose prominent characteristic will be versatility in addition to an exponential growth in speed of execution and memory capacity.

1 IMPACT OF COMPUTATIONAL METHODS IN AIRCRAFT DESIGN

We may illustrate the merits of computers by taking as an example the aerospace engineering community with its entire research, academic and industrial institutions which rely heavily upon computing. This specific area is one of the largest users of the one hundred or so Crays installed worldwide.

Every aircraft generation has tremendously increased the

time spent on wind tunnel testing because of the rising configuration complexity and the widening of performance envelopes. These factors together with other cost rises have resulted in a manifold cost increase of wind tunnel testing on any one single project. On the contrary, computer processing costs have declined by 20% every year in the past ten years, amounting to a decrease of computing costs by a factor of two over the last decade. Moreover, if wind tunnels are constrained by limits on Reynolds and Mach numbers and effect of wall- and support-interferences, computers are only restricted by size and speed. In the interest of brevity, we have summarized an article of "Aviation Week and Space Technology" (August 29, 1983, pp. 50-72) in Fig. I.1.

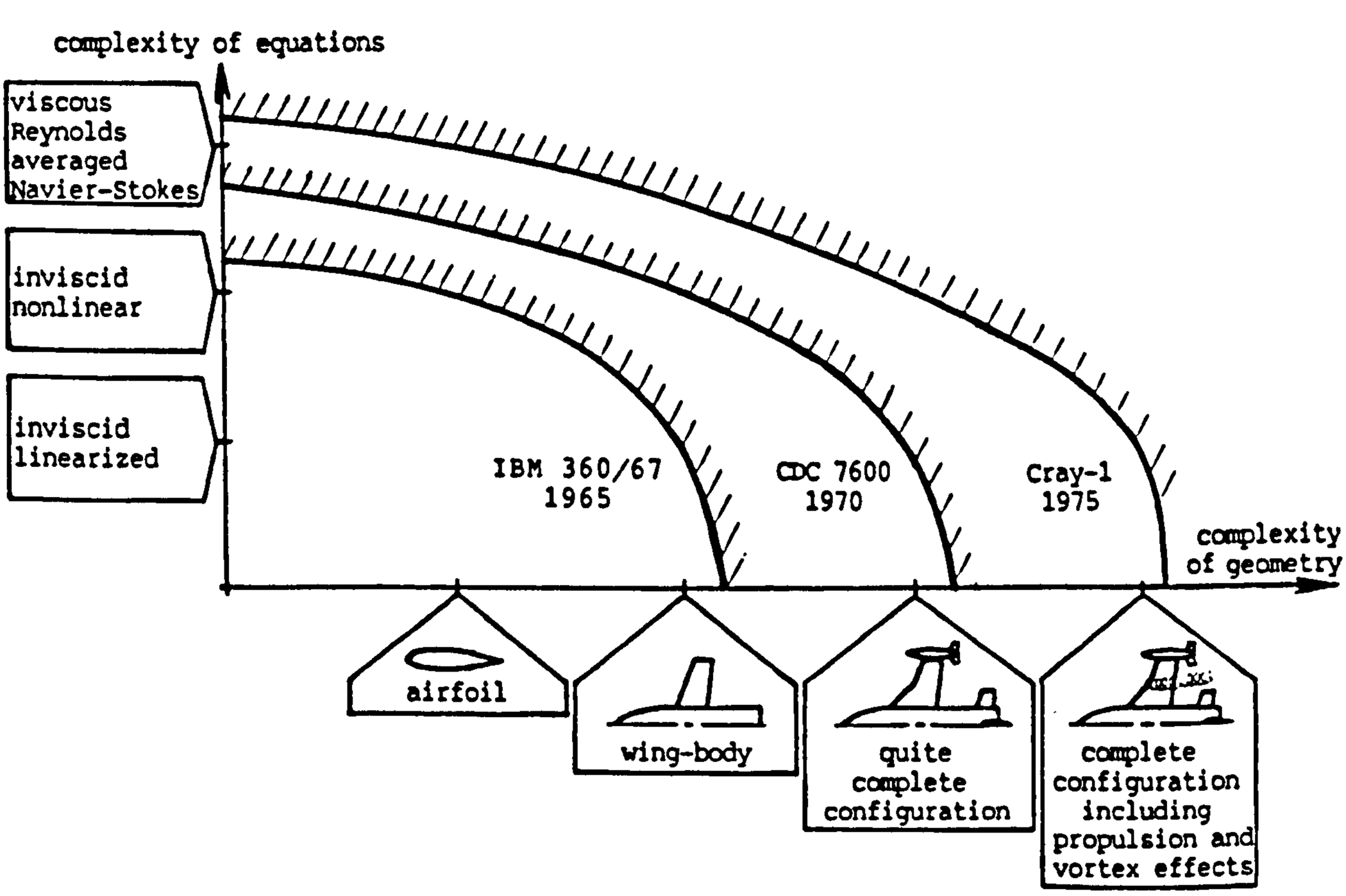

Fig. I.1 Widenining over the years of the complexity of the problems that can be computed

It can be seen that over the years the relative reduction in computational costs and the "inflation of computer muscles" have spurred the examination of either more complex physics or more complex geometries. Nowadays, computational codes are enthusiastically used by airframe manufacturers to economically study several configurations before the start of most wind tunnel test programs. An analogy to computational fluid dynamics in aerodynamic design is finite element methods in structural design: no ground or flight structural testing of large components are being performed without prior finite element analyses.

Another asset of computers is that they can reveal details that testing can hardly or may not produce such as boundary layer behavior, separation of drag into its different components, localized stresses around a crack tip and many other applications. Such particular studies are leading to a better understanding of these different problems and consequently better designs can be achieved.

2 LIMITATIONS OF COMPUTERS

We do not wish to dwell too much on the benefits of computational simulation. However, neither are we deliberately trying to ignore the need for testing to backup or sometimes refine numerical results. The above short paragraphs are intended to merely show the strength of computers as illustrated by their growing use in areas where more traditional tools have prevailed. Our aim now is to

concern ourselves with placing the limitations of these electronic machines into perspective so that the necessity of efficiency and convergence of computational methods becomes apparent. For this purpose, we reproduced in Fig. I.2 a graph from the aforementioned magazine. This figure shows the difference between engineering and research in terms of computing needs.

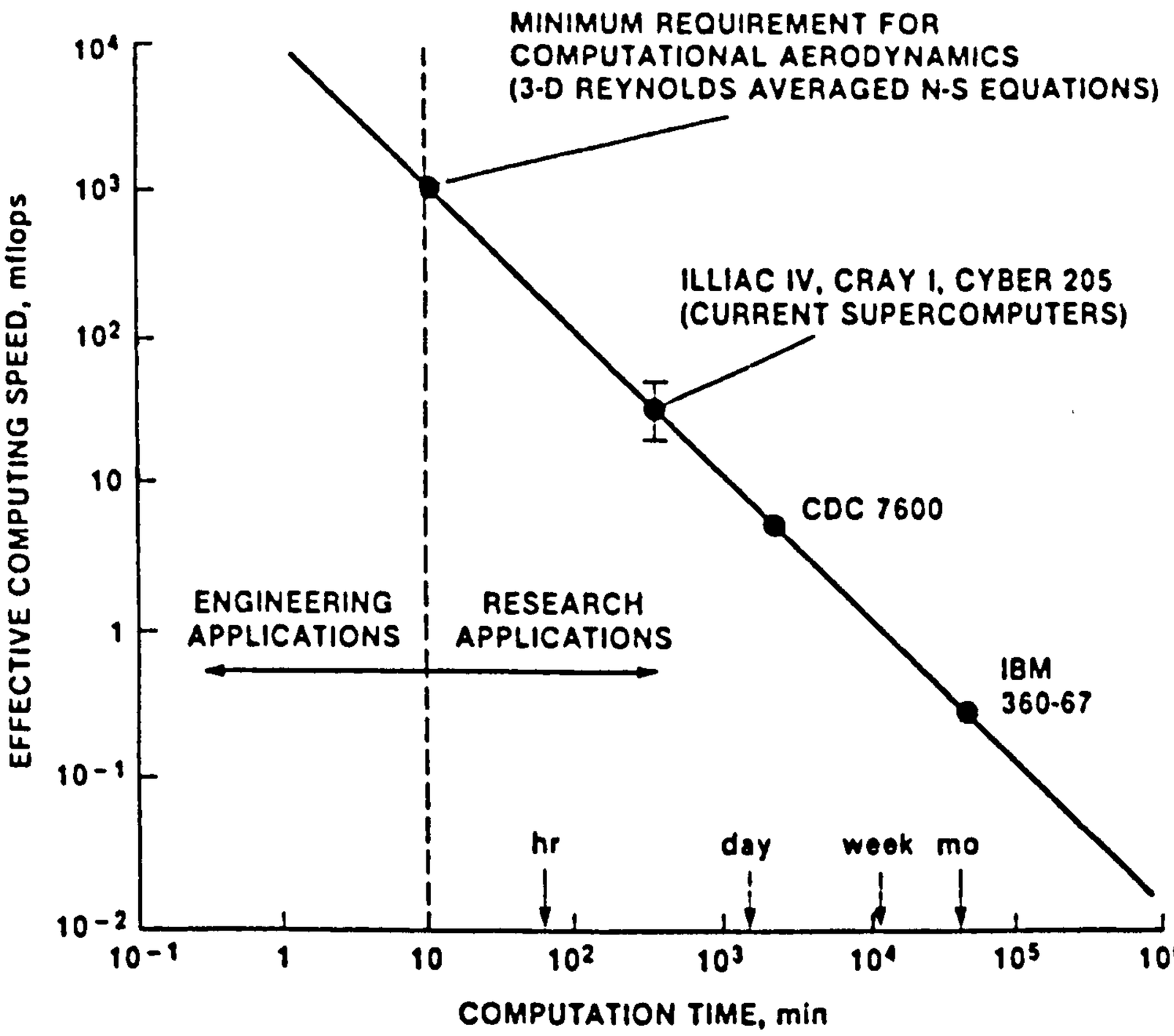

Source: Aviation Week and Space Technology (August 29, 1983, page 72)

Fig. I.2

Engineering problems require a much greater performance from computers than research work for two reasons. Firstly, better spatial resolutions are necessary for engineering purposes. In other words, realistic problems which are usually large and have complicated geometric contours should be modeled by bigger and finer aerodynamic and structural

grid meshings. Some programming codes which can tackle extremely complex phenomena are readily available. However, they are rarely applied to real size problems because of computer capacity restrictions.

Secondly, a few design options are usually studied at least on a trial-an-error basis so that the most adequate can be selected. Due to the complexity of today's engineering problems, the selection of the changes to be made from one option to the other will depend very much upon the intuition and artistry of the individual. A more rational way to seek the best design solution is to automate and consequently ease the choice of design changes by using optimization codes. However, in a number of situations that are characterized by either complexity or size, or both, the cost of an analysis is far from being moderate and hence modifications and reanalyses to search for an optimum will be prohibitely expensive.

In view of the foregoing, we can infer that economic reasons and desires to solve exceedingly more challenging problems is stimulating not only the development of more powerful and cheaper to run computing machines but also the development of equally imperative efficient algorithms. Nevertheless, the point of emphasis is that the development of efficient hardware and software is most of all dictated by engineering needs to establish the best of all possible designs by combining analysis and optimization.

3 DESIGN PHILOSOPHIES FOR FLUTTER PREVENTION

In the past, the prevention of flutter has relied heavily on "rules of thumb" methods. It has been a practice of conventional design procedures to focus firstly and mostly on the strength of the aircraft. To comply with aeroelastic mandates and regulations from aviation authorities, rudimentary flutter checks are then carried out using empirical formulaes. These checks were confined, most of the times, to binary flutter, beam idealization of structures and sometimes simply to a two-dimensional "representative airfoil" section. If the flutter speed of the structure is less than the one required, the necessary corrections are made by stiffening and "mass-balancing" the lifting and control surfaces resulting in heavy designs. Obviously, the accuracy of these simplified theoretical analysis applied to such a complex airplane behavior is very doubtful. It is likely that experimental observations and checks, such as ground resonance and flight flutter tests would lead to further design modifications or limitations and/or performance changes.

Another technique which permits a more complete flutter analysis is to build scaled down models and perform wind tunnel tests. These models are unfortunately several orders of magnitude more expensive to design and build than models for ordinary wind tunnel tests. The reason is that flutter models are reduced replicas that should reproduce as faithfully as possible not only the external geometry of the

aircraft but its dynamics as well with appropriate stiffness and inertia distributions. This is proving to be too constrictive for general applications. Hence, flutter models have been rarely used except for relatively complex structures and unconventional layouts.

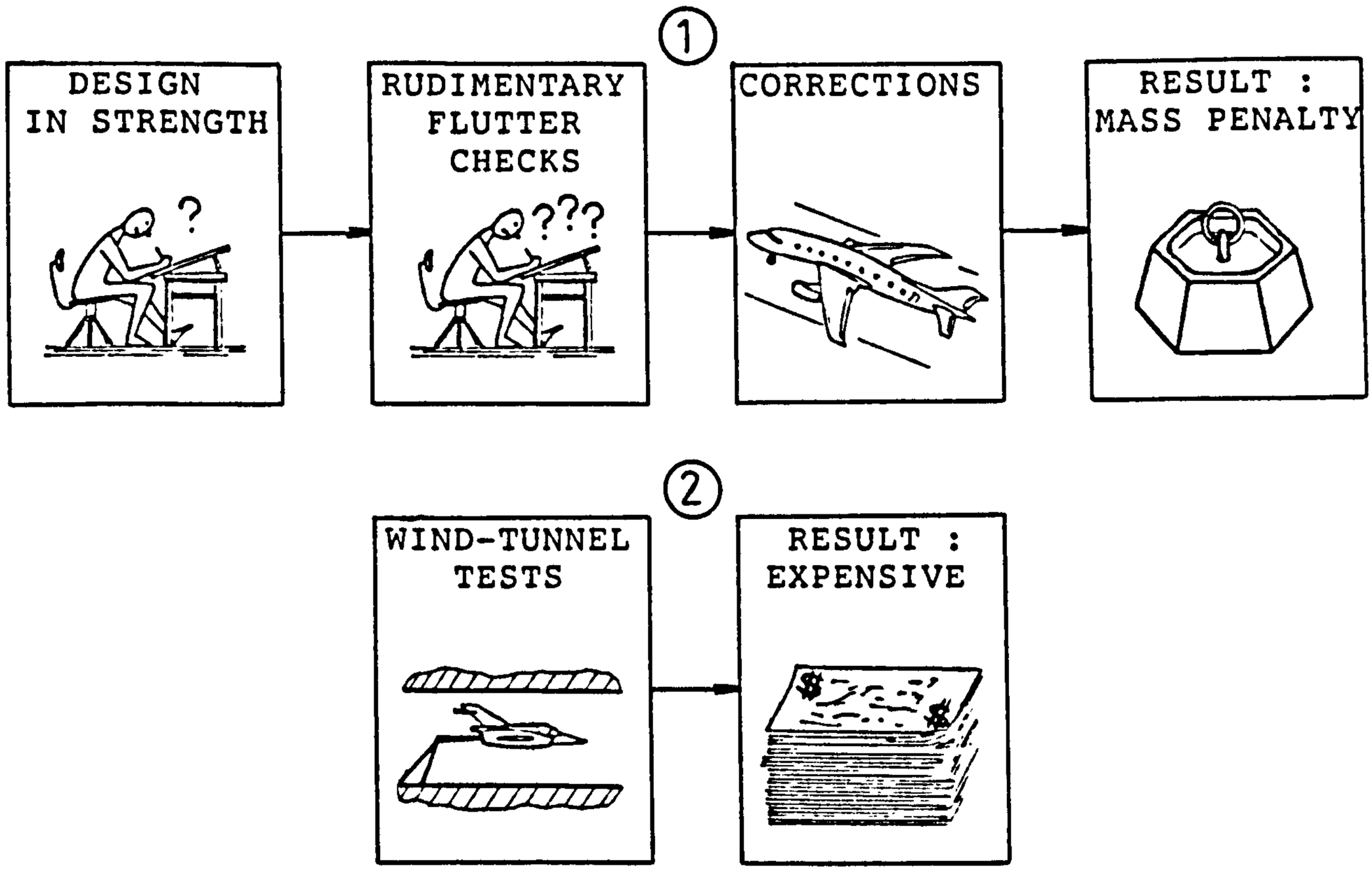

Fig. I.3 Classical flutter prevention techniques

It took two essential steps to evolve to a new concept of designing structures to perform adequately in an aeroelastic environment.

The necessity of making drastic assumptions in the treatment of flutter problems has been deemphasized with the advent of high-speed digital computing machines featuring large memory capacities and with the introduction of efficient analysis techniques and algorithms for handling matrices of high dimensions. It became obvious that one

should be able to derive economically flutter solutions for large types of structures. Indeed, much valuable information about inertia and stiffness distributions, modes of oscillations of structures and unsteady airloads can be obtained by finite element methods and computational aerodynamics.

As computing costs decreased and as more and more efficient and convergent optimization techniques appeared, it was realized that one should be able to design ab-initio structures that are optimum in terms of weight and which are flutter-free.

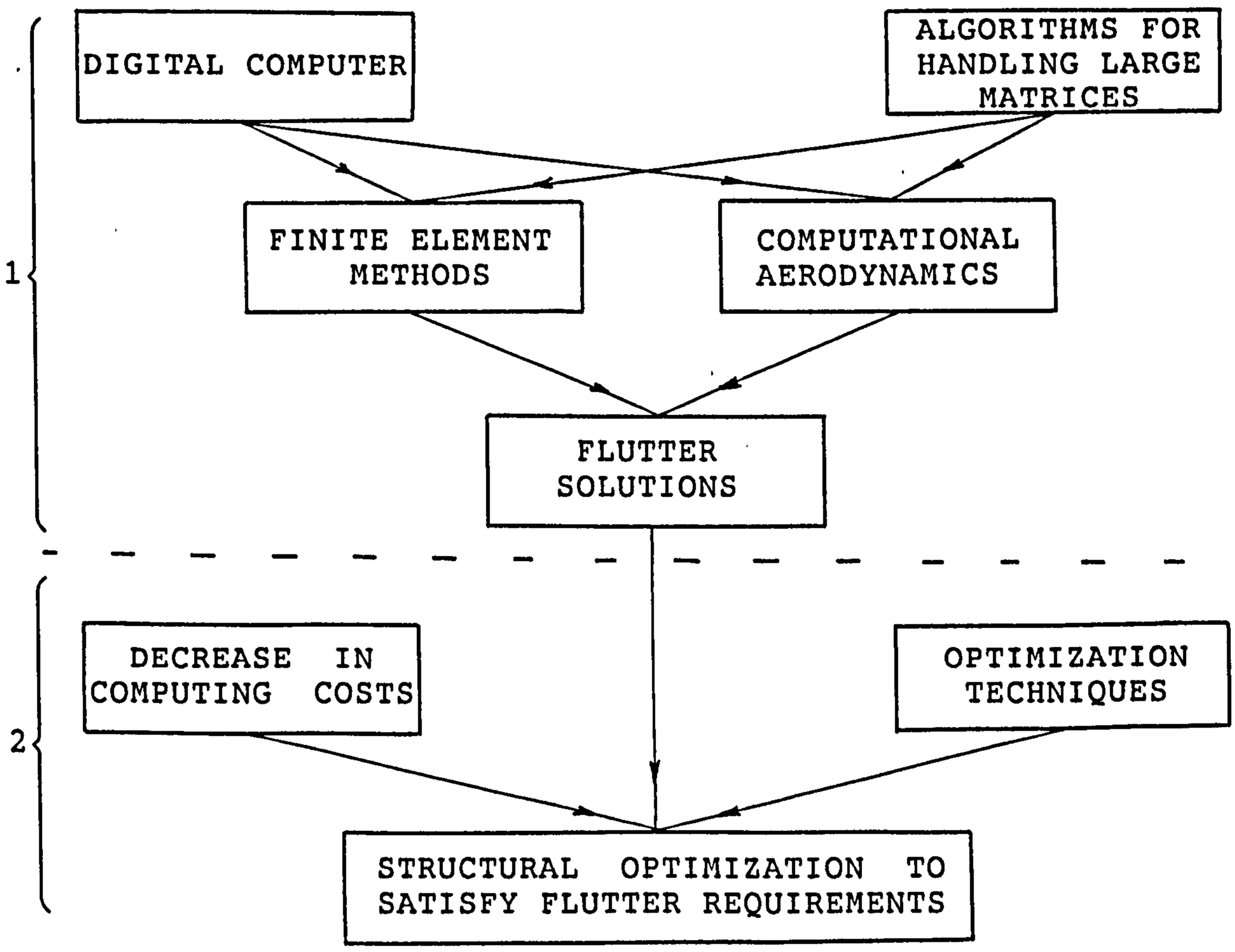

Fig. I.4 Milestones in automated flutter design

This leads us to the point which provides the incentive of the material presented in the next chapters: "structural optimization to satisfy flutter requirements".

4 IMPORTANCE OF ALGORITHMIC EFFICIENCY AND CONVERGENCE IN FLUTTER SYNTHESIS

Clearly, computational methods are today preferred as the mean of ascertaining whether a structure may flutter or not in given conditions because they are both economical and reasonably rigorous. However, repetitive analysis to guide the structural weight towards an optimum while simultaneously satisfying flutter requirements is a more ambitious task and may be paid with an exorbitant price of long (or worse non-convergent) computer runs.

The flutter constrained problem inherently demands more effort in terms of computing resources than, for instance, stress or displacement constrained problems. The criticality of algorithmic efficiency is, therefore, more acute in the case of flutter synthesis.

The enormity of the flutter synthesis task is due to the fact that a complete aeroelastic behavior of the structure must normally be determined at each step of the optimization routine which requires the solution of a free-vibration eigenvalue problem, the interconnection of structural and aerodynamic grids and the generation of unsteady airforces. The most challenging aspect resides in the peculiar nature of

the flutter eigenvalue problem. Its solution is defined in terms of complex eigenvalues — compounds of frequencies and damping parameters — and the corresponding complex eigenvectors. The dependence of the unsteady aerodynamics on these same frequencies imposes scanning through a whole range of frequencies until the starting frequencies are matched with the solved ones for all the flutter modes. Thus, a number of bulk complex aerodynamic matrices will be calculated. These calculations are by far the most time consuming in the entire design process making flutter synthesis emerge as a concrete example of a candidate for algorithmic efficiency.

5 SCOPE OF THE WORK

Even though few algorithms have been proposed for the minimum-weight design of wing structures under flutter constraints, their efficiency, accuracy and reliabiltity, when applied to practical large wing structures has yet to be demonstrated. Unlike conventional minimum-weight structural design where commercially available and fully supported programs are available (STARS, Ref. 34; DOCS, Ref. 35; ...), packages specifically designed for flutter synthesis are not forthcoming. This shows to some extent the need for further exploration in the field of automated aeroelastic design. The object of this research as set two and a half years ago is centered around how to efficiently yield sensible minimization of the structural weight when it is subjected to flutter constraints.

There are two activities that must be looked at to design a program that can cope efficiently with realistic aircraft structures idealized by large numbers of finite elements and degrees of freedom:

— the procedures used to produce the necessary numerical information for analysis[1] and synthesis[2];

— the way such procedures have been written and assembled[3].

Our concern should be aimed at applying the criteria of algorithmic efficiency and convergence to the synthesis area(2). An essential prerequisite to such a task is a program which will perform the necessary preliminary analyses and compute the flutter stability points. Although programs for the calculation of flutter speeds exist, they have not been designed with a view to linking with a structural optimizer. It was, therefore, necessary to embark on building such a program laying special emphasis on efficiency of areas (1) and (3) as well: dynamic dimensioning of arrays and modular approach at the internal language level and at the compilation and linking levels. Use has been made of techniques with high efficiency and reliability such as eigenvalue economizer and surfaces splines. For optimization work, the primary interest is to assess the most critical speed. Hence, we opted for the American method of flutter solutions. For general investigations or previous to flight

flutter tests, prediction of decays at subcritical speeds are crucial and the British method developed by RAE may give better subcritical trends (Ref. 31).

Armed with an aeroelastic program, the next task is to attack the problem of the efficiency of the resizing process. The first logical step is to identify from a literature survey any area that, in our viewpoint, may need further explorations.

Previous work on flutter synthesis has relied on the use of the initial natural modes of the base design throughout the whole optimization process although free-vibration analysis should be carried out at each iteration as the sizes of the design variables are changed. One slight benefit of such an approach is that it avoids the recomputation of the mode shapes at each resizing step. Its potential benefit is that it permits the optimization routine with aerodynamic matrices not dependent on the mode shapes simplifying considerably the flutter analyses and any derivatives expressions. The main concern is that solutions obtained from such an approach may leave a lot to be desired in terms of satisfying the minimum flutter speed. Our proposal to overcome this obstacle without any sensible detriment to efficiency is the exploitation of dual theory. A scheme of this kind has not been applied before to aeroelastic constrained problems.

Thus, the object of this research is, firstly, the

development of a program package for optimizing structures to satisfy flutter requirements incorporating most recent economical and accurate analysis techniques and, secondly, to provide a coherent method aimed at improving the efficiency of synthesis method for flutter prevention.

CHAPTER II

ON FLUTTER

1 DEFINITIONS OF FLUTTER

In order to quantify the problem we are attacking, it is necessary to clarify what is meant by flutter. Unfortunately, no clear definition exists and, within the literature on aeroelasticity, several are given:

— aeroelastic and self-excited vibration, in which the external source of energy is the air stream;

— aerodynamic self-excited oscillations;

— self-sustained oscillatory instability;

— cyclic and high frequency oscillation of the aerofoil caused by a struggle between the aerodynamic forces and the stiffness of the surfaces;

— dynamic instability of an elastic body in an airstream produced by aerodynamic forces which result from the deflection of the elastic body from its undeformed state;

— dynamic aeroelastic instability;

— dynamic instability occurring in an aircraft in flight at a certain speed where the elasticity of the structure plays an essential part in the instability;

— self-excited or unstable oscillation arising out of the simultaneous action of elastic, inertia and aerodynamic lift forces upon a mass or a system of masses;

— oscillatory instability arising from the condition where one degree of freedom is driven at resonance by a second degree of freedom, both oscillating at the same frequency;

— unstable divergent motion or vibration caused by aerodynamic forces.

While it may be an exaggeration to say that such definitions render flutter even more obscure, it is admitted that one has to resort to simple examples rather than to dictionary types of definitions in order to gain some insight into the flutter mechanism.

2 INTRODUCTION TO FLUTTER

The most popular, because very instructive, way for introducing the subject of flutter is a flat plate in which bending and torsion stiffnesses are idealized by springs and with the further simplifying assumption of steady aerodynamics. Pines (Ref. 38, 1958) used this system to give an elementary, but remarkable, description of how certain parameters such as the relative positions of centre of gravity, elastic axis and aerodynamic centres can have salutary or detrimental effects on a classical class of flutter commonly referred to as "binary bending-torsion"

flutter. The outstanding feature of this example is its pedagogic simplicity because it does not demand too great a prior knowledge of the physics and mathematics needed to study the behavior of this instability. Since then, the flat plate has stimulated widespread interest in the academic institutions. A remarkable result, inferred from this rudimentary example, is that the flat plate would not encounter classical flutter if the centre of gravity is ahead of the elastic axis.

Bisplinghoff and Ashley (see bibliography: Principles of Aeroelasticity, page 264) and Dowell, et al. (see bibliography: A Modern Course on Aeroelasticity, pp. 76-89) extended the study of the flat plate with the use of a slightly more respectable approximation of quasi-steady aerodynamics.

An alternative but somewhat more systematic attempt to probe into the nature of flutter is through the energy exchange of the whole aeroelastic system. Elastic and inertia forces caused by stiffness and mass distributions are both conservative forces and the result is that they do zero net work on the system. In other words, they do neither feed into nor extract energy from the system during a cycle of oscillation. If flutter is a self-excited instability that can maintain itself without the help of any external source of energy, then there remains the question of how the oscillations can persist and be amplified to structural failure. Under certain circumstances involving diversified

parameters, namely reduced frequency (ratio of frequency to velocity), Mach number, phase lag between deflection and its aerodynamic reaction or between flexural and torsional wing oscillations..., energy may be drawn from the airstream by the structure. Depending on whether the energy absorbed is smaller or higher than dissipated through damping, the amplitude of oscillations may die out or remain and diverge.

A practical demonstration on flutter and the associated energy exchange can be made by means of the "flutter engine". This is an apparatus that consists of a rigid airfoil allowed to pitch and roll freely at its root (Ref. 14). The energy pumped from the airstream by the airfoil is imparted through connecting rods and cranks to a flywheel which is then forced to rotate.

3 BRIEF REVIEW OF BIBLIOGRAPHY

The bibliography, currently available in English and dealing with aeroelasticity in general and flutter in particular, is listed herein. It begins with the excellent text book of Bisplinghoff (in collaboration with Ashley and Halfman), first published in 1955 and representing a pioneering compilation of what was known on and applied to the study of aeroelasticity. Most technical papers on flutter have this book in their lists of references and it is being pointed out whenever the V-g solution (see appendix A) is mentioned although the V-g solution method can be traced as far back as 1942 and is attributed by Ref. 32 (page 1.1-2) to

the Air Material Command (USA). Another valuable contribution to the general understanding of aeroelasticity is the book by Fung also published in 1955. A recent book on the same field by Dowell, et al., titled "A modern course in aeroelasticity", is, however, preferably recommended because it is very educational (chapters 1 and 2 on static and dynamic aeroelasticity) and contains a wealth of up-dated information specially on non-steady aerodynamics and aeroelaticity of rotorcrafts and an authoritative account on stall flutter. "Aeroelasticity of plates and shells (Dowell only)" represents the most extensive document of the very special case of aeroelasticity of panels. Other additional books listed in the bibliography are there to do justice to other authors' share to the comprehension of aeroelastic phenomena. These are also recommended though to a much lesser degree.

All the aforementioned books do not represent a complete survey of the subject. Thus, the profusion of papers or articles referred to by these books or consistently published in the relevant journals (Journal of Aircraft, AIAA Journal, Journal of Sound and Vibration...) must be consulted if specific areas of interest require further explanation.

4 FORMS OF FLUTTER PHENOMENA OF INTEREST TO THE AIRCRAFT DESIGNER

A host of instabilities in systems such as aircraft, helicopter rotors, air deflectors or spoilers on automobiles,

turbomachinery, pipes, electrical power transmission cables, towers, chimneys, bridges, flags, venetian blind slats... can be identified as flutter. We are concerned here not so much with exhaustive coverage and treatment on all the flutter problems encountered in everyday life. This paragraph has been instead restricted to a basic classification of the flutter phenomena of particular interest to the aircraft designer.

The text is enhanced with a suite of figures. These illustrations do need few clarifications and they are given below.

Investigations of the stability of a system can be made by assuming that the generalized motions are damped harmonic functions of the form

$$\{q\} = \{\bar{q}\}e^{ist} = \{\bar{q}\}e^{i\left(\omega+i\omega_i\right)t} = \{\bar{q}\}e^{i\omega t}e^{\left(-\omega_i t\right)} \qquad \text{(II.4.1)}$$

$\{q\}$ vector of generalized coordinates

$\{\bar{q}\}$ vector of complex amplitudes

s complex frequency

$\omega \equiv Re(s)$

$\omega_i \equiv Im(s)$

Formally, we recall that ω is the circular frequency of oscillation and that ω_i is a measure of the true damping. The sign of ω_i determines whether the motion is stable or unstable. If ω_i is positive, the system is stable. If ω_i is

negative, then the motion diverges exponentially with time and the system flutters.

Alternatively, stability may be looked at through the mathematical concept of artificial damping (more about this in appendix A). Negative artificial damping shows that the structure is not fluttering in a specific mode and it represents the amount of fictious damping that must be substracted from the system to make it undergo neutrally stable oscillations in that mode. When one of the modes of vibration of the structure becomes unstable, artificial damping of that mode is positive which can be seen as the amount of fictious damping that must be added to the system to force it to undergo neutrally stable oscillations.

Now, we proceed to enumerate the types of flutter encountered by aircraft structures.

4.1 "Zero frequency" flutter

This is generally known as divergence and is usually dealt with in static aeroelasticity. Although the nature of divergence is entirely different from that of flutter, it can be as well investigated as a special single-degree-of-freedom flutter. Fig. II.1 is to show that this steady state instability occurs when one of the values of s has a zero real part and a negative imaginary part.

Out-of-phase structural and aerodynamic damping forces

are less amenable to reliable theoretical treatment than the in-phase forces. Since divergence can be considered to be a time-independent instability, these damping forces together with the inertia forces can be excluded making divergence emerge as a simple and well predicted aeroelastic problem. The theory is generally reliable even when divergence becomes of acute practical importance such as in forward swept wings.

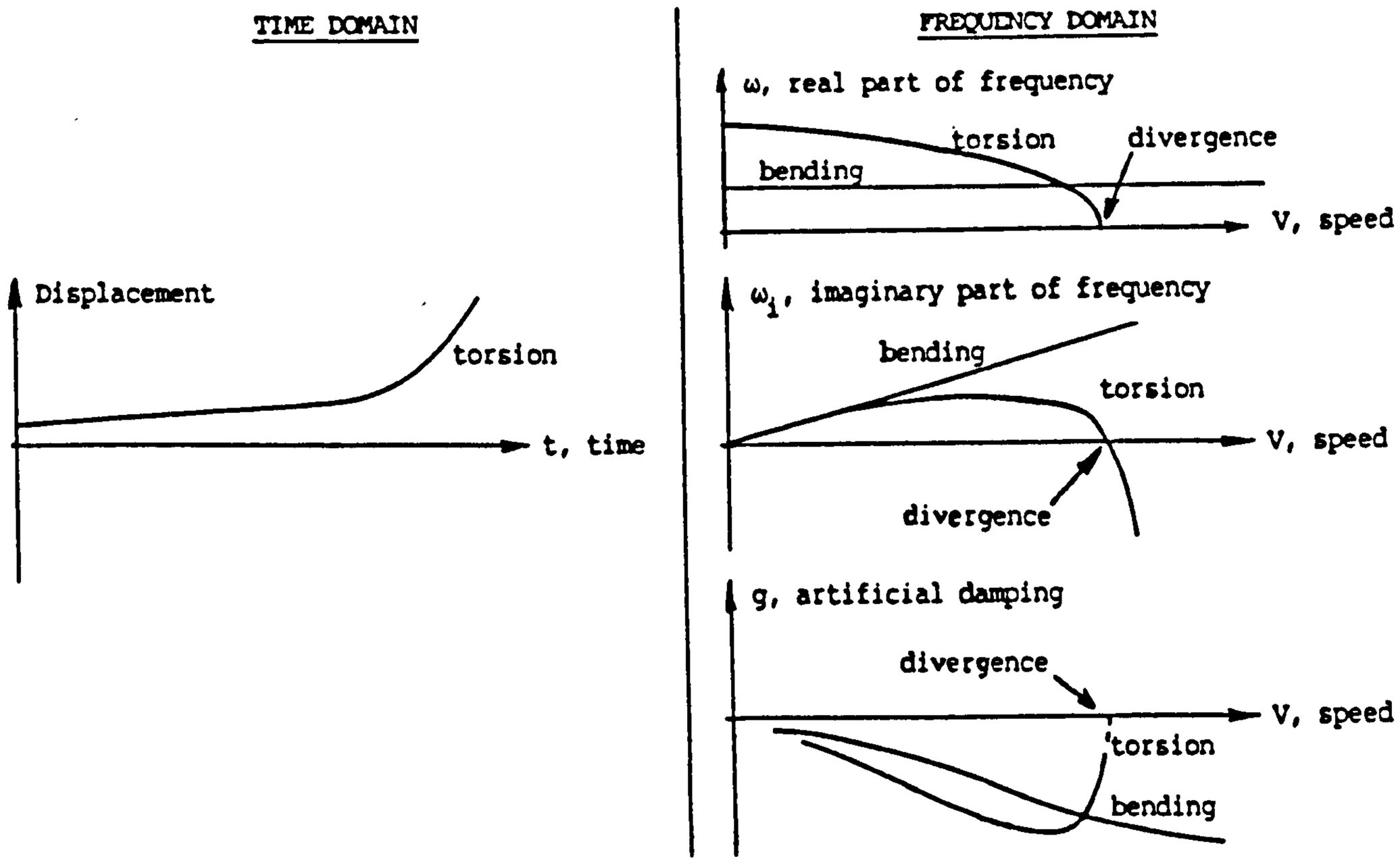

Fig. II.1 Divergence in time and frequency domains

4.2 "Coalescence", "merging frequency" or "coupled-mode" flutter

Broadly speaking, the characteristics of this class of flutter is that two or more distinct types of structural deformation are converging towards oscillating at the same frequency as the flutter condition is approached. The onset of this dynamic instability happens when one of the imaginary

parts of s changes sign from a positive value to a negative value. however, in contrast to divergence the real parts of s do not vanish (see Fig. II.2).

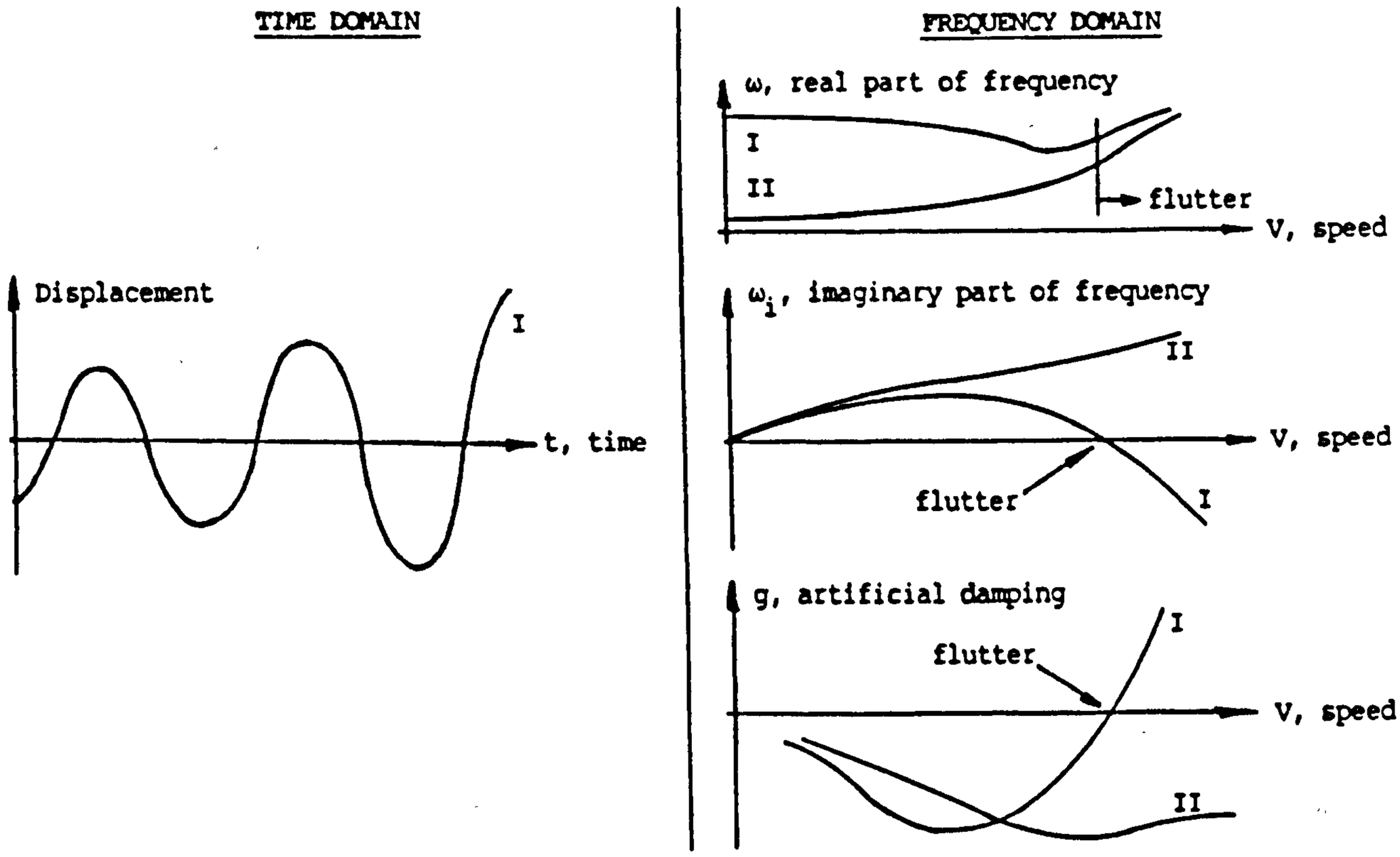

Fig. II.2 Coalescence flutter in time and frequency domains

"Coupled-mode" flutter is quite — but not crucially — sensitive to out-of-phase damping forces. In fact, reasonably good results can sometimes be obtained by neglecting structural damping and by making yet another drastic assumption of quasi-steady aerodynamics.

4.3 Stall or stalling flutter

This class of flutter can be treated as prominently involving just one degree of freedom, say torsion or bending. However, this not universally true as stall flutter in more

than one degree of freedom may occur under certain circumstances adding a further complication to this already non-linear problem.

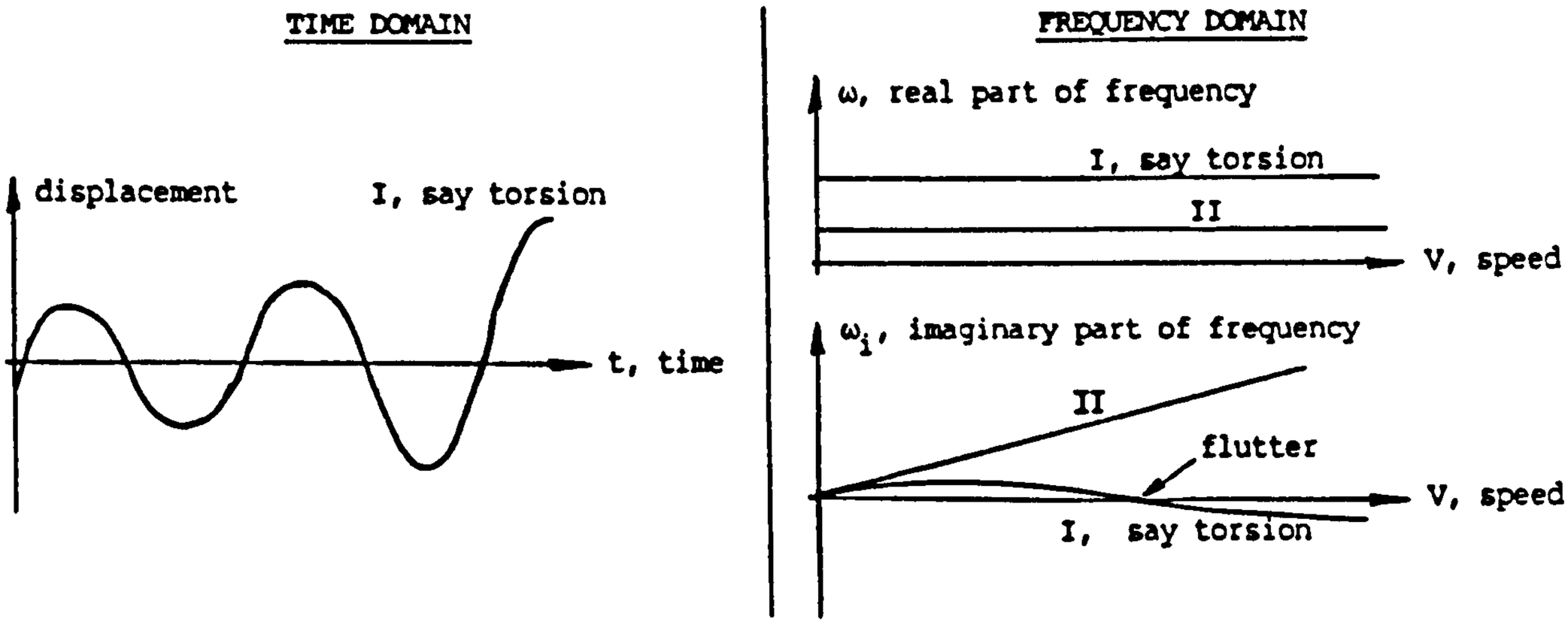

Fig. II.3 Stall flutter in time and frequency domains

Examination of Fig. II.3 shows that stall flutter exhibits the destabilization of a very lightly damped mode (usually torsion). This sensitivity towards such trivial damping forces coupled with the uncertainty surrounding the out-of-phase load predictions, on the one hand, and the notable aerodynamic non-linearity, on the other hand, are the two factors that make stall flutter difficult to approach analytically. Experimental or semi-empirical methods appear to be the only solution techniques for the foreseeable future.

Stall flutter can be a serious concern only for designs of airfoils expected to operate in very high angle of attack conditions.

4.4 Transonic buzz

Like divergence, this can be considered as a one-degree-of-freedom type of flutter. It is traditionally called aileron buzz. However, it is not confined to ailerons only but to trailing-edge controls in general. It is even possible for clean airfoils to undergo transonic buzz. This latter peculiar form of transonic buzz is caused by shock waves oscillations, specially in high aspect ratio wings, and inducing torsional vibrations of the airfoil. The problem of control buzz is somewhat similar but involves oscillations of shock waves on the upper and lower airfoil surfaces and oscillations of a control surface.

4.5 Panel flutter

As with the airframe as a whole, aircraft skins may locally suffer sustained and sometimes destructive vibrations very much similar to overall structural flutter.

Simplistic theoretical approaches (see both books of Dowell in bibliography list) supported by experimental evidence (Ref. 17) show that the different aspects of the aeroelasticity of plates and shells can be basically grouped into divergence and coupled-mode flutter. The divergence type of instability resembles the classic form of buckling but is influenced by the aeroelastic feedback of the airstream whereas the coupled-mode type is characterized by the coming together of buckle wave frequencies.

4.6 Other types of flutter

Airframe distortions are the result of mutual structural and aerodynamic interactions and this problem is dealt with under the interdisciplinary heading of aeroelasticity. At supersonic speeds, aerodynamic heating may introduce thermal stresses and deformations and deteriorations of mechanical properties. If kinetic heating is important, the study of flutter must be extended to the broader field of aerothermoelasticity.

Other topics, not included in the survey of flutter outlined above, are those related to rotary-wing and propeller whirl flutter. It is possible to conceive of conditions wherein any amalgam of different sorts of flutter and thermal effects interacts on the structure.

5 FLUTTER PHENOMENON CONSIDERED IN THIS WORK

To obviate certain difficulties and problems such as unavailability of adequate theoretical modeling, lack of time or of financial resources, we found it necessary to confine the flutter phenomenon considered in this treatise to within certain boundaries. These restrictions are in a way fairly academic, though they are in no way affecting the generality of certain results or the validity of certain conclusions drawn throughout this work. In some instances, these sets of simplifying assumptions do not prevent the computer code

developed to be applied to practical real-life problems.

5.1 Operational envelope

There is no an all-embracing aerodynamic code that can assess unsteady airloads at any Mach number. The one we are using is exclusively for airflows that have subsonic velocity all around the airfoil.

5.2 Type

Well established linearized mathematical analysis on which "coalescence" flutter relies cannot be expected to be of any validity for aeroelastic phenomena such as stall and buzz flutter or any other type of flutter that exhibit flow separation. This latter category of flutter is characterized by highly non-linear behavior. There is as yet no adequate theory which can investigate unsteady aerodynamics or assess the value of the airloads with any reasonable accuracy for these flutter phenomena. Thus, state-of-the-art of computational aerodynamics restricts the scope of the present work to the classical form of flutter in which frequencies of oscillations are merging towards the same value to render one mode unstable. Whenever the term "flutter" is henceforth mentioned the "coupled-mode" type is implied unless otherwise specified.

Incidentally, the skin thickness on which panel flutter may be triggered off is so small in subsonic flight that it

is not of any practicality (Ref. 17). Panel flutter is, therefore, assumed not to be a source of concern in our case. However, if for any reason, structural integrity is governed by panel flutter rather than strength, the skin thickness required to prevent panel flutter from occurring may be used as a minimum gauge.

5.3 Interference and coupling effects

The aerodynamic interference between adjacent wings and bodies and the inertia and elastic coupling between the major aircraft parts can sometimes be so marked as to make the modeling of at least a group of components a prerequisite of any sensible flutter analysis. For instance, a T-tail arrangement cannot be reduced to two flutter analyses of disconnected fin and tailplane. A lot of skepticism must be displayed towards flutter results that separate the wing from its close-coupled canard, the fully retracted variable geometry wing from the empennage...

The aerodynamic code that computes the unsteady airloads for our optimization purposes does not incorporate interference effects. Thus, we are limited to consider only flutter of isolated lifting planforms.

5.4 External stores

Because the aerodynamic code is exclusively for clean surfaces, external stores (powerplants, fuel tanks,

missiles...) are precluded from our analysis although their effects upon airloads and frequencies and modes of oscillations can modify appreciably the flutter characteristics of a wing.

5.5 Thermal effect

Aerodynamic thermal effects are insignificant for the subsonic regime we are considering. Aerothermoelasticity problems are therefore not of practical concern for this work.

6 AEROSERVOELASTICITY

The historical trend of the aircraft industry has been towards more and more flexible structural components whose member sizes are very likely to be designed to meet stiffness rather than static strength requirements. This highlights how potentially significant it is to investigate ways of efficiently distributing the structural mass while preventing aeroelastic distortions beyond acceptable limits. Optimum distribution of mass and optimum orientation of stiffness such as allowed by advanced composite materials form the passive control technique of aeroelastic deformations.

Equipping the aircraft with an active control system is the other avenue towards tightly managing the aeroelastic behavior of the vehicle. It is done by actuating the control surfaces or by shaping the airfoil (wing with variable

camber) through feedback signals from acceleration, velocity and displacement sensors on the structure. Extensive research in this technique is nowadays paving the way to aeroservoelasticity, a fascinating subtopic of aeroelasticity.

The use of servo-systems to artificially remove aeroelastic instabilities can be at times more rewarding in terms of weight savings and mission flexibility gains than the optimum alteration of the structural members. This is definitely the case for aging aircrafts that need to have their aeroelastic performance stretched during an upgrading program. Moreover, modern military aircrafts experience during their service life new combinations or introductions of external stores, armaments and electronic pods. If one of these arrangements brings in a flutter problem, it appears that provision of an active flutter suppression system would be a more appropriate solution than severing or bridging across major structural members.

Ref. 55 reports the case of the Rockwell Forward Swept Wing design, probably the one that entered the competition for building a demonstrator. Because this configuration is particularly prone to divergence, the initial attention focused on exploring the wing as cantilevered. A problem of a coupling between the rigid body mode and a wing bending mode remained unnoticed until after the design was frozen. It was then discovered that the flutter speed caused by this coupling was much lower than the divergence speed for which

the wing was optimized. Changes in sweep angle, aspect ratio, thickness-to-chord ratio, skin thickness and Young modulus of the fibers of the composite materials were investigated as parameters to raise the flutter speed. Each of these palliatives either degraded other design performances or did not increase the flutter speed enough to move it outside the operational envelope. The only feasible solution to this design dead-lock was to enhance the aircraft with an active control system to suppress this unstable mode coupling.

Finally, one can propose active controls (automatic suppression of aeroelastic instabilities) as a redundant technique to the passive control (aeroealstic tailoring of the structure). This could prove very valuable as an extra safeguard in case of a damage to the structure of a combat aircraft or in designs where explosive flutter onsets are predicted.

The conclusion that may be drawn in this section is that it may be delusive to believe that structural optimization is the best answer to satisfy aeroelastic constraints. There are instances where active controls may complement or sometimes supplant structural optimization and may achieve better cost-effective design solutions with less weight and performance penalties.

CHAPTER III

ON STRUCTURAL OPTIMIZATION

In contemporary life, the manufacture of complex products or the bringing to fruition of an important project will definitely be the result of a compromise between numerous factors. Each compromise represents a balance between sets of conflicting demands some of which are rational and hence can be more or less easily represented by mathematical models and others which are subjective and can hardly be defined in terms of heuristic formalisms. Lift to drag ratio, strength of a structure, manufacturing costs, mass, speed, etc... fall in the first category. Whereas aesthetic, market appeal, public or trade unions reactions, social changes, fashion, etc... fall in the second category.

To strive for the realization of the best or the optimum product is a trait of human nature. This can be motivated by any combination of a desire for perfection, a search for prestige, economical necessities, competition drives... It is obvious that this definition of an optimum is too abstract. In addition, such optimae cannot be achieved if all the relevant factors affecting every aspect of the project are required to be taken simultaneously into consideration. Therefore, one has to decompose the work into a series of more specific tasks. Some of these tasks can be separately optimized but may demand massive mathematical and numerical effort. In a number of situations, some other tasks could be very much a matter of individual judgment and art.

In view of this, our interest will be limited to the

dimensioning aspect of structures when subjected to loading and design restrictions that can be clearly identified and quantified. This is traditionaly known as structural optimization. Before embarking on this subject, it may be essential to state clearly at this point the definitions of some specific words from amongst the rich structural optimization terminology.

1 OBJECTIVE FUNCTION IN STRUCTURAL OPTIMIZATION

Within the optimization process is defined a function called objective or cost function whose minimum or maximum value must be sought. By far the most important design objective for the aircraft engineer is lightness because of the dominant effect that weight has on the performance of air and spacecrafts. So, in the field of aircraft and spacecraft structural synthesis, the objective function is the mass or weight of the vehicle.

Unlike some authors, we will refer to this function only as objective function rather than cost function, for weight is not necessarily representative of cost and in some instances any reduction of weight beyond a certain limit may inevitably result in a sudden and exponential rise of the cost of a vehicle.

2 DESIGN VARIABLES IN STRUCTURAL OPTIMIZATION

By describing the idealized structural system by a

finite set of parameters one can define the variables that compose the objective function. Amongst these parameters, there are those that are, a priori, prescribed and not altered by the algorithm of optimization. The rest, that is those that are modified in the process, are called design variables.

The design variables can define (in ascending order of difficulty they would pose if taken into account in the optimization process): (i) the dimensions of the elements of the structure; (ii) the geometry (configuration) of the structure; (iii) the material types used in the structure; (iv) the topology of the structure.

2.1 Dimensional design variables

These may be thicknesses (of membranes or plates), cross-sectional areas (of bars, rods or beams), moments of inertia, or even individual element masses or volumes. Engineering standards imposes that only certain discrete values can be taken by these design variables. However, in practice, they are usually assumed to be continuous.

2.2 Configurational or geometrical design variables

The geometry of the structure such as lengths, areas or angles between elements can affect significantly the final mass. For instance, one approach to satisfying divergence speed requirement on forward swept wings is to reduce the

wing wash-in by increasing the flexural and/or torsional stiffnesses and this will lead to an increase in wing and aircraft weights. If the orientation of the stringers of a wing relatively to the longitudinal axis of the aircraft is made variable in the design process, aeroelastic divergence on forward swept wings can be overcome with a minimum weight penalty because stringers set a at certain optimum angle can favorably couple bending and twisting modes. Refinement can be carried out even further by tailoring composite materials. These materials, while having superior specific strength and stiffness properties when compared to conventional aircraft metals, possess strength and stiffness that are predominantly uni-directional. Deformation of a wing can be controlled by proper selection of ply angle and laminate thickness distribution. This is referred to as anisotropic aeroelasticity or aeroelastic tailoring and is having a drastic impact on aircraft design no matter whether the wing is swept fore or aft.

2.3 Material design variables

Although the mass of a structure can be appreciably improved with a proper choice of materials, the use of material as a design variable seems not to have received much attention. This may be due to the fact that material types are selected by experience for each major item of a structure and that any algorithm including the feature of material choice would be too complex. However, as more and more new materials are certified by airworthiness authorities, it

would be worth looking at ways of optimizing structures with material as one of the variable factors.

2.4 Topological design variables

These may describe the number, spatial sequence and mutual connectivity of members and joints. We can anticipate in this category modifications in the discretized structure such as the replacement of elements by other element types which may be connected differently. In construction terms, the choice can be about braced, stressed skins or sandwich designs.

3 CONSTRAINTS

After having adopted an objective function and having selected the variables composing it, one is left with the task of quantifying the performance that we require from the structure. In optimization terminology, the constraints describe a set of imposed restrictions or limitations on certain quantities so that the structure can assume its rôle in its operational environment.

Side constraints usually refer to upper and lower limits on certain quantities. Gauge constraints are side constraints on the dimensions of the elements of the structure as laid down by manufacturing requirements.

Behavior constraints are so called because they refer to

the structural response such as stresses, local and global instability, deflections, frequencies, flutter, divergence...

4 SOLUTION METHODS

The numerical problem of structural optimization can be summarized as the search of values of design variables so as formally achieve minimization of the objective function (mass or weight) while at the same time satisfying associated conditions of minimum/maximum gauge constraints and of diverse behavior constraints. Numerous methods are available to solve this problem. Our intention in this section is not to produce an exhaustive comparative essay on these methods. Instead, we will aim at giving a brief classification of and general commentaries on these solution techniques.

The first impression that one has when reading early literature on structural optimization is that solution methods are classified into two conflicting schools of teaching that were developed in parallel streams and in almost dogmatic ways: indirect and direct methods.

The indirect or optimality criteria (OC) methods attempt, through recursive relations, to drive the initial design towards the satisfaction of intuitive or strict optimality criteria. In buckling constrained designs, the intuitive definition of structural efficiency was that local buckling of the sheet panel should occur at the same stress level as over-all buckling. In stress constrained designs,

the intuitive approach is inspired by a "fully-stressed" philosophy. In flutter constrained designs, the intuitive criteria is similar and requires that the strain energy density is uniform throughout the structure in its deformed flutter mode. The interest in intuitive optimality criteria has been fading out since MP (mathematical programming) have brought to light that in the design space optimum weights are not necessarily fully-stressed (Schmit, Ref. 44, 1960). Another important criticism of this approach is that it is potentially hazardous in the case of buckling constraints. The collapse of the so-called least-weight design (simultaneous mode failure) is a sudden explosive snap of the structure and is very sensitive to initial imperfections as observed by Koiter and Skaloud (Ref. 7, 1962). The alternate rigorous OC are derived mathematically from the equations governing the optimization problem. These OC are valid only at the optimum and it is imperative to convert them into recurrence relations which might on occasions diverge away from any optimum solution.

The direct methods or MP based methods work directly to minimize the objective function. As opposed to OC techniques, MP techniques are more versatile design tools and possess far wider practical applications. The main drawback, however, is that the cost of MP optimization may be very expensive even for moderately sized finite element models.

The MP procedure is the most laborious but most commonly converges to at least a near optimum design whereas the OC

procedure usually entails least labor but does not guarantee convergence. These led the protagonists of both approaches to separately redouble their efforts in overcoming the MP computational burdens and the risks of OC impasses. However, it was soon discovered that the attributes of each of these techniques can be exploited simultaneously and mixed-approach programs that combine both procedures into one single program were introduced. In many practical applications, it was found that the FSD (fully-stressed-design) approach can be used in the initial few iterations to speed up convergence to pseudo-optimum points and then one can proceed from there to the search of a true optimum (Ref. 34 and 35). In the program described in Ref. 47, gross overall material distribution of the fuselage is tackled with an FSD concept and the component design of panels consisting of skins and stringers is handled with greater care by an MP concept.

Apart from the differences in computational performances, OC or MP based methods should merge to one unique and natural goal: satisfaction of the Kuhn-Tucker conditions of optimality. This viewpoint has recently been propounded by Fleury and Sander (Ref. 16) when they conclusively reconciled the mathematics behind the two approaches (see also Ref. 15 and chapter 10 of the book in the bibliography list edited by Morris).

In view of this changed perspective, it might now be argued that one may cover the large spectrum of solutions techniques in a three-category classification: primal,

transformation and dual techniques.

The two papers by Belegundu and Arora (Ref. 4 and 5, 1985) testify this new strong viewpoint. The intention of these authors was to present an analytical and numerical comparison on solution techniques applicable to structural optimization and their work identified:

(a) recursive quadratic programming;	primal techniques
(b) method of Bard and Greenstadt;	
(c) sequential linear programming;	
(d) gradient projection;	
(e) reduced gradient;	
(f) feasible directions;	
(g) projection methods;	
(h) and also optimality criteria;	
(i) sequential unconstrained minimization techniques (penalty functions and barrier functions);	transformation techniques
(j) multiplier (or augmented Lagrangian) methods.	

For completeness, however, their comparative study should have included dual techniques. The auxiliary dual problem is to maximize the Lagrangian function in which the Lagrange multipliers have the rôle of dual variables. One aspect of dual theory put into perspective by Bartholomew (Ref. 2) is that of dual bounding of the structural weight which can be favorably used to monitor the convergence of the

solution method. This provides a more reliable cut-off criterion when compared to the termination criterion that specifies limits on the difference between certain quantities on two successive iterations or somewhat arbitrary criterion such as stopping the program after the completion of a maximum permissible number of iterations.

Finally, to supplement this overall view, we must digress here to present an alternative way of thinking that might have important repercussions on automated design: namely knowledge-based expert systems (KBES). KBES is claimed to be capable of addressing challenging tasks that need specialized knowledge and expertise gained only through long experience. Possibly one of the justifications for the integration of KBES in structural optimization is that some design problems are ill-structured for classical algorithmic solutions. For instance, including material into the set of design variables is probably one typical example of such problems.

5 STRUCTURAL OPTIMIZATION WITH FLUTTER CONSTRAINTS

5.1 Situation of the problem in the overall design process

After the phase of defining the need for a product and the performance required from it, the structural design process whether partly or entirely automated follows a pattern of three chronological stages:

— the conceptual or early preliminary design stage which consists of carrying out approximate analysis and comparisons possibly with statistical data to select a potential baseline configuration that may be expected to be most promising in satisfying few key constraints (cost, performance...);

— the intermediary design stage with more elaborate analyses in order to compile information on the worst loading cases over the entire operational envelope;

— the detailed design stage in which the proportioning of all structural components is finally made.

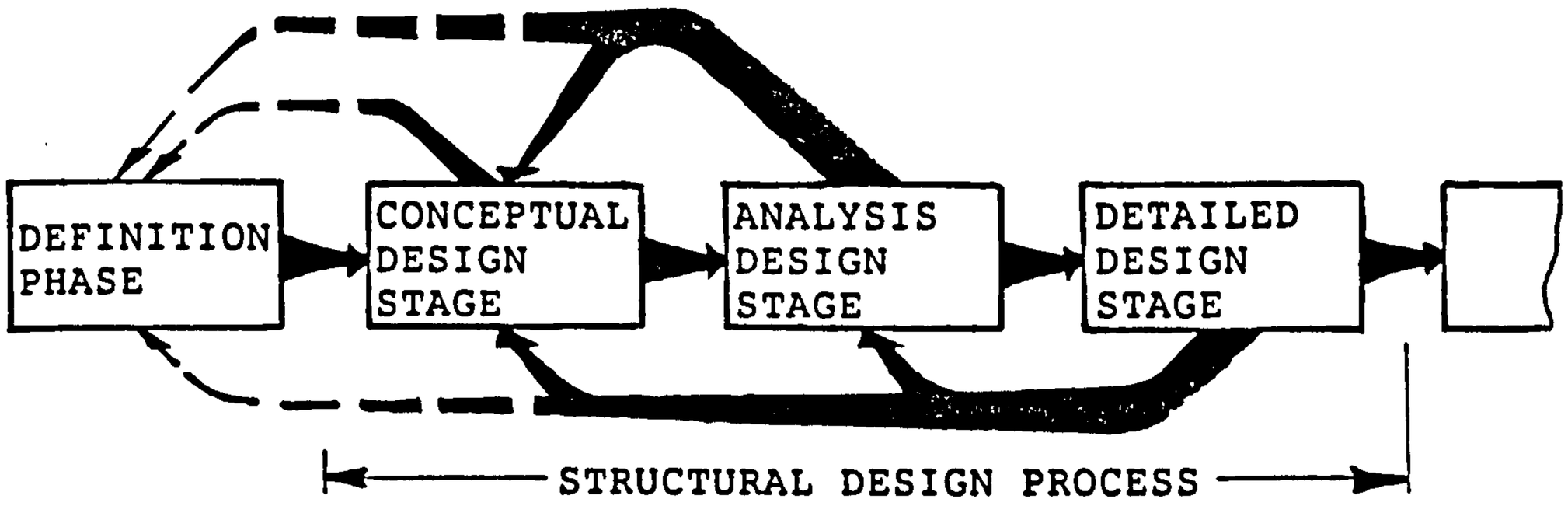

Fig. III.1 Structural design process

Undoubtedly, in an effort to steer the final product to within close bounds of the best solution while maintaining design feasibility and satisfactory levels of safety, "reliability", "affordability", "serviceability", "...bility":

— there will be, within each design stage, localized

synthesis loops to achieve optimum solutions related to each design stage;

— major and minor cycles of redesign will occur as the structural design process is forced to loop around the conceptual-analysis-detailed stages (Fig. III.1).

In most applications, the complexity of the project will partition each design stage level into sub-design stages. For instance, the detailed design stage where the context of this work is located must be subdivided into a convenient series of hierarchically performed design tasks. Such a breakdown is inevitable if this stage is to encompass the multitude and diversified constraints that govern the proportioning of the components, i.e, constraints on stresses, deflections, frequencies, flutter instability, divergence, response to atmospheric turbulences, post-buckling response, crippling, gauges...

A proposed breakdown of the detailed design stage may be as depicted in Fig. III.2 (see the following page) where an overall mass distribution of the structure is made based on some controlling constraints (load-carrying capacity, overall buckling, flutter instability, divergence...) followed by the consideration of secondary constraints (local buckling, crippling, bearing strength, panel flutter, connections...) which set out the structural subcomponent sizes.

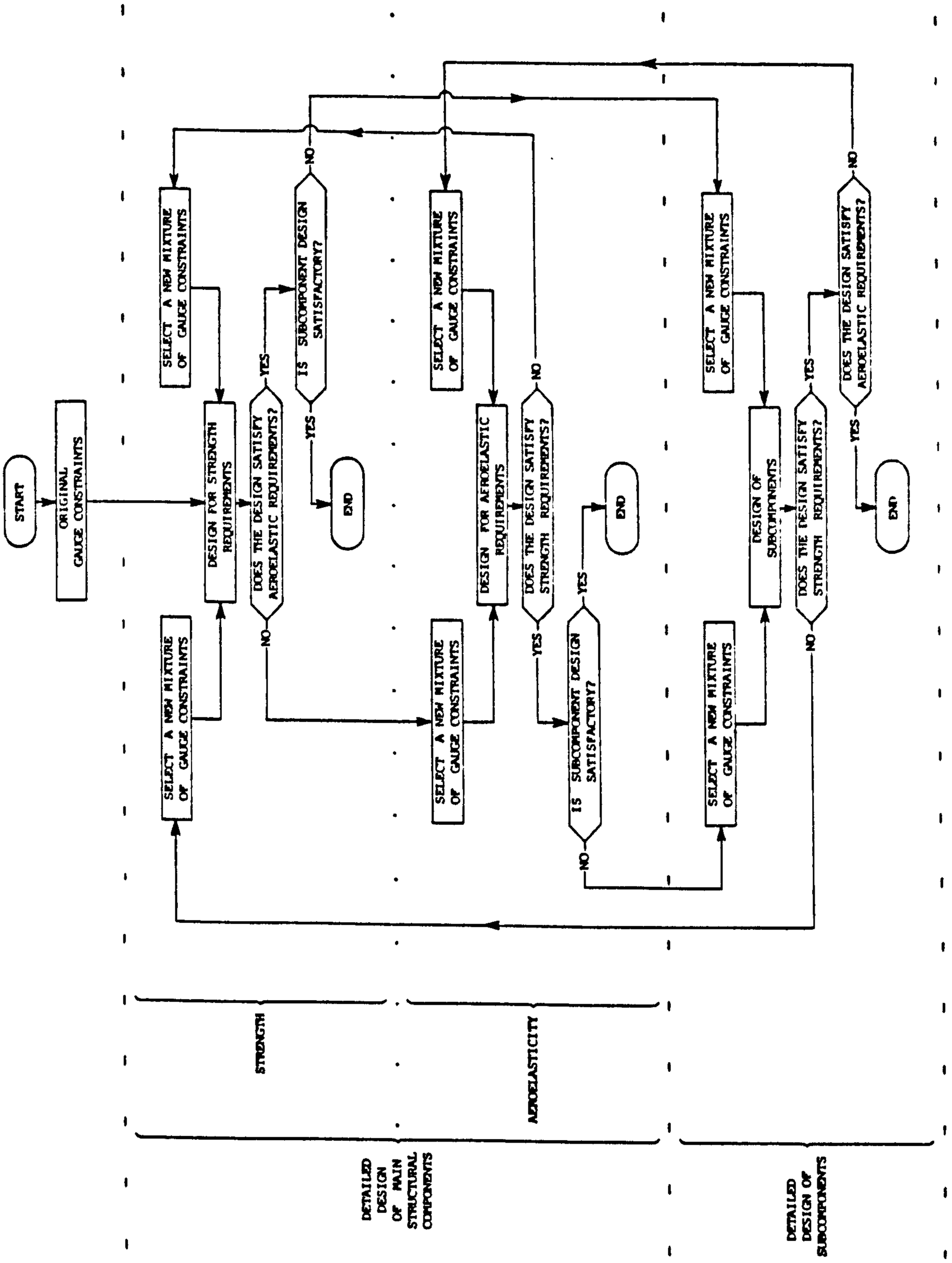

Fig. III.2 Possible breakdown of the detailed design stage

The complexity of the structural design process does not stop here. It may be imperative to decompose the structure into several substructures. It is of course the lifting surfaces which are the substructure concerned herein.

A shortcoming of the afore-described detailed design process is that there is no guarantee of ideal solutions that are assured of meeting the original specifications and fulfill all the preassigned rôles as set in the definition phase. The pronounced sensitivity of aircraft general performances to any increase of weight makes the establishment of designs and the release of drawings on the sole basis of structural optimization no longer sufficient. Concurrent with this, active control systems must be introduced as a means of alleviating loads or suppressing aeroelastic instabilities. They must be included if there are sound economic reasons and if they can improve the aircraft performance when the distribution of structural weight inhibits it.

To attain the ultimate objective of an optimum solution, the philosophy of designing structures must strike a good balance between over-all mass distributions and interacting servo-mechanisms in the form of active controls. However, structural optimization is underlying the approach of this research work and therefore, we will purposely refrain from making any more allusion to aeroservoelasticity, load alleviation or to active flutter suppression.

5.2 Type of design variables

Although the weight of aircraft is sensitive to the material types used in building the structure, we will not commit ourselves to consider material as a design variable because this does not lend itself easily to traditional automated design. Moreover, for convenience (see § IV.2.3), materials will be supposed to be only isotropic even though multilayered filamentary composites offer much broaden latitude than metals in meeting strength and stiffness requirements independently of one another. This eliminates the need to take ply orientation angles and ply thicknesses as design variables.

To simplify the problem even further and on account of what has already been said in § II.5.4, spanwise and chordwise locations for massive items such as engines will not be treated as design variables albeit the decisive part that engine position takes on removing undesirable wing-flutter. Perhaps, the strongest argument in favor of such an omission is that engine locations are fixed at the much earlier stage of conceptual design where the most apposite wing-engine layout in terms of flutter and in terms of other performance indexes (aerodynamics, thrust...) are appreciated.

Hence, we limit ourselves to the simplest case where only the dimensions of the elements composing the structure

are taken as design variables and their modification during the process of optimization is not discrete but continuous.

5.3 Types of constraints

Relatively to structural optimization with strength or displacement constraints, there has been a much more modest effort devoted to minimum-weight design wherein constraints are placed on aeroelastic instabilities. As more thorough investigations are needed in this field, the interest of this research is nested around aeroelasticity rather than strength.

In appendix D, the equation of motion is introduced in lieu of the flutter speed constraint. This behavior equality constraint as shown in the next section (Eq. III.5.4.1) embraces both flutter and divergence. The method as developed is therefore applicable to both aeroelastic instabilities. The word divergence was, nevertheless, omitted from the title of this thesis because we are not considering anisotropic materials that must be included in any relevant work on divergence.

The inequality equations in Eq. III.5.4.1 enforce minimum-gauge dimensions on the structural members and are the second type of constraints considered. Strictly speaking, these minimum-gauge limits incorporate both structural members sized by strength or by practical

manufacturing considerations depending on whichever is the least (see Fig. III.2).

5.4 Mathematical formulation

Taking the mass of the structure as the objective function the structural optimization problem with aeroelastic and gauge constraints can be formulated in mathematical jargon as (see appendix D):

$$\left.\begin{aligned} &\text{minimize} \quad m = m_0 + \sum_{j=1}^{N} m_j x_j \\ &\text{subject to} \quad [F]\{\bar{q}\} = \{0\} \\ &\text{and to} \quad x_j \geq \underline{x}_j \qquad j = 1,\ldots,N \end{aligned}\right\} \quad \text{(III.5.4.1)}$$

with

m total mass of the structure

m_0 mass of fixed structural items

m_j mass per unit length (for bar elements) or per unit area (for quadrilateral or triangular elements) of jth variable element

x_j jth design variable

N number of design variables

$[F]$ flutter matrix

$\{\bar{q}\}$ aeroelastic eigenvector

$\underline{x}_j$ jth minimum gauge constraints; minimum value imposed on jth design variable

CHAPTER IV

PROGRAM APPRAISAL

1 GENERAL LAYOUT

In this section, we present the FORTRAN-based program that has been developed on VAX minicomputers. But, prior to any narrative description, it may be helpful and instructive to visualize, in a block diagram, the general layout of the modules that make up the system for the design optimization of lifting surface structures subjected to flutter constraints.

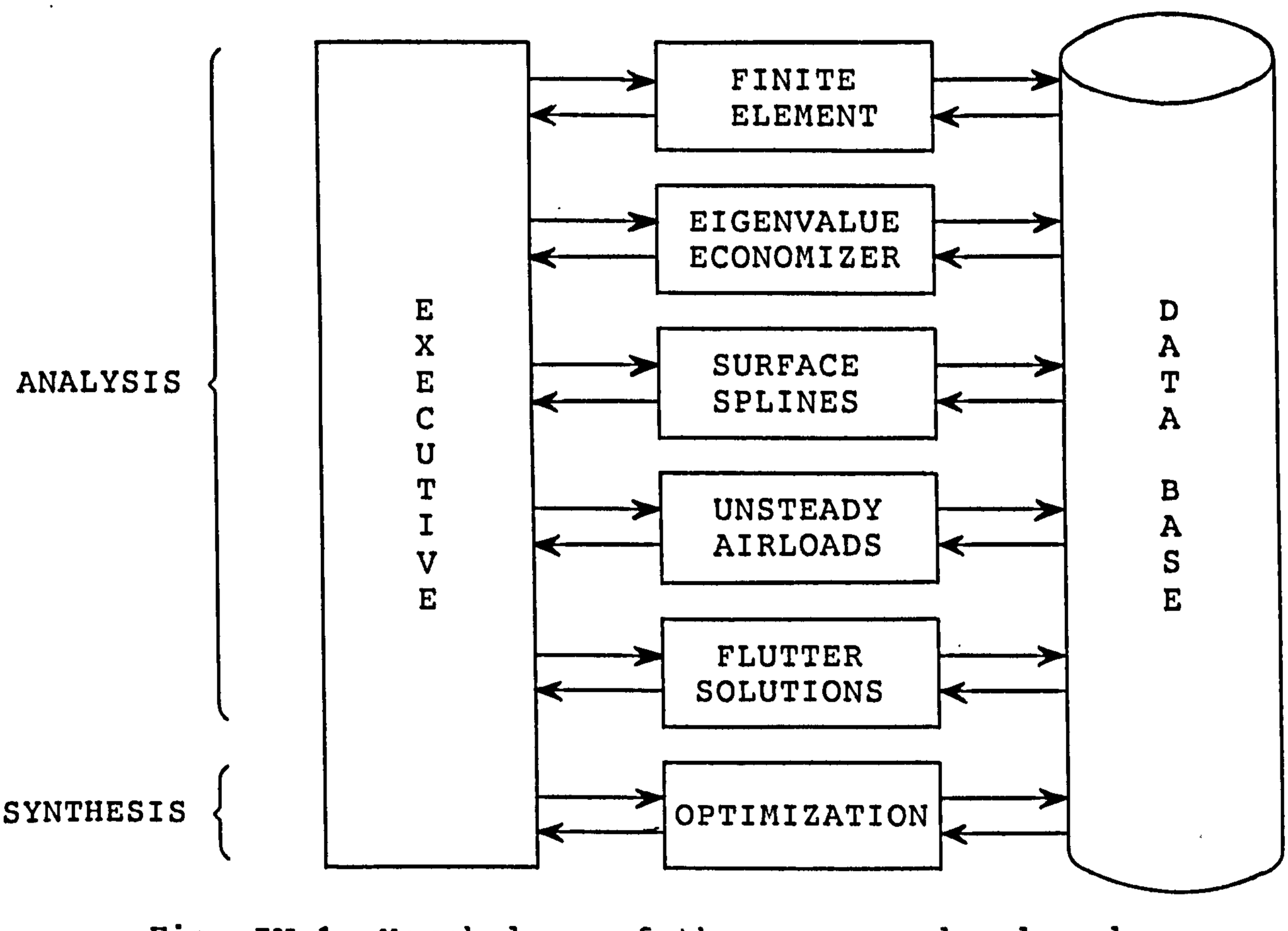

Fig. IV.1 Morphology of the program developed

As highlighted by the above diagram, the program has been fragmented into a chain of modules. This modular organization was found to be crucial for the optimization scheme in the sense that it permits flexibility in scheduling

the succession of analyses to be performed. Moreover, by virtue of this architecture, it would be possible to independently carry out any analyses without having recourse to the whole process.

2 GENERAL DESCRIPTION OF THE MODULES

2.1 Executive

The complexities associated with blending all the modules to perform optimization are hidden from the reader and are greatly simplified and displayed under the "executive" heading. The "executive" can be virtually seen as the block that monitors the order of execution of the analyses and the looping operation where the results of all analyses are used by the optimization algorithm to make rational adjustments to the structure until an optimum design is reached.

2.2 Data transfer

It is clear that, in any kind of program of the character and size described in the previous paragraphs, there is an abundance of data flowing between the numerous routines. Thus, some kind of management is necessary to handle the voluminous amount of data and this must be embedded in the pre- and post-processors of each sub-program with some form of data interface.

Considering that, in our case, there is no simple sequential execution of the analyses, it would be ineffective to directly transfer between the different program segments the large arrays generated. Thus, to keep the merits of a modular designed program, the bulk of data needed to be communicated is exchanged via a common Data Base.

Another, but less sophisticated form of data access, is carried out through various COMMON blocks. The data allocated to these areas is kept to minimal levels and is chiefly for small data items or for variables that control the information between the routines.

2.3 Finite element

FINEL is a general purpose program developed in the Imperial College of Science and Technology, London, which uses the well-known finite element method of analysis to solve certain engineering problems (Ref. 24, 25 and 26). In our context, FINEL is asked to perform only two tasks: first to generate the structural grid and secondly to integrate and assemble the consistent inertia and stiffness matrices.

Although FINEL is less complete and capable than other finite element programs readily available in the Cranfield Institute of technology, it has been selected because privileged access to the source file and not simply to object or execution files is possible. This allowed us to carry out on FINEL alterations, improvements or adaptations to suit our

ends. Nevertheless, this advantage has been counterbalanced by the sparse element library and by the lack of support from the Imperial College of Science and Technology.

A rather restrictive condition on the use of FINEL is that material must be isotropic. It was, nevertheless, judged wiser to guard against departing from the main topic of the work by not rewriting the FINEL code to accept anisotropic materials.

2.4 Eigenvalue economizer

By stating that the displacement field of the fluttering structure may be decomposed into a limited number of mode shapes, the solutions of the free vibration problem are required to serve a dual purpose: first, to find out the unsteady airloads that are functions of the mode shapes and, second, to construe the flutter equation whose solutions is sought by the optimization process.

In an attempt to simplify the expression of the unsteady airloads, it is further assumed that only transverse (out of the plane of the lifting planform) modes of oscillations play a rôle in the flutter mechanism.

The "eigenvalue economizer" subprogram has been written to accommodate four jobs and begins by retrieving from the Data Base the global mass and stiffness matrices already prepared by FINEL. It then reduces these matrices by

automatically discriminating the master degrees of freedom (out-of-plane) from the slave degrees of freedom (inplane). Finally, it culminates by obtaining the solution of the reduced eigenvalue problem and consequently to the reproduction in the Data Base of the transverse mode shapes and their associated natural frequencies.

2.5 Surface splines

This module is responsible, but only at the very first iteration run, for the generation of the points of the two aerodynamic grid and the storing of their coordinates in the Data Base. Those grid points which model the aerodynamic planform do not coincide with the locations of the structural grid nodes despite that structural and aerodynamic analyses are both based upon a finite element approach. The mismatch between structural and aerodynamic grids may be due to various reasons of which one deserve formal mention.

The discretization of the wing structure is essentially an exercise of engineering judgment and experience. Topology, abrupt changes in geometrical and material properties, types of elements chosen to idealize the structure... are matters which are addressed in laying out a structural mesh. On the other hand, only the grading of the aerodynamic mesh from coarse to fine tends to depend on individual judgment and relies on an intuitive trade-off between computational accuracy and computational effort. Putting aside this human intervention, it is the aerodynamic theory that forces the

geometry of the grid to follow a regular pattern even for rather complex vehicles. For instance, the positions of the nodes of the aerodynamic panels are uniquely defined in Dr. Davies' work (Ref. 11 and 12) because they are enforced by analytical equations. This pragmatic procedure of subdividing the lifting surface into aerodynamic finite elements is dictated by convenience: it is to judiciously facilitate the numerical evaluation of certain terms of the unsteady airforces.

As the formulation of the unsteady airloads is, amongst other factors, dependent upon the deformation shape of the lifting surface, the "surface splines" module has provision to generate deflections and slopes of the surface at any aerodynamic grid point. It achieves this by applying splining techniques on the structural mode shapes computed by the previously described routine.

2.6 Unsteady airloads

The aerodynamic loading on the lifting surfaces in unsteady motion is obtained using the program WLST1 from RAE (Farnborough, UK) developed by Dr. Davies who both released the source code and assisted in its implementation. The procedure upon which this code is based uses a development of the lifting surface theory of Multhopp type (Ref. 12).

WLST1 has been programmed in ICL 1900 FORTRAN and this entailed the rewriting of several statements so that it could

be accepted by more modern compilers and run on DEC VAX machines. To gain a higher degree of accuracy, the program has been refined with DOUBLE PRECISION statements. The code was further reformulated by the deletion of the READ/WRITE statements. The passing of data to and from WLST1 is now achieved by means of COMMON blocks or the Data Base depending on the size of storage needed.

The sharp constraint of the fixed dimensioned arrays in WLST1 has been relaxed with the implementation of dynamic dimensioning. This feature has been incorporated in all the subroutines and real and integer vectors or matrices are, when needed, expanded into strings and placed into one single vector array. As far as editing programs is concerned, this is rather laborious and increases the risk of making errors because, in each major routine, pointers must be set to identify the locations of each vector and each matrix in the working array and checks must be made not to exceed the allowable space. Nevertheless, dynamic sizing is worth the effort because it permits the operation of the whole program with minimum core storage requirements and keeps computing costs down.

2.7 Flutter solutions

When all ingredients (inertia and stiffness matrices, natural frequencies and modes of oscillations and unsteady airloads) are made available, what is missing is a tool for setting up and solving the modal flutter equation.

The "flutter solutions" module concludes the repertoire of analysis blocks. Because WLST1 gives unsteady loads for steady-state harmonic motions, the flutter solutions can be obtained in the frequency domain rather than in the time domain. Hence, the rôle of this module is to deduce the aeroelastic stability by using the traditional American method also known as k or V-g method.

2.8 Optimization

As outlined above, the program bulges with a whole range of subprograms which are grouped to cover the analysis aspect. The other aspect, the synthesis side of the program, is represented by one single module that attempts to proceed to the satisfaction of an optimality criterion and hence to achieve the computation of a minimum weight design while not violating the flutter constraint.

3 GENERAL DISCUSSIONS

We have attempted to describe above some salient features of the program developed. We now proceed to show two other major aspects.

Certain members sizes of fixed structural regions can be kept as invariant at user request. The rest of structural components that compose the set of design variables may be reduced by any choice of design variable linking imposed by

fabrication requirements or suggested by heuristic judgment. The linked design variables do not need to have the same size, e.g, different bar elements of the same design variable may have different lengths. This is also allowed for in the assessment of the weight status.

Not represented in the diagram (Fig. IV.1) but still fitting well within the flutter-optimization framework is a module that was written to give the derivative expressions of several quantities relatively to the design variables or to the reduced frequency.

By way of a conclusion to this chapter, we may note that, because of the problems encountered with FINEL and WLST1 and because the work presented herein is not particularly well suited to be performed on mini-computers, there was a restriction in the range of problems that were treated. However, the routines presented in the previous section are relatively well-structured and thoroughly debugged such that subsequent transfer to larger capacity computers should allow the solution of more extensive design problems.

CHAPTER V

ILLUSTRATIVE EXAMPLES

Our current purposes is to implement the program to typical planforms and illustrate, with numerical results, the different techniques applied. Two demonstration problems are used and their physical descriptions along with their finite-element modeling are presented below. Only half of each structure is needed because symmetry can be exploited.

1 RECTANGULAR-PLANFORM WING

As a first simple numerical application, we consider a rectangular-planform wing which was introduced by Rudisill and Bathia (Ref. 42) and has been studied by many other authors. This has an aspect ratio of 7.2, a thickness-to-chord ratio of 8%, and is represented in Fig. V.1. The structural box is divided by ribs into three equal-length bays. In each bay, the cover sheets, spar webs and rib are idealized by quadrilateral in-plane elements and the spar booms by pin-jointed bar elements. The finite-element model of the structure is shown in Fig. V.2 and is assumed to be rigidly fixed at the root. Tables V.1 and V.2 give the generated mesh-coordinates and the element numbering.

2 SWEPT TAILPLANE

This second problem is a more realistic configuration with a leading-edge sweep angle of 25°, a taper ratio of 1.58 and has more structural components and degrees of freedom

than the previous example. Fig. V.3 illustrates the dimensions and the geometry pertinent to grid generation. As above, the basic structural idealization is once again a representation of the spars, ribs and skin covers with quadrilateral elements and the spar booms with bar elements (Fig. V.4). This structure is assumed to be cantilevered and the eight nodes at the tailplane-body intersection are completely fixed. The generated mesh-coordinates and the element topology are tabulated respectively in tables V.3 and V.4

3 OTHER PARAMETERS

Other parameters considered are cited below and taken to be the same for both examples although provision is made in the program so that any other values can be incorporated into the input data stream.

The material constants are that of aluminum:

Young modulus $E = 69000\ MN/m^2$

Poisson's ratio $\nu = 0.3$

material density $\rho = 2816\ kg/m^3$

The first six transverse mode shapes are used for modal analysis to define the generalized flutter equation. The effect of the number of mode shapes on both flutter analysis parameters and optimization parameters is shown in tables V.5 and V.6. There is little discernible differences between the

use of six and much higher numbers of modes of vibration and it appears that higher than six modes cannot be expected to emulate the results appreciably to justify the extra-computational effort.

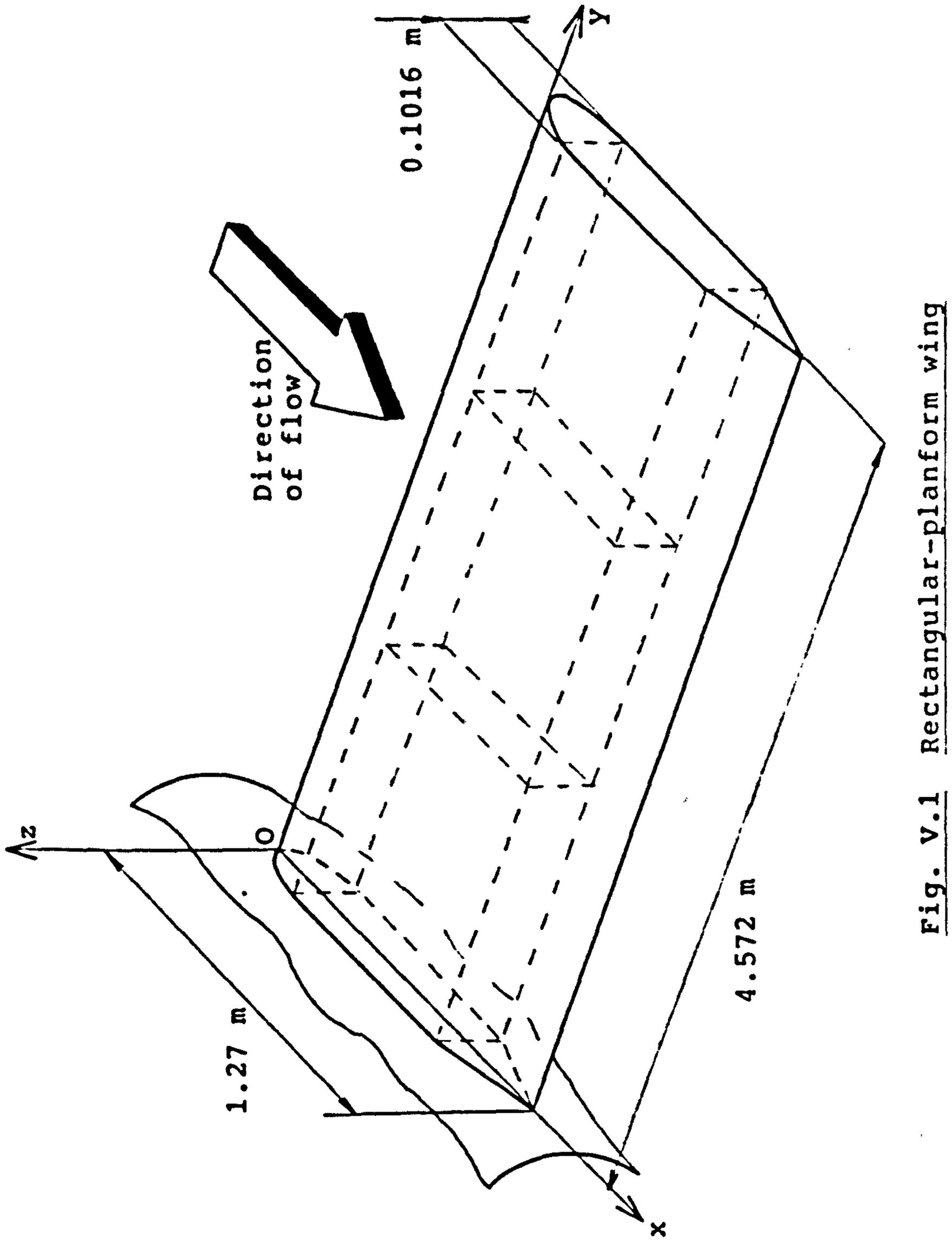

Fig. V.1 Rectangular-planform wing

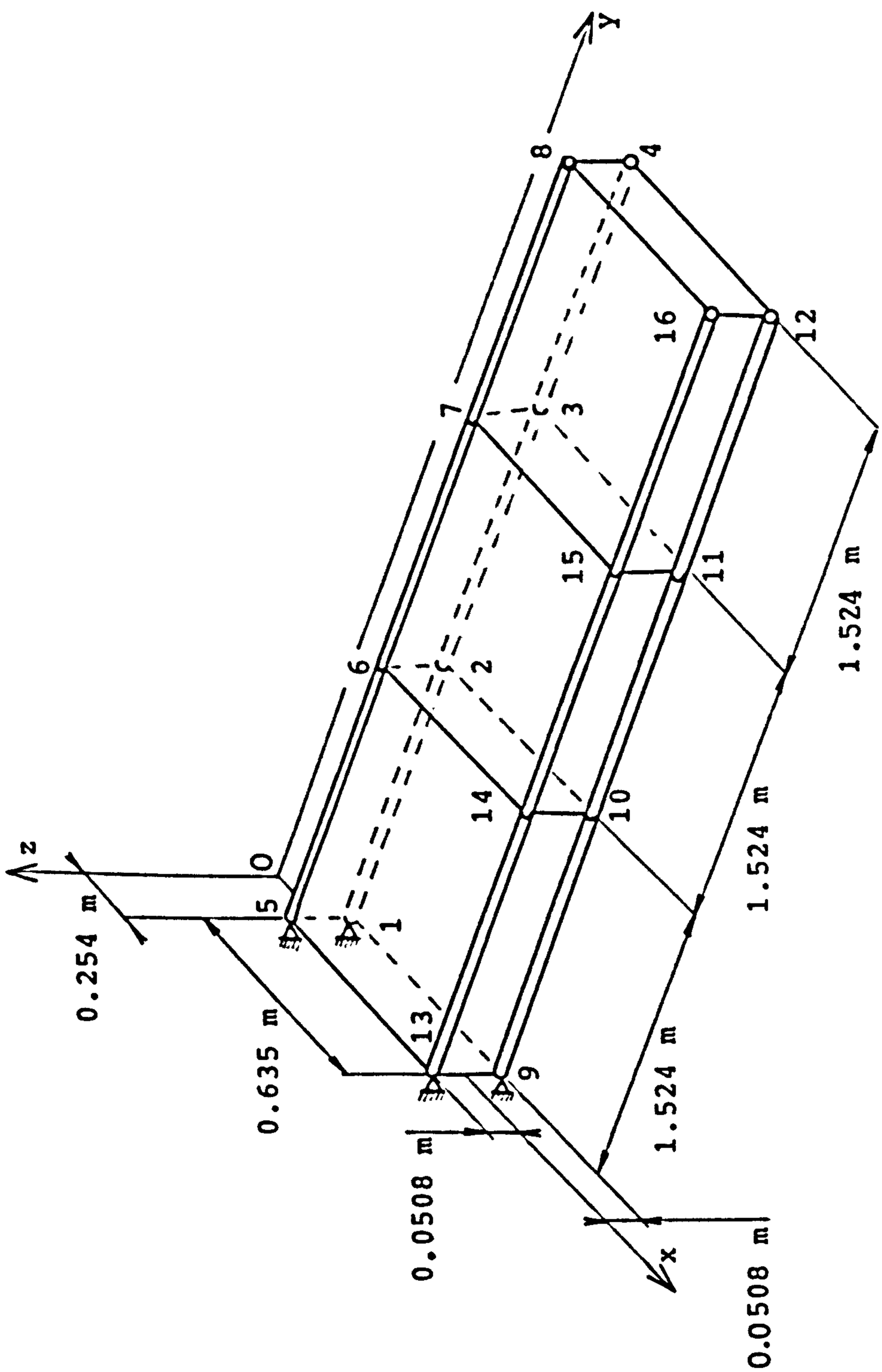

Fig. V.2 Finite-element idealization of rectangular-planform wing

Table V.1 Generated mesh coordinates for rectangular-planform wing

Nodal point	x-coordinate in m	y-coordinate in m	z-coordinate in m
1	0.254	0.000	-0.0508
2	0.254	1.524	-0.0508
3	0.254	3.048	-0.0508
4	0.254	4.572	-0.0508
5	0.254	0.000	0.0508
6	0.254	1.524	0.0508
7	0.254	3.048	0.0508
8	0.254	4.572	0.0508
9	0.889	0.000	-0.0508
10	0.889	1.524	-0.0508
11	0.889	3.048	-0.0508
12	0.889	4.572	-0.0508
13	0.889	0.000	0.0508
14	0.889	1.524	0.0508
15	0.889	3.048	0.0508
16	0.889	4.572	0.0508

Table V.2 Element topology for rectangular-planform wing

Element No	Nodal point				Element type
1	1	2			Pin-jointed bar element
2	2	3			Pin-jointed bar element
3	3	4			Pin-jointed bar element
4	1	2	5	6	Quadrilateral in-plane element
5	2	3	6	7	Quadrilateral in-plane element
6	3	4	7	8	Quadrilateral in-plane element
7	5	6			Pin-jointed bar element
8	6	7			Pin-jointed bar element
9	7	8			Pin-jointed bar element
10	1	2	9	10	Quadrilateral in-plane element
11	2	3	10	11	Quadrilateral in-plane element
12	3	4	11	12	Quadrilateral in-plane element
13	5	6	13	14	Quadrilateral in-plane element
14	6	7	14	15	Quadrilateral in-plane element
15	7	8	15	16	Quadrilateral in-plane element
16	9	10			Pin-jointed bar element
17	10	11			Pin-jointed bar element
18	11	12			Pin-jointed bar element
19	9	10	13	14	Quadrilateral in-plane element
20	10	11	14	15	Quadrilateral in-plane element
21	11	12	15	16	Quadrilateral in-plane element
22	13	14			Pin-jointed bar element
23	14	15			Pin-jointed bar element
24	15	16			Pin-jointed bar element
25	2	6	10	14	Quadrilateral in-plane element
26	3	7	11	15	Quadrilateral in-plane element
27	4	8	12	16	Quadrilateral in-plane element

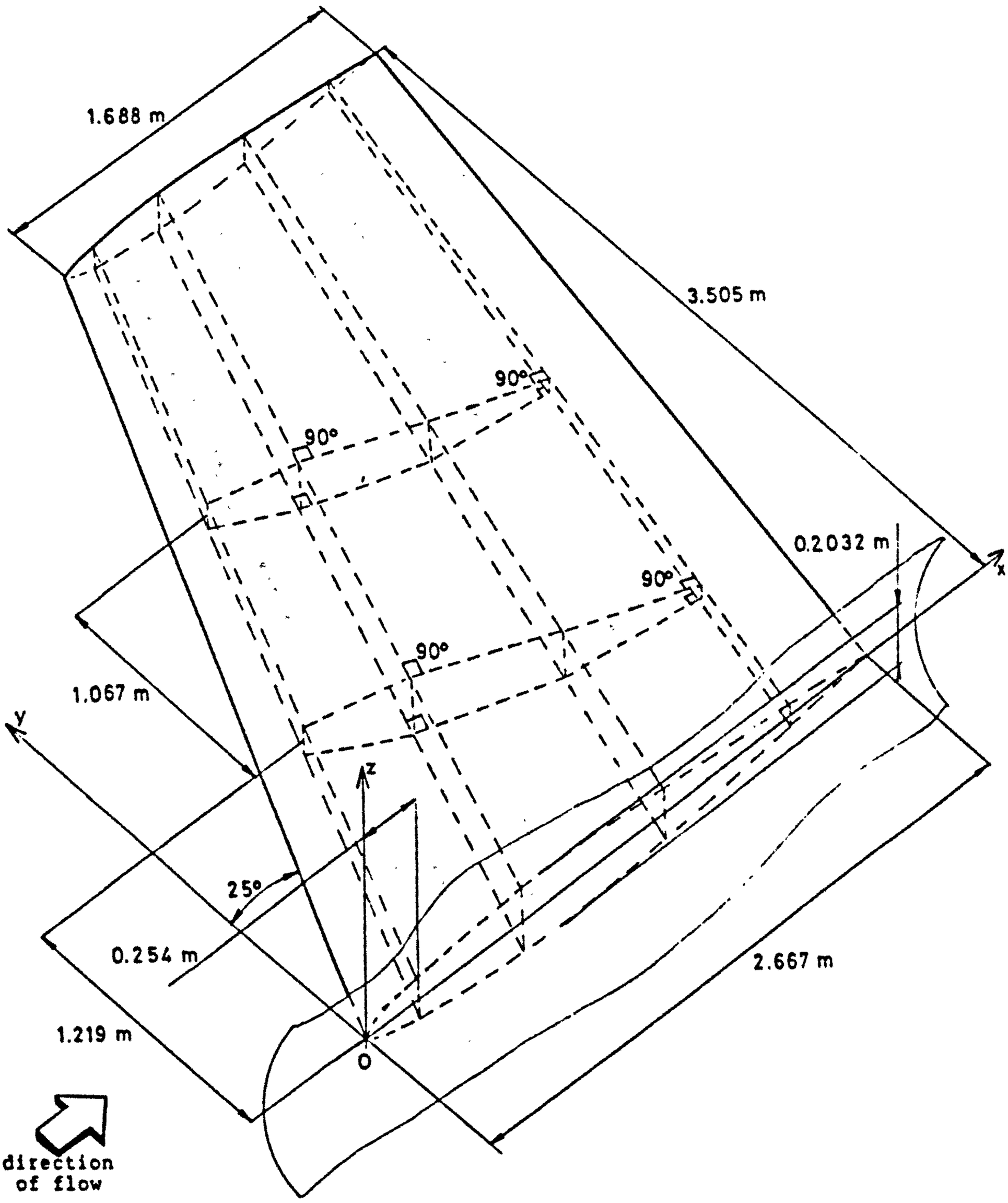

Fig. V.3 Swept tailplane

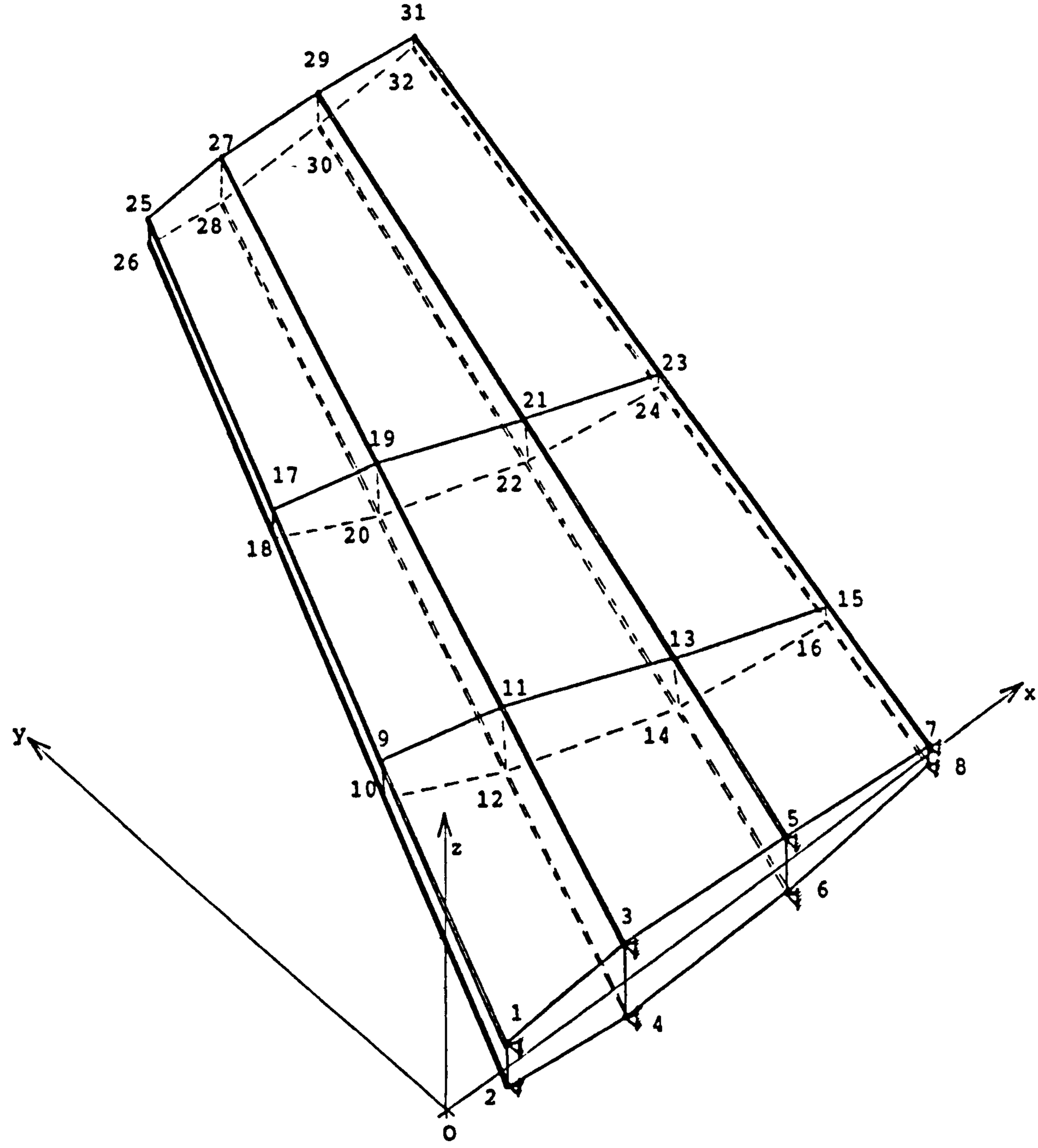

Fig. V.4 Finite-element idealization of swept tailplane

Table V.3 Generated mesh coordinates for swept tailplane

Nodal point	x-coordinate in m	y-coordinate in m	z-coordinate in m
1	0.2540	0.0000	0.1270
2	0.2540	0.0000	-0.1270
3	0.8128	0.0000	0.2032
4	0.8128	0.0000	-0.2032
5	1.5748	0.0000	0.1524
6	1.5748	0.0000	-0.1524
7	2.2606	0.0000	0.0508
8	2.2606	0.0000	-0.0508
9	0.7901	1.2192	0.1108
10	0.7901	1.2192	-0.1108
11	1.2157	1.0570	0.1807
12	1.2157	1.0570	-0.1807
13	1.8235	0.8253	0.1392
14	1.8235	0.8253	-0.1392
15	2.4187	0.6886	0.0471
16	2.4187	0.6886	-0.0471
17	1.2592	2.2860	0.0966
18	1.2592	2.2860	-0.0966
19	1.6302	2.1445	0.1576
20	1.6302	2.1445	-0.1576
21	2.1602	1.9425	0.1214
22	2.1602	1.9425	-0.1214
23	2.6792	1.8234	0.0411
24	2.6792	1.8234	-0.0411
25	1.7953	3.5052	0.0804
26	1.7953	3.5052	-0.0804
27	2.1489	3.5052	0.1286
28	2.1489	3.5052	-0.1286
29	2.6312	3.5052	0.0964
30	2.6312	3.5052	-0.0964
31	3.0653	3.5052	0.0322
32	3.0653	3.5052	-0.0322

Element No	Nodal points				Element type
1	2	1	10	9	Quadrilateral in-plane element
2	4	3	12	11	Quadrilateral in-plane element
3	6	5	14	13	Quadrilateral in-plane element
4	8	7	16	15	Quadrilateral in-plane element
5	1	3	9	11	Quadrilateral in-plane element
6	2	4	10	12	Quadrilateral in-plane element
7	3	5	11	13	Quadrilateral in-plane element
8	4	6	12	14	Quadrilateral in-plane element
9	5	7	13	15	Quadrilateral in-plane element
10	6	8	14	16	Quadrilateral in-plane element
11	1	9			Pin-jointed bar element
12	2	10			Pin-jointed bar element
13	3	11			Pin-jointed bar element
14	4	12			Pin-jointed bar element
15	5	13			Pin-jointed bar element
16	6	14			Pin-jointed bar element
17	7	15			Pin-jointed bar element
18	8	16			Pin-jointed bar element
19	10	9	12	11	Quadrilateral in-plane element
20	12	11	14	13	Quadrilateral in-plane element
21	14	13	16	15	Quadrilateral in-plane element
22	10	9	18	17	Quadrilateral in-plane element
23	12	11	20	19	Quadrilateral in-plane element
24	14	13	22	21	Quadrilateral in-plane element
25	16	15	24	23	Quadrilateral in-plane element
26	9	11	17	19	Quadrilateral in-plane element
27	10	12	18	20	Quadrilateral in-plane element
28	11	13	19	21	Quadrilateral in-plane element
29	12	14	20	22	Quadrilateral in-plane element
30	13	15	21	23	Quadrilateral in-plane element
31	14	16	22	24	Quadrilateral in-plane element
32	9	17			Pin-jointed bar element
33	10	18			Pin-jointed bar element
34	11	19			Pin-jointed bar element
35	12	20			Pin-jointed bar element
36	13	21			Pin-jointed bar element
37	14	22			Pin-jointed bar element
38	15	23			Pin-jointed bar element
39	16	24			Pin-jointed bar element
40	18	17	20	19	Quadrilateral in-plane element
41	20	19	22	21	Quadrilateral in-plane element
42	22	21	24	23	Quadrilateral in-plane element
43	18	17	26	25	Quadrilateral in-plane element
44	20	19	28	27	Quadrilateral in-plane element
45	22	21	30	29	Quadrilateral in-plane element
46	24	23	32	31	Quadrilateral in-plane element
47	17	19	25	27	Quadrilateral in-plane element
48	18	20	26	28	Quadrilateral in-plane element
49	19	21	27	29	Quadrilateral in-plane element
50	20	22	28	30	Quadrilateral in-plane element
51	21	23	29	31	Quadrilateral in-plane element
52	22	24	30	32	Quadrilateral in-plane element
53	17	25			Pin-jointed bar element
54	18	26			Pin-jointed bar element
55	19	27			Pin-jointed bar element
56	20	28			Pin-jointed bar element
57	21	29			Pin-jointed bar element
58	22	30			Pin-jointed bar element
59	23	31			Pin-jointed bar element
60	24	32			Pin-jointed bar element
61	26	25	28	27	Quadrilateral in-plane element
62	28	27	30	29	Quadrilateral in-plane element
63	30	29	32	31	Quadrilateral in-plane element

Table V.4 Element topology for swept tailplane

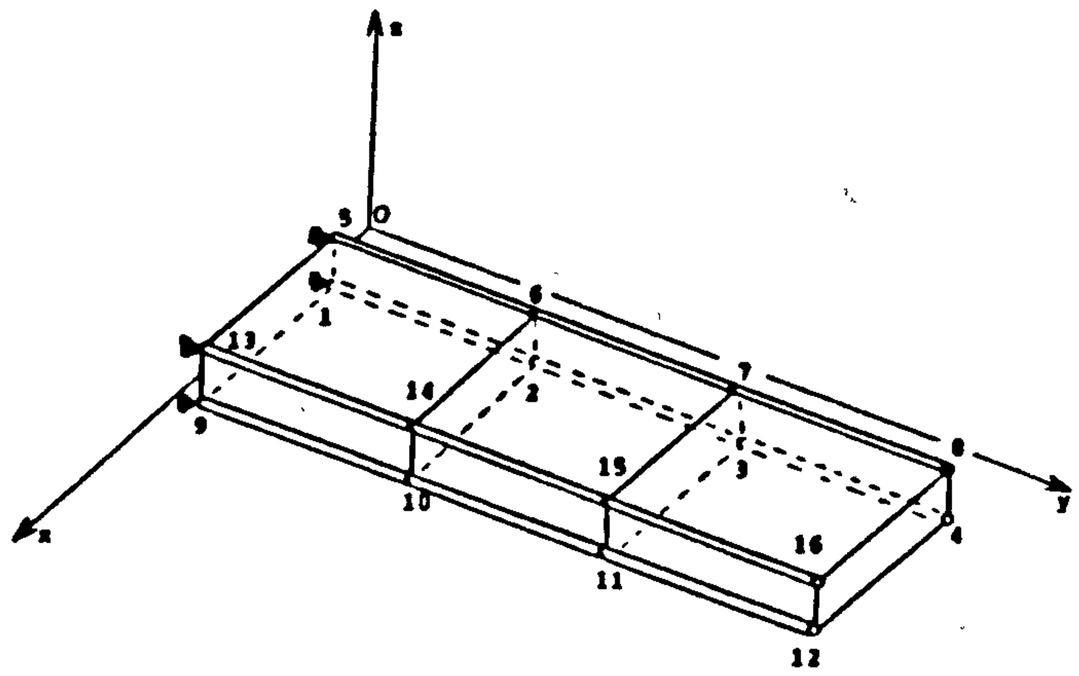

Rectangular-planform wing

Element No.	Element dimensions
1, 2, 3, 7, 8, 9, 16, 17, 18, 22, 23 and 24	0.3225×10^{-3} m^2
4, 6, 19 and 21	0.508×10^{-3} m
5 and 20	1.409×10^{-3} m
10, 11, 12, 13, 14, 15, 25, 26 and 27	0.254×10^{-3} m

Altitude: 1372 m

Flight speed: 213.36 m/s

2nd flutter mode

	Number of mode shapes used: 2	4	6	12
Reduced frequency	0.6517	0.6438	0.6437	0.6437
Circular frequency	109.5 rad/s	108.2 rad/s	108.1 rad/s	108.1 rad/s
Artificial damping	-0.1951	-0.1981	-0.1986	-0.1987
Real part of aeroelastic eigenvector (real part of generalized coordinates)	0.9885	0.9888	0.9888	0.9888
	-0.5399×10^{-1}	-0.5495×10^{-1}	-0.5498×10^{-1}	-0.5499×10^{-1}
		-0.2064×10^{-1}	-0.2063×10^{-1}	-0.2064×10^{-1}
		-0.2422×10^{-3}	-0.1861×10^{-3}	-0.1812×10^{-3}
			0.2222×10^{-3}	0.2231×10^{-3}
			-0.1493×10^{-3}	-0.1503×10^{-3}
				⋮
Imaginary part of aeroelastic eigenvector (imaginary part of generalized coordinates)	0.0000	0.0000	0.0000	0.0000
	0.1411	0.1363	0.1364	0.1364
		0.1146×10^{-1}	0.1159×10^{-1}	0.1161×10^{-1}
		0.9796×10^{-2}	0.9856×10^{-2}	0.9864×10^{-2}
			-0.1191×10^{-2}	-0.1193×10^{-2}
			-0.3794×10^{-3}	-0.3810×10^{-3}
				⋮
Real part of aeroelastic adjoint eigenvector (real part of Lagrange multipliers)	-0.4614	-0.4680	-0.4678	-0.4678
	0.7260	0.7190	0.7191	0.7191
		0.9025×10^{-2}	0.8976×10^{-2}	0.8977×10^{-2}
		0.3508×10^{-1}	0.3537×10^{-1}	0.3540×10^{-1}
			-0.5287×10^{-3}	-0.5305×10^{-3}
			-0.2541×10^{-2}	-0.2547×10^{-2}
				⋮
Imaginary part of aeroelastic adjoint eigenvector (imaginary part of Lagrange multipliers, but with opposite signs)	0.5100	0.5124	0.5124	0.5124
	0.0000	0.0000	0.0000	0.0000
		-0.1075×10^{-1}	-0.1082×10^{-1}	-0.1083×10^{-1}
		0.7701×10^{-2}	0.7453×10^{-2}	0.7452×10^{-2}
			0.6874×10^{-3}	0.6887×10^{-3}
			0.4786×10^{-3}	0.4782×10^{-3}
				⋮

Table V.5 Variations of aeroelastic and optimization parameters with the number of mode shapes used (rectangular-planform wing)

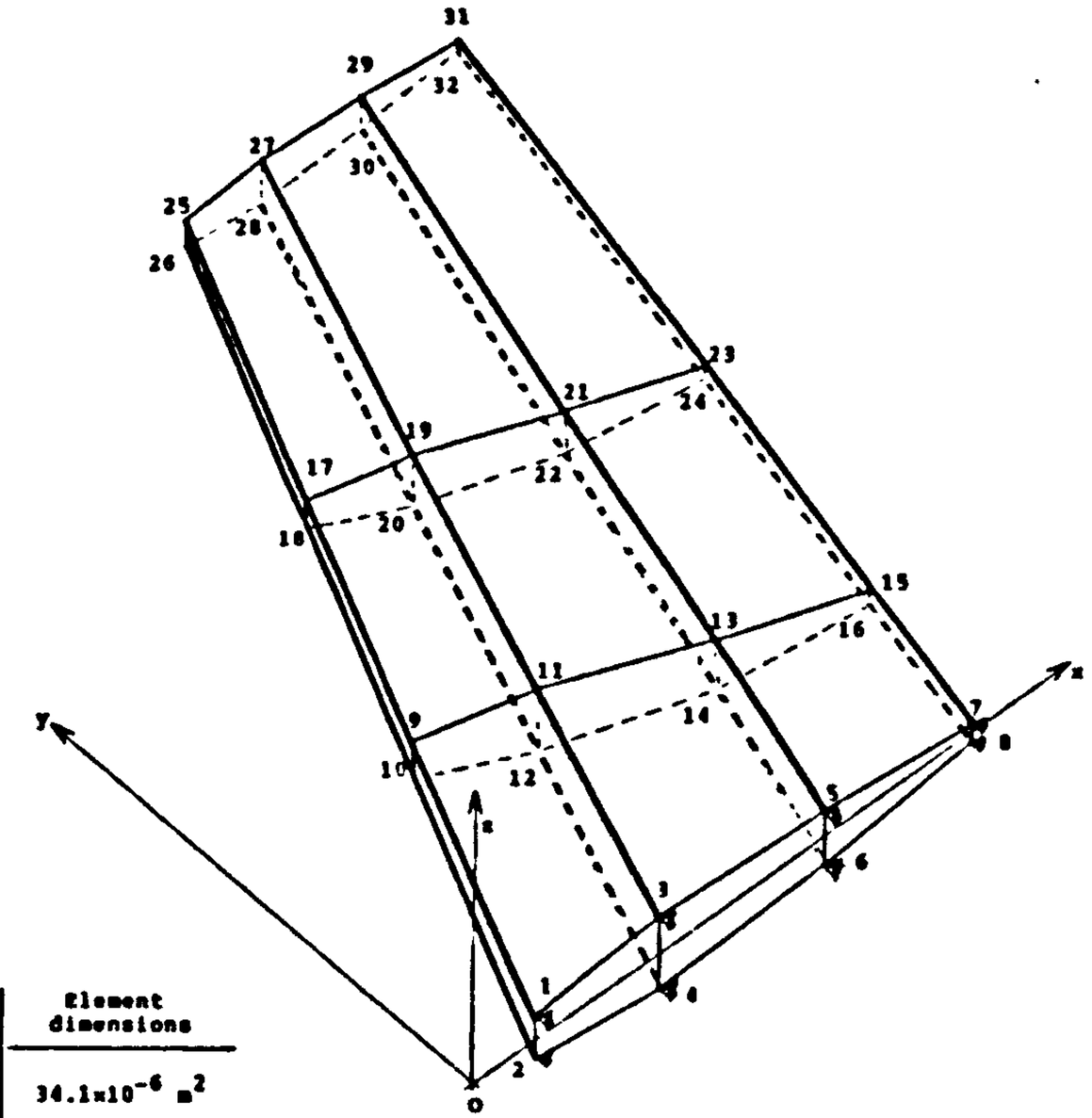

Swept tailplane

Element No.	Element dimensions
11, 12, 13, 14, 15, 16, 17 and 18	34.1×10^{-6} m^2
32, 33, 34, 35, 36, 37, 38 and 39	25.4×10^{-6} m^2
53, 54, 55, 56, 57, 58, 59 and 60	25.9×10^{-6} m^2
1, 2, 3, and 4	0.9×10^{-3} m
5, 6, 7, 8, 9, 10, 26, 27, 28, 29, 30, 31, 40, 41, 42, 43, 44, 45, 46, 47, 48, 49, 50, 51, 52, 61, 62 and 63	0.7×10^{-3} m
19, 20, 21, 22, 23, 24 and 25	0.8×10^{-3} m

Altitude: 3000 m

Flight speed: 243.84 m/s

1st flutter mode

	Number of mode shapes used: 3	4	6	20
Reduced frequency	2.231	2.228	2.230	2.228
Circular frequency	203.9 rad/s	203.7 rad/s	203.9 rad/s	203.7 rad/s
Artificial damping	-0.8318	-0.8355	-0.8378	-0.8361
Real part of aeroelastic eigenvector (real part of generalized coordinates)	0.9982 -0.3855×10^{-1} -0.1083×10^{-1}	0.9881 -0.3910×10^{-1} -0.1102×10^{-1} -0.4165×10^{-2}	0.9881 -0.3928×10^{-1} -0.1099×10^{-1} -0.4177×10^{-2} 0.1473×10^{-2} 0.5007×10^{-3}	0.9881 -0.3904×10^{-1} -0.1099×10^{-1} -0.4170×10^{-2} 0.1475×10^{-2} 0.4972×10^{-3} ⋮
Imaginary part of aeroelastic eigenvector (imaginary part of generalized coordinates)	0.0000 -0.4188×10^{-1} 0.1651×10^{-1}	0.0000 -0.4234×10^{-1} 0.1672×10^{-1} 0.1019×10^{-2}	0.0000 -0.4215×10^{-1} 0.1680×10^{-1} 0.1057×10^{-2} -0.3623×10^{-3} 0.3177×10^{-3}	0.0000 -0.4234×10^{-1} 0.1679×10^{-1} 0.1042×10^{-2} -0.3608×10^{-3} 0.3058×10^{-3} ⋮
Real part of aeroelastic adjoint eigenvector (real part of Lagrange multipliers)	0.9723 0.4302×10^{-1} -0.2284×10^{-1}	0.9719 0.4192×10^{-1} -0.2320×10^{-1} -0.1409×10^{-1}	0.9718 0.4225×10^{-1} -0.2327×10^{-1} -0.1421×10^{-1} -0.6023×10^{-3} -0.5118×10^{-2}	0.9716 0.4213×10^{-1} -0.2331×10^{-1} -0.1431×10^{-1} -0.6186×10^{-3} -0.5159×10^{-2} ⋮
Imaginary part of aeroelastic adjoint eigenvector (imaginary part of Lagrange multipliers, but with opposite signs)	0.0000 0.2283 0.8304×10^{-2}	0.0000 0.2297 0.7988×10^{-2} 0.5149×10^{-2}	0.0000 0.2301 0.8062×10^{-2} 0.5260×10^{-2} -0.2171×10^{-2} -0.5049×10^{-2}	0.0000 0.2307 0.8138×10^{-2} 0.5311×10^{-2} -0.2152×10^{-2} -0.5084×10^{-2} ⋮

Table V.6 Variations of aeroelastic and optimization parameters with the number of mode shapes used (swept tailplane)

CHAPTER VI

EIGENVALUE ECONOMIZER

It may be assumed that flutter of aircraft lifting planforms predominantly involves deflections normal to the surface. This is a rather drastic but nevertheless useful simplification that makes the evaluation of the already complex unsteady airloads somewhat more approachable. Owing to the fact that airfoil sections are much stiffer in the chordwise direction, this assumption may be quite apposite.

There is a growing interest for the extension of unsteady theory to include in-plane oscillations. This interest seems to be aroused much more for the exploration of rotary-wing flutter rather than fixed wing flutter (Ref. 27, 28 and 29). The motion of a helicopter blade cannot be conveniently regarded as consisting of only transverse (out of the plane of rotation) modes of oscillations and lead-lag (in the plane of rotation) oscillations are not to be ignored.

1 CONDENSATION OF THE EIGENVALUE PROBLEM

In the course of setting up the flutter equation (appendix A), modalization or modal analysis is desirable for economical solutions of this complex eigenvalue equation. This in turn requires performing a dynamic analysis on the structure.

The truncation of the degrees of freedom of the flutter problem to produce fewer freedoms suggests implementing the

"eigenvalue economizer" technique. This technique, sometimes referred to as dynamic condensation, retains only a small number of the nodal displacements called masters which, for our purposes, are the transverse degrees of freedom in the z-direction. By convention, the flow is in the positive x-direction of the Cartesian coordinate system, the y-axis is along the wing (or lifting surface) and the z-axis is out of the wing plane (see Fig. V.1, V.2, V.3 and V.4). The remaining inplane degrees of freedom (in the x- and y-directions) are called slaves and are removed by condensing the mass and stiffness matrices.

The original eigenvalue problem,

$$\left[[K] - \left(\omega_N\right)^2 [M] \right] \{\zeta\} = \{0\} \qquad \text{(VI.1.1)}$$

when partitioned would take the form

$$\left[\left[\begin{array}{c|c} [K_{mm}] & [K_{ms}] \\ \hline [K_{sm}] & [K_{ss}] \end{array} \right] - \left(\omega_N\right)^2 \left[\begin{array}{c|c} [M_{mm}] & [M_{ms}] \\ \hline [M_{sm}] & [M_{ss}] \end{array} \right] \right] \left\{ \begin{array}{c} \{\zeta\}_m \\ \hline \{\zeta\}_s \end{array} \right\} = \{0\} \qquad \text{(VI.1.2)}$$

[K] stiffness matrix

[M] mass or inertia matrix

$\left(\omega_N\right)^2$ eigenvalue

ω_N circular natural frequency

$\{\zeta\}$ mode shape

$\{\zeta\}_m$, $\{\zeta\}_s$ respectively master and slave mode shapes

After the appropriate transformation (Eq. A.7 and A.9), one can derive the reduced stiffness and mass matrices as complex combinations of stiffness and mass matrices

$$\left[K_r \right] = \left[K_{mm} \right] - \left[K_{ms} \right]\left[K_{ss} \right]^{-1}\left[K_{sm} \right] \qquad \text{(VI.1.3)}$$

$$\begin{aligned}\left[M_r \right] = \left[M_{mm} \right] &- \left[M_{ms} \right]\left[K_{ss} \right]^{-1}\left[K_{sm} \right] \\ &- \left[K_{ms} \right]\left[K_{ss} \right]^{-1}\left[M_{sm} \right] \\ &+ \left[K_{ms} \right]\left[K_{ss} \right]^{-1}\left[M_{ss} \right]\left[K_{ss} \right]^{-1}\left[K_{sm} \right]\end{aligned} \qquad \text{(VI.1.4)}$$

$\left[K_r \right]$, $\left[M_r \right]$ reduced stiffness and reduced mass matrices

The condensed eigenvalue system can now be stated as

$$\left[\left[K_r \right] - \left(\omega_N\right)^2\left[M_r \right]\right]\{\zeta\}_m = \{0\} \qquad \text{(VI.1.5)}$$

2 RESULTS

The quadrilateral and bar elements used to model the two types of structures considered permits three transational degrees of freedom at each node. With the root nodes fixed, the total number of degrees of freedom is 36 for the rectangular-planform wing and 72 for the swept tailplane which are then condensed to respectively 12 and 24 degrees of freedom normal to the planforms.

The results of the condensed eigenvalue problem for both structural examples are compared with that of the full eigenvalue problem. A perusal of table VI.1 through to table VI.8 highlights the good agreement between the results of the two eigenvalue problems for at least the first six master modes which is adequate for flutter work (see § V.3). The reduced eigenvalue problem generates spurious modes and frequencies but only for much higher modes. Tables VI.1 and VI.5 show also that the lowest mode shapes of typical aircraft lifting surfaces are dominated by transverse modes of vibration.

Comparison of computer times needed to get the mode shapes with subspace iteration and with eigenvalue economizer show that, if six natural vibration modes are required, the CPU time is nearly as much as sixteen times higher for subspace iteration:

— the CPU time of the subspace iteration method applied to the non-reduced problem, when six modes are required but twelve are computed to achieve good convergence and reasonable accuracy on the first six, is one minute and fifty five seconds;

— the CPU time of the eigenvalue economizer technique is just seven seconds for twelve computed natural modes.

The above CPU times are those required by a DEC VAX 11/750 for the "rectangular-planform wing" example.

The CPU time ratio of sixteen is not surprising because the time needed to solve an eigenvalue problem of size N is usually approximately proportional to N^3. Moreover, the ratio of CPU times should in actual fact be higher than sixteen. This is because of two reasons:

— amongst the lowest selected modes, few modes will be inplane modes and as such do not contribute in the formulation of the unsteady aerodynamic coefficients;

— for very large and detailed finite element models of realistic structures, subspace iteration method would be applied to the "master-and-slaves" condensed problem also.

It is worth noting that another advantage of reducing the problem through eigenvalue condensation is that the space necessary for storing frequencies and associated eigenvectors is three times less than for the original full problem.

Table VI.1 Natural frequencies of the rectangular-planform wing

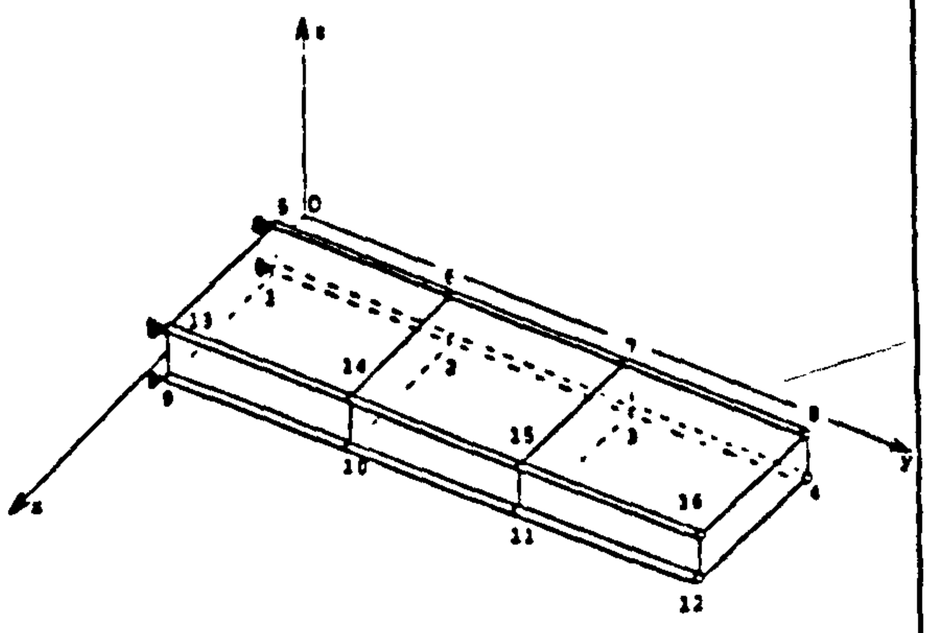

Rectangular-planform wing

Element No.	Element dimensions
1, 2, 3, 7, 8, 9, 16, 17, 18, 22, 23 and 24	1.290×10^{-3} m^2
4, 5, 6, 19, 20 and 21	2.032×10^{-3} m
10, 11, 12, 13, 14, 15, 25, 26 and 27	1.016×10^{-3} m

Mode	Frequency in Hz	
	Full problem	Eigenvalue economizer
1	10.78	10.78
2	28.67	28.67
3	37.00	*
4	69.20	69.20
5	104.2	104.2
6	165.9	*
7	190.5	190.5
8	222.9	223.0
9	273.4	
10	378.0	
11	791.7	685.9
12	855.7	
13	889.8	
14	1093.	
15	1159.	
16	1233.	
17	1244.	
18	1296.	
19	1347.	
20	1413.	
21	1600.	
22	1606.	
23	1634.	
24	1775.	
25	2423.	
26	2571.	
27	2700.	
28	2833.	
29	2905.	3083.
30	3137.	3580.
31	4305.	4257.
32	4430.	
33	4451.	
34	4500.	4588.
35	4652.	4698.
36	4817.	

* Predominantly in-plane modes

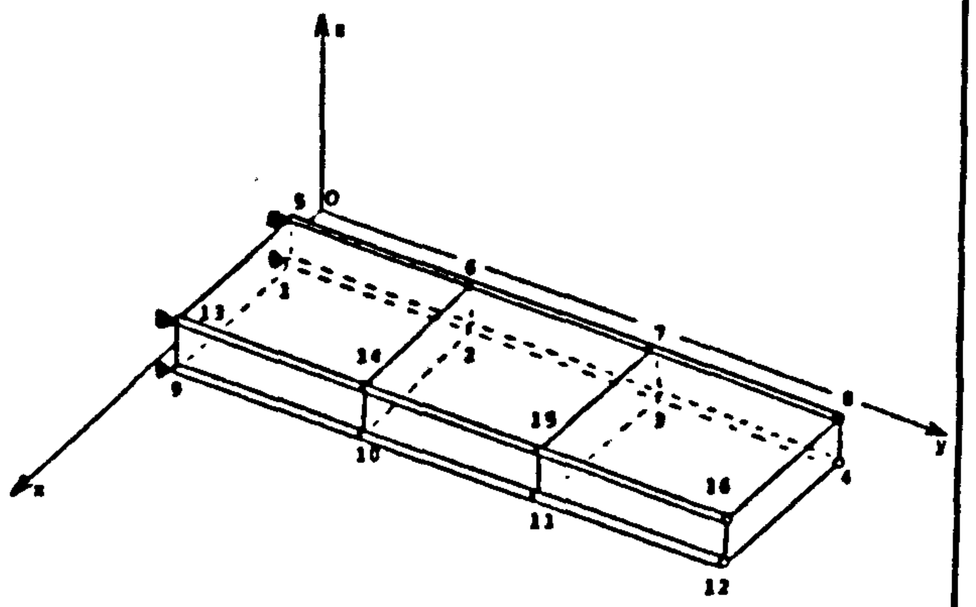

Rectangular-planform wing

Element No.	Element dimensions
1, 2, 3, 7, 8, 9, 16, 17, 18, 22, 23 and 24	1.290×10^{-3} m^2
4, 5, 6, 19, 20 and 21	2.032×10^{-3} m
10, 11, 12, 13, 14, 15, 25, 26 and 27	1.016×10^{-3} m

Nodal point	Full 1st mode shape, displacement in x-direction	displacement in y-direction	displacement in z-direction	1st master mode shape, displacement in z-direction
1	0.0000	0.0000	0.0000	0.0000
2	0.1072×10^{-3}	0.2044×10^{-2}	0.3538×10^{-1}	-0.3538×10^{-1}
3	0.2101×10^{-4}	0.2986×10^{-2}	0.1147	-0.1147
4	0.6629×10^{-5}	0.3204×10^{-2}	0.2093	-0.2093
5	0.0000	0.0000	0.0000	0.0000
6	-0.1070×10^{-3}	-0.2044×10^{-2}	0.3538×10^{-1}	-0.3538×10^{-1}
7	-0.2179×10^{-4}	-0.2985×10^{-2}	0.1147	-0.1147
8	-0.6990×10^{-5}	-0.3204×10^{-2}	0.2093	-0.2093
9	0.0000	0.0000	0.0000	0.0000
10	-0.1072×10^{-3}	0.2044×10^{-2}	0.3538×10^{-1}	-0.3538×10^{-1}
11	-0.2085×10^{-4}	0.2986×10^{-2}	0.1147	-0.1147
12	-0.6697×10^{-5}	0.3204×10^{-2}	0.2093	-0.2093
13	0.0000	0.0000	0.0000	0.0000
14	0.1069×10^{-3}	-0.2044×10^{-2}	0.3538×10^{-1}	-0.3538×10^{-1}
15	0.2175×10^{-4}	-0.2986×10^{-2}	0.1147	-0.1147
16	0.6849×10^{-5}	-0.3204×10^{-2}	0.2093	-0.2093

Table VI.2 Comparison of 1st full and 1st master mode shapes (1st bending mode)

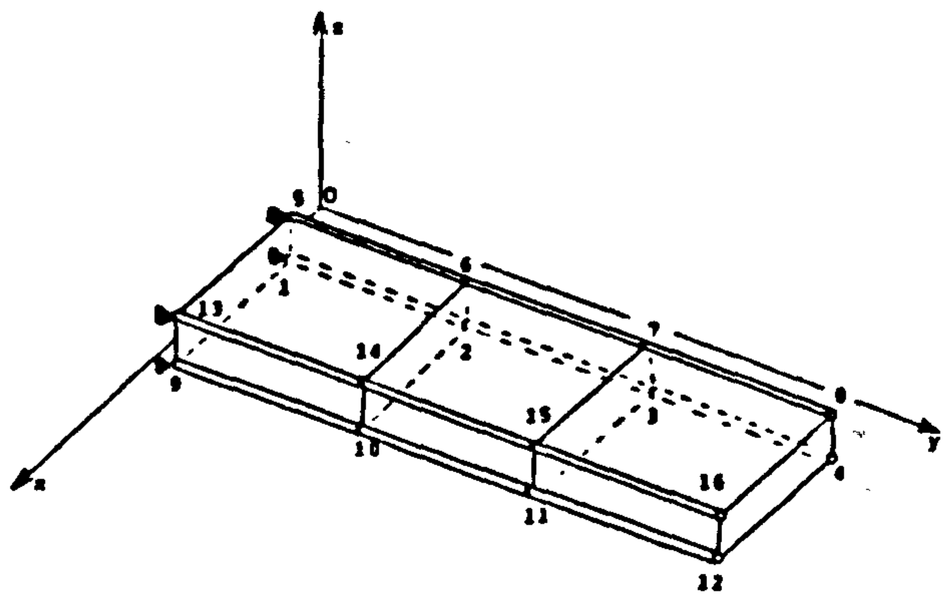

Rectangular-planform wing

Element No.	Element dimensions
1, 2, 3, 7, 8, 9, 16, 17, 18, 22, 23 and 24	1.298×10^{-3} m^2
4, 5, 6, 19, 20 and 21	2.032×10^{-3} m
10, 11, 12, 13, 14, 15, 25, 26 and 27	1.016×10^{-3} m

Nodal point	Full 8th mode shape, displacement in x-direction	Full 8th mode shape, displacement in y-direction	Full 8th mode shape, displacement in z-direction	6th master mode shape, displacement in z-direction
1	0.0000	0.0000	0.0000	0.0000
2	0.2586×10^{-1}	0.3894×10^{-2}	-0.1731	-0.1733
3	-0.2964×10^{-1}	0.1634×10^{-2}	0.2143	0.2143
4	0.2999×10^{-1}	-0.1687×10^{-1}	-0.2048	-0.2048
5	0.0000	0.0000	0.0000	0.0000
6	-0.2591×10^{-1}	-0.3892×10^{-2}	-0.1732	-0.1733
7	0.2964×10^{-1}	-0.1638×10^{-2}	0.2142	0.2143
8	-0.2998×10^{-1}	0.1687×10^{-1}	-0.2048	-0.2048
9	0.0000	0.0000	0.0000	0.0000
10	0.2590×10^{-1}	-0.3897×10^{-2}	0.1731	0.1733
11	-0.2963×10^{-1}	-0.1636×10^{-2}	-0.2142	-0.2143
12	0.2998×10^{-1}	0.1688×10^{-1}	0.2048	0.2048
13	0.0000	0.0000	0.0000	0.0000
14	-0.2586×10^{-1}	0.3896×10^{-2}	0.1733	0.1733
15	0.2965×10^{-1}	0.1636×10^{-2}	-0.2142	-0.2143
16	-0.2999×10^{-1}	-0.1687×10^{-1}	0.2047	0.2048

Table VI.3 comparison of 8th full and 6th master mode shapes (3rd torsion mode)

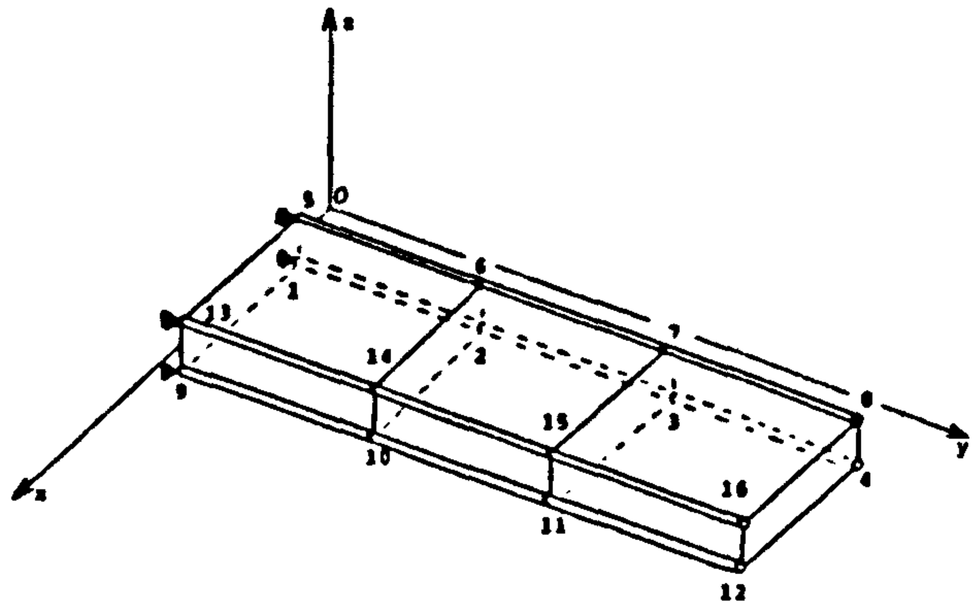

Rectangular-planform wing

Element No.	Element dimensions
1, 2, 3, 7, 8, 9, 16, 17, 18, 22, 23 and 24	1.290×10^{-3} m^2
4, 5, 6, 19, 20 and 21	2.032×10^{-3} m
10, 11, 12, 13, 14, 15, 25, 26 and 27	1.016×10^{-3} m

Nodal point	Full 11th mode shape, displacement in x-direction	displacement in y-direction	displacement in z-direction	7th master mode shape, displacement in z-direction
1	0.0000	0.0000	0.0000	0.0000
2	0.5786×10^{-2}	0.9017×10^{-1}	0.1058×10^{-2}	0.3599×10^{-1}
3	0.3363×10^{-1}	0.1373	0.1328×10^{-3}	0.5702×10^{-2}
4	-0.8921×10^{-1}	0.1452	-0.1572×10^{-3}	0.2950×10^{-2}
5	0.0000	0.0000	0.0000	0.0000
6	0.5787×10^{-2}	0.9027×10^{-1}	-0.1047×10^{-2}	-0.3599×10^{-1}
7	0.3362×10^{-1}	0.1373	-0.1417×10^{-3}	-0.5702×10^{-2}
8	-0.8918×10^{-1}	0.1451	0.1565×10^{-3}	-0.2950×10^{-2}
9	0.0000	0.0000	0.0000	0.0000
10	0.5722×10^{-2}	-0.9025×10^{-1}	-0.8553×10^{-3}	-0.3599×10^{-1}
11	0.3360×10^{-1}	-0.1373	-0.2215×10^{-3}	-0.5702×10^{-2}
12	-0.8920×10^{-1}	-0.1451	-0.1830×10^{-3}	-0.2950×10^{-2}
13	0.0000	0.0000	0.0000	0.0000
14	0.5726×10^{-2}	-0.9015×10^{-1}	0.8689×10^{-3}	0.3599×10^{-1}
15	0.3359×10^{-1}	-0.1373	0.2131×10^{-3}	0.5702×10^{-2}
16	-0.8918×10^{-1}	-0.1452	0.1945×10^{-3}	0.2950×10^{-2}

Table VI.4 Comparison of 11th full and 7th master mode shapes

Table VI.5 Natural frequencies of swept tailplane

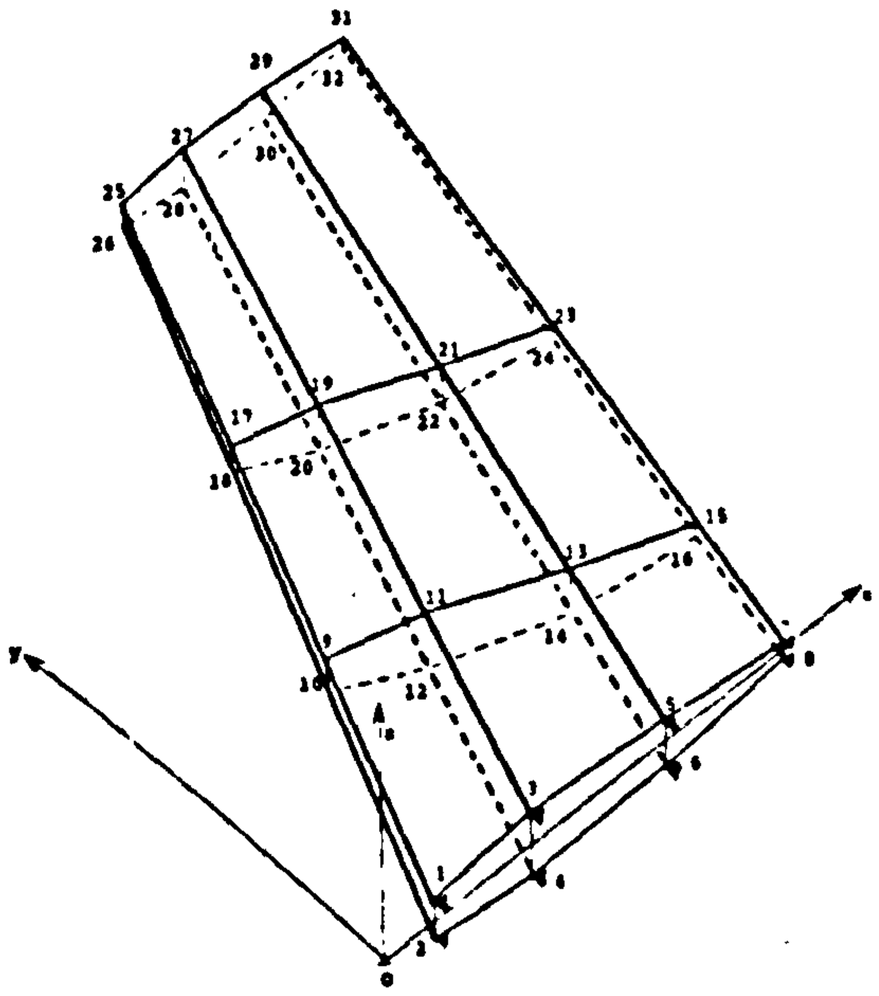

Swept tailplane

Element No.	Element dimensions
11, 12, 13, 14, 15, 16, 17 and 18	34.1×10^{-6} m^2
32, 33, 34, 35, 36, 37, 38 and 39	25.4×10^{-6} m^2
53, 54, 55, 56, 57, 58, 59 and 60	25.9×10^{-6} m^2
1, 2, 3, and 4	0.9×10^{-3} m
5, 6, 7, 8, 9, 10, 26, 27, 28, 29, 30, 31, 40, 41, 42, 43, 44, 45, 46, 47, 48, 49, 50, 51, 52, 61, 62 and 63	0.7×10^{-3} m
19, 20, 21, 22, 23, 24 and 25	0.8×10^{-3} m

Mode	Frequency in Hz Subspace iteration	Eigenvalue economizer
1	35.39	35.39
2	111.6	*
3	118.5	118.6
4	177.2	177.2
5	308.0	308.2
6	355.7	*
7	393.1	*
8	448.2	448.3
9	565.0	565.4
10	575.5	575.9
11	750.5	751.4
12	804.7	
13	836.4	842.1
14	953.4	955.0
15	983.3	
16	1098.	1097.
17	1100.	1104.
18	1354.	
19	1394.	
20	1409.	
21	1481.	1490.
22	1554.	
23	1700.	
24	1743.	
25	1810.	
26	1907.	
27	2000.	
28	2024.	
29	2153.	
30	2181.	
31	2281.	
32	2324.	
33	2398.	
34	2529.	
35	2641.	
36	2648.	
37	2756.	2736.
38	2775.	
39	2867.	
40	2997.	
41	3089.	
42	3145.	
43	3219.	
44	3478.	
45	3560.	3567.
⋮	⋮	⋮

* Predominantly in-plane modes

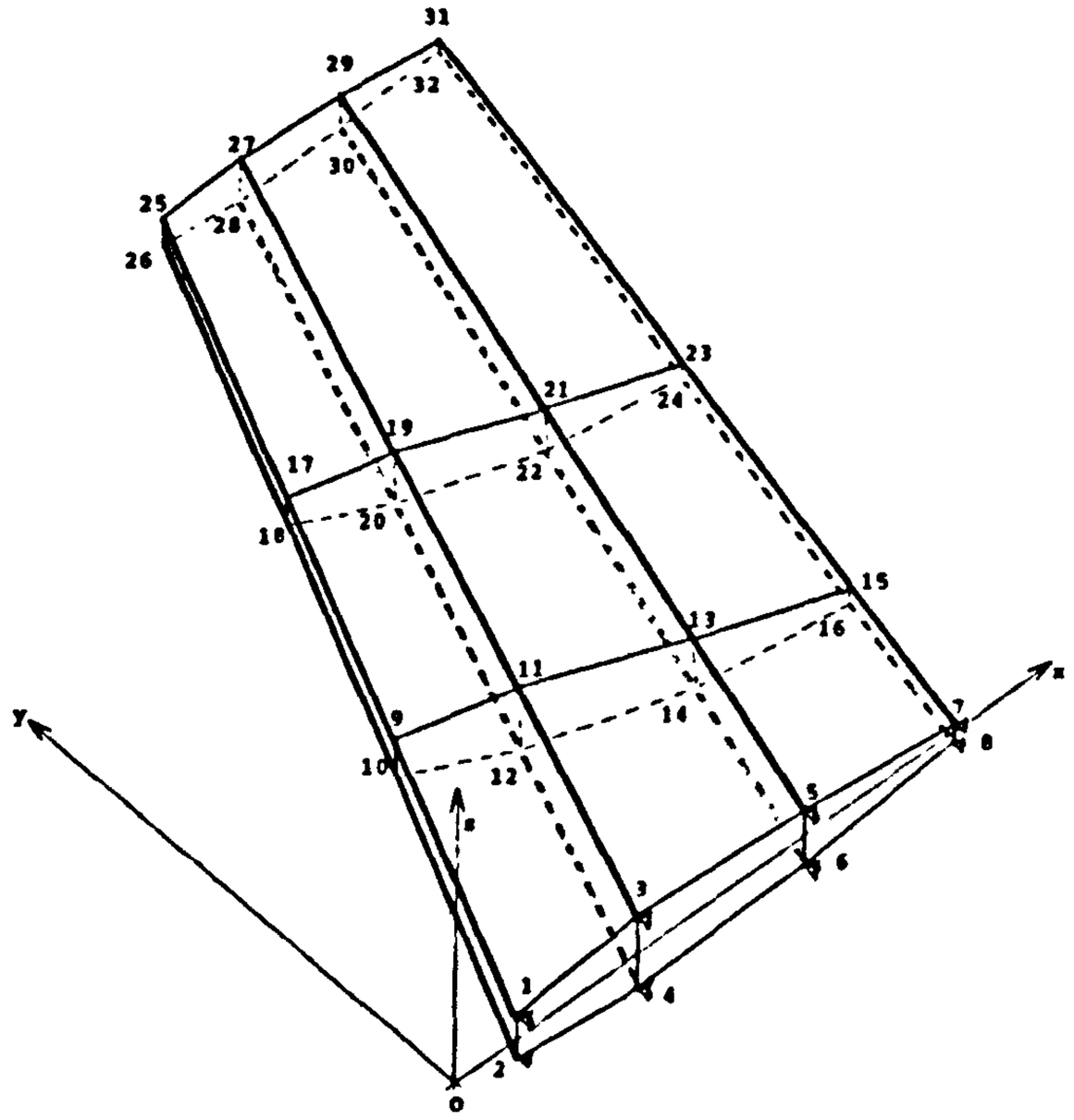

Swept tailplane

Element No.	Element dimensions
11, 12, 13, 14, 15, 16, 17 and 18	34.1×10^{-6} m^2
32, 33, 34, 35, 36, 37, 38 and 39	25.4×10^{-6} m^2
53, 54, 55, 56, 57, 58, 59 and 60	25.9×10^{-6} m^2
1, 2, 3, and 4	0.9×10^{-3} m
5, 6, 7, 8, 9, 10, 26, 27, 28, 29, 30, 31, 40, 41, 42, 43, 44, 45, 46, 47, 48, 49, 50, 51, 52, 61, 62 and 63	0.7×10^{-3} m
19, 20, 21, 22, 23, 24 and 25	0.8×10^{-3} m

Nodal point	Full 1st mode shape, displacement in x-direction	displacement in y-direction	displacement in z-direction	1st master mode shape, displacement in z-direction
1	0.0000	0.0000	0.0000	0.0000
2	0.0000	0.0000	0.0000	0.0000
3	0.0000	0.0000	0.0000	0.0000
4	0.0000	0.0000	0.0000	0.0000
5	0.0000	0.0000	0.0000	0.0000
6	0.0000	0.0000	0.0000	0.0000
7	0.0000	0.0000	0.0000	0.0000
8	0.0000	0.0000	0.0000	0.0000
9	-0.3803×10^{-2}	-0.5716×10^{-2}	0.3991×10^{-1}	0.3991×10^{-1}
10	0.3803×10^{-2}	0.5716×10^{-2}	0.3991×10^{-1}	0.3991×10^{-1}
11	-0.4608×10^{-2}	-0.1061×10^{-1}	0.4184×10^{-1}	0.4184×10^{-1}
12	0.4608×10^{-2}	0.1061×10^{-1}	0.4184×10^{-1}	0.4184×10^{-1}
13	-0.2433×10^{-2}	-0.9167×10^{-2}	0.3828×10^{-1}	0.3828×10^{-1}
14	0.2433×10^{-2}	0.9167×10^{-2}	0.3828×10^{-1}	0.3828×10^{-1}
15	-0.4917×10^{-3}	-0.3930×10^{-2}	0.3650×10^{-1}	0.3650×10^{-1}
16	0.4918×10^{-3}	0.3930×10^{-2}	0.3650×10^{-1}	0.3650×10^{-1}
17	-0.4931×10^{-2}	-0.1009×10^{-1}	0.1496	0.1496
18	0.4931×10^{-2}	0.1009×10^{-1}	0.1496	0.1496
19	-0.7622×10^{-2}	-0.1666×10^{-1}	0.1535	0.1535
20	0.7622×10^{-2}	0.1666×10^{-1}	0.1535	0.1535
21	-0.5441×10^{-2}	-0.1358×10^{-1}	0.1569	0.1569
22	0.5441×10^{-2}	0.1358×10^{-1}	0.1569	0.1569
23	-0.1684×10^{-2}	-0.4998×10^{-2}	0.1669	0.1669
24	0.1684×10^{-2}	0.4999×10^{-2}	0.1669	0.1669
25	-0.5066×10^{-2}	-0.9733×10^{-2}	0.3225	0.3225
26	0.5066×10^{-2}	0.9733×10^{-2}	0.3225	0.3225
27	-0.8342×10^{-2}	-0.1583×10^{-1}	0.3453	0.3453
28	0.8342×10^{-2}	0.1583×10^{-1}	0.3453	0.3453
29	-0.6292×10^{-2}	-0.1232×10^{-1}	0.3778	0.3778
30	0.6292×10^{-2}	0.1232×10^{-1}	0.3778	0.3778
31	-0.2019×10^{-2}	-0.4258×10^{-2}	0.4070	0.4070
32	0.2019×10^{-2}	0.4258×10^{-2}	0.4070	0.4070

Table VI.6 Comparison of 1st full and 1st master mode shapes

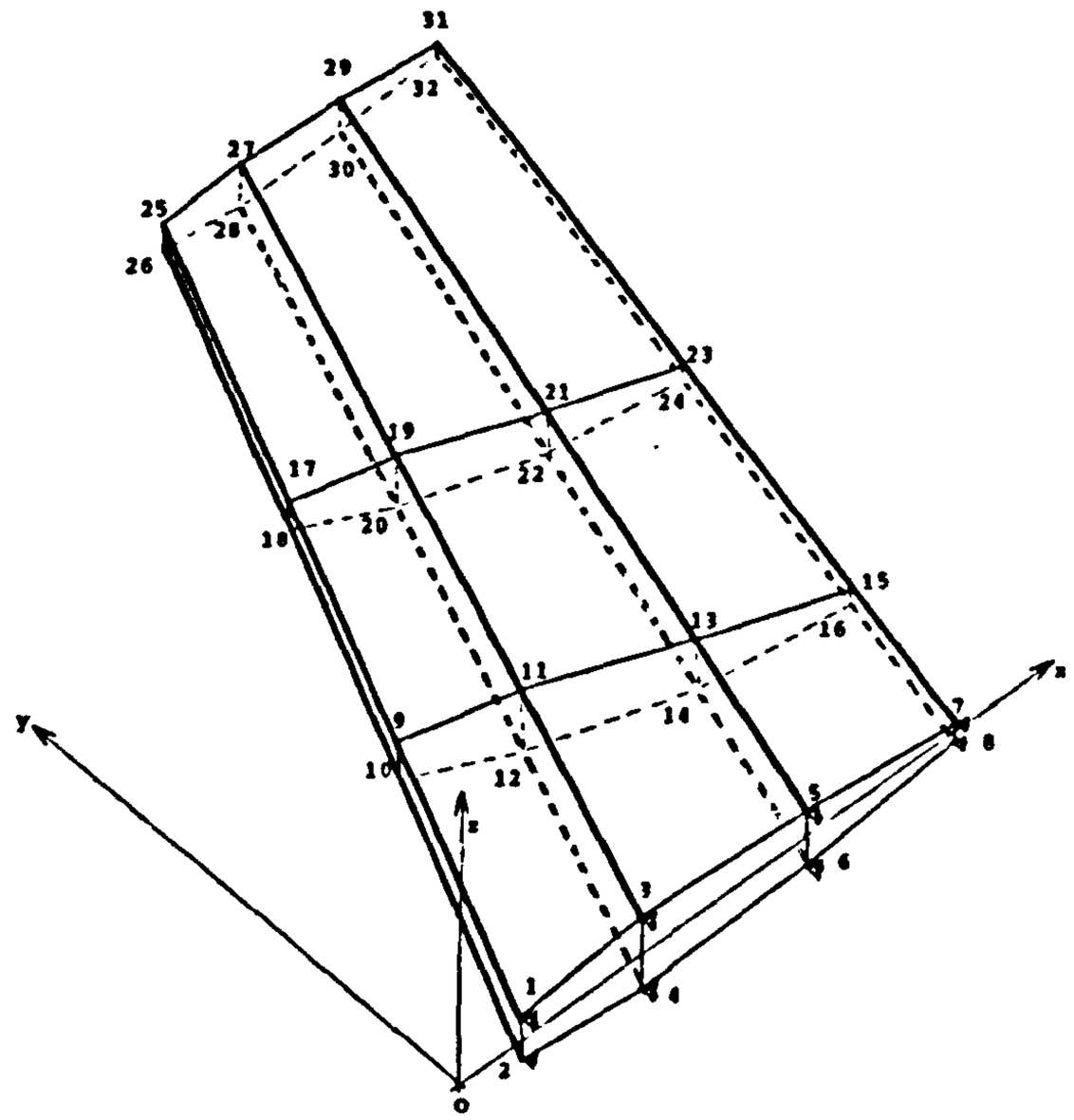

Swept tailplane

Element No.	Element dimensions
11, 12, 13, 14, 15, 16, 17 and 18	34.1×10^{-6} m^2
32, 33, 34, 35, 36, 37, 38 and 39	25.4×10^{-6} m^2
53, 54, 55, 56, 57, 58, 59 and 60	25.9×10^{-6} m^2
1, 2, 3, and 4	0.9×10^{-3} m
5, 6, 7, 8, 9, 10, 26, 27, 28, 29, 30, 31, 40, 41, 42, 43, 44, 45, 46, 47, 48, 49, 50, 51, 52, 61, 62 and 63	0.7×10^{-3} m
19, 20, 21, 22, 23, 24 and 25	0.8×10^{-3} m

Nodal point	Full 9th mode shape, displacement in x-direction	displacement in y-direction	displacement in z-direction	6th master mode shape, displacement in z-direction
1	0.0000	0.0000	0.0000	0.0000
2	0.0000	0.0000	0.0000	0.0000
3	0.0000	0.0000	0.0000	0.0000
4	0.0000	0.0000	0.0000	0.0000
5	0.0000	0.0000	0.0000	0.0000
6	0.0000	0.0000	0.0000	0.0000
7	0.0000	0.0000	0.0000	0.0000
8	0.0000	0.0000	0.0000	0.0000
9	0.2737×10^{-1}	-0.3389×10^{-2}	0.4652	0.4644
10	-0.2739×10^{-1}	0.3356×10^{-2}	0.4652	0.4644
11	0.6909×10^{-1}	-0.6981×10^{-2}	0.1868	0.1850
12	-0.6909×10^{-1}	0.6991×10^{-2}	0.1868	0.1850
13	0.2346×10^{-1}	-0.1934×10^{-2}	-0.1746	-0.1762
14	-0.2345×10^{-1}	0.1937×10^{-2}	-0.1746	-0.1762
15	0.1604×10^{-2}	-0.1764×10^{-1}	-0.1531	-0.1471
16	-0.1595×10^{-2}	0.1763×10^{-1}	-0.1531	-0.1471
17	-0.1439×10^{-1}	0.2182×10^{-1}	-0.2274	-0.2209
18	0.1442×10^{-1}	-0.2177×10^{-1}	-0.2274	-0.2209
19	-0.2746×10^{-1}	0.1400×10^{-1}	-0.2872	-0.2862
20	0.2746×10^{-1}	-0.1400×10^{-1}	-0.2872	-0.2862
21	-0.8272×10^{-1}	0.1438×10^{-1}	-0.1648	-0.1695
22	0.8272×10^{-1}	-0.1438×10^{-1}	-0.1648	-0.1695
23	-0.8187×10^{-2}	-0.1882×10^{-2}	0.6451	0.6488
24	0.8167×10^{-2}	0.1890×10^{-2}	0.6451	0.6488
25	-0.1669×10^{-2}	-0.4287×10^{-1}	0.3515	0.3520
26	0.1673×10^{-2}	0.4283×10^{-1}	0.3515	0.3520
27	0.3302×10^{-1}	-0.6234×10^{-1}	0.2589	0.2573
28	-0.3302×10^{-1}	0.6231×10^{-1}	0.2589	0.2573
29	0.5018×10^{-1}	-0.1379×10^{-1}	-0.4726×10^{-1}	-0.4940×10^{-1}
30	-0.5018×10^{-1}	0.1383×10^{-1}	-0.4726×10^{-1}	-0.4940×10^{-1}
31	0.3076×10^{-1}	0.1764×10^{-1}	-0.3177	-0.3118
32	-0.3077×10^{-1}	-0.1768×10^{-1}	-0.3177	-0.3118

Table VI.7 Comparison of 9th full and 6th master mode shapes

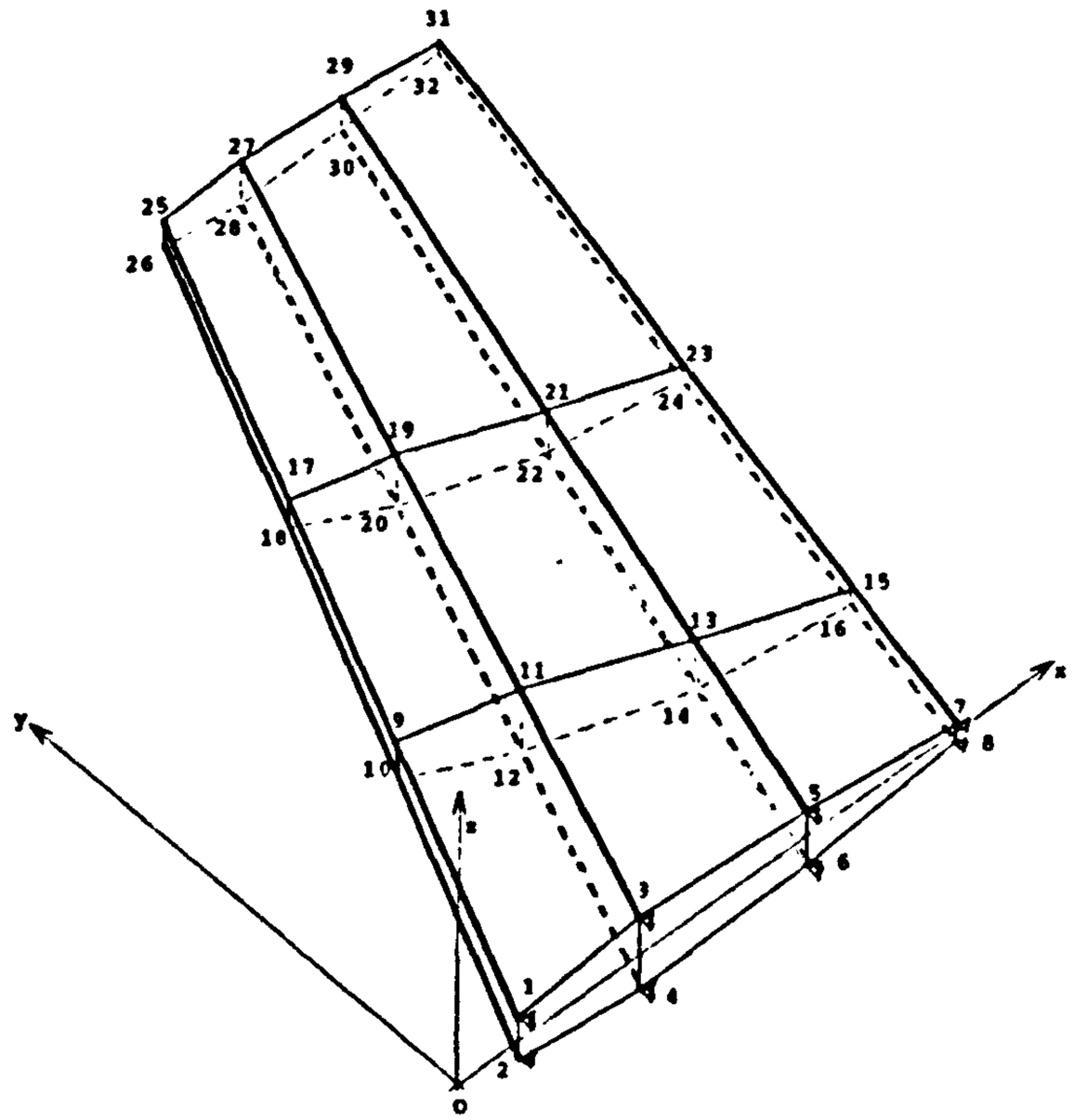

Swept tailplane

Element No.	Element dimensions
11, 12, 13, 14, 15, 16, 17 and 18	34.1×10^{-6} m^2
32, 33, 34, 35, 36, 37, 38 and 39	25.4×10^{-6} m^2
53, 54, 55, 56, 57, 58, 59 and 60	25.9×10^{-6} m^2
1, 2, 3, and 4	0.9×10^{-3} m
5, 6, 7, 8, 9, 10, 26, 27, 28, 29, 30, 31, 40, 41, 42, 43, 44, 45, 46, 47, 48, 49, 50, 51, 52, 61, 62 and 63	0.7×10^{-3} m
19, 20, 21, 22, 23, 24 and 25	0.8×10^{-3} m

Nodal point	Full 13th mode shape, displacement in x-direction	displacement in y-direction	displacement in z-direction	9th master mode shape, displacement in z-direction
1	0.0000	0.0000	0.0000	0.0000
2	0.0000	0.0000	0.0000	0.0000
3	0.0000	0.0000	0.0000	0.0000
4	0.0000	0.0000	0.0000	0.0000
5	0.0000	0.0000	0.0000	0.0000
6	0.0000	0.0000	0.0000	0.0000
7	0.0000	0.0000	0.0000	0.0000
8	0.0000	0.0000	0.0000	0.0000
9	-0.6100×10^{-2}	0.1719×10^{-1}	-0.1905	-0.2057
10	0.6062×10^{-2}	-0.1722×10^{-1}	-0.1905	-0.2057
11	-0.5039×10^{-1}	-0.4006×10^{-2}	0.2329	0.2384
12	0.5040×10^{-1}	0.4025×10^{-2}	0.2329	0.2384
13	-0.4867×10^{-1}	0.2794×10^{-1}	-0.2369	-0.2357
14	0.4868×10^{-1}	-0.2797×10^{-1}	-0.2369	-0.2357
15	-0.2416×10^{-1}	0.1160×10^{-2}	0.1911	0.1934
16	0.2415×10^{-1}	-0.1166×10^{-2}	0.1911	0.1934
17	-0.6607×10^{-2}	0.9523×10^{-2}	-0.3815	-0.3921
18	0.6621×10^{-2}	-0.9530×10^{-2}	-0.3815	-0.3921
19	-0.7549×10^{-1}	0.4016×10^{-1}	0.4067	0.4115
20	0.7550×10^{-1}	-0.4016×10^{-1}	0.4067	0.4115
21	-0.7972×10^{-1}	0.1282×10^{-1}	-0.2505	-0.2569
22	0.7973×10^{-1}	-0.1276×10^{-1}	-0.2505	-0.2569
23	-0.3143×10^{-1}	0.1341×10^{-1}	0.1081	0.1248
24	0.3141×10^{-1}	-0.1346×10^{-1}	0.1081	0.1248
25	-0.2374×10^{-1}	-0.9909×10^{-2}	-0.3629	-0.3682
26	0.2378×10^{-1}	0.9944×10^{-2}	-0.3629	-0.3682
27	-0.6096×10^{-1}	0.3559×10^{-1}	0.1740	0.1721
28	0.6096×10^{-1}	-0.3564×10^{-1}	0.1740	0.1721
29	-0.4036×10^{-2}	-0.5276×10^{-2}	0.6630×10^{-1}	0.6301×10^{-1}
30	0.4013×10^{-2}	0.5246×10^{-2}	0.6630×10^{-1}	0.6301×10^{-1}
31	-0.1139×10^{-2}	0.5266×10^{-2}	-0.1837	-0.1744
32	0.1126×10^{-2}	-0.5220×10^{-2}	-0.1837	-0.1744

Table VI.8 Comparison of 13th full and 9th master mode shapes

CHAPTER VII

CONTRIBUTIONS TO FLUTTER SYNTHESIS

1 SURVEY OF OTHER PEOPLE'S CONTRIBUTIONS TO FLUTTER SYNTHESIS

Although work on flutter synthesis has been limited when compared to other behavioral related synthesis work, the processus of weight minimization subjected to flutter speed constraints, like any other structural optimization problem, is amenable to direct minimization and to methods that attempt to satisfy optimality criteria in an indirect recursive fashion.

Prior to 1969, it seems that the research into the optimum structural design with dynamic requirements was confined to natural frequency constraints, perhaps, awaiting the consolidation of the theory of nonstationary aerodynamics and further developments in theoretical structural dynamics and in the digital computer. One of the earliest contribution was made by Turner (Ref. 53, 1969) who first employed Lagrange multipliers to find the relative proportions of selected elements in an aircraft structure to achieve a specified flutter speed.

This was followed two years later by the formulation of the equations that give the partial derivatives of the flutter velocity and of the frequency with respect to structural parameters (Rudisill and Bathia, Ref. 42). These authors were then able to incorporate this into a combination of direct searches for the minimum weight of a box beam. In

this approach, whenever there is a deficiency in the flutter speed, a velocity-gradient move is made to step the parameters towards the direction of maximum increase in flutter speed. A mass-gradient routine moves the design in the direction of the maximum reduction in the structural mass whenever it is desired to decrease the flutter velocity. The velocity-gradient-projection searchs to find a design having relatively maximum flutter speed on a constant mass hyperplane.

In another attack on the problem, Gwin, McIntosh and Taylor employed the rates of changes of the flutter speed constraint and information on the rates of changes of the objective function as part of a feasible-direction method (Ref. 20, 1972; followed by Ref. 21, 1973).

In what can be seen as a brute approach equivalent to its stress constrained counterpart, the familiar FSD concept, Siegel (Ref. 46, 1972) presented an intuitive resizing algorithm based on the criterion that the strain energy per unit volume in every structural component should be constant throughout the deformed structure in the critical flutter mode. Using the classical linear recurrence relation

$$x_j^{(k+1)} = C_j^{(k)} \cdot x_j^{(k)} \qquad \text{(VII.1.1)}$$

he devised the redesign factor reproduced below. In our notation, it shows that

$$C_j^{(k)} = \left(\left(\frac{V_r}{V_f^{(k)}} \right)^2 \left(\frac{(e_v)_j^{(k)}}{(e_{avav})^{(k)}} \right)^{1/2} \right) \qquad \text{(VII.1.2)}$$

C_j redesign factor for jth design variable

x_j jth design variable

k iteration counter

V_r required speed

V_f flutter speed

$(e_v)_j$ strain energy density of jth design variable

(e_{avav}) average of $(e_v)_j$ that exceeds (e_{av})

(e_{av}) average of all $(e_v)_j$

In requiring that the design variables do not fall below the minimum specified gauges, Siegel performed his recursive relation over a selection of elements whose strain energy is above the average (e_{av}) of all $(e_v)_j$, thus, permitting only incremental structural changes but with the major drawback that some elements may become too large too early in the design process. Siegel claims both accuracy which is suprising and unprecedented rapid computation which is very probable.

Rudisill and Bathia complemented their earlier first

order derivatives with second order derivatives of the flutter velocity (Ref. 43, 1972). Their intention was to improve the move distance in the velocity-gradient-projection search which was performed previously by trial. These authors take credit for their finding of analytical expressions for first and second flutter parameters derivatives.

Pines and Newman (Ref. 39, 1973) gave a major thrust to indirect methods by deriving optimality criteria straight from the equations governing the flutter optimization problem. Their OC are somewhat akin to that of Siegel and hence can be correlated to pseudo-strain-energy densities. Their work has shortcomings because of their assumption of quasi-steady aerodynamics.

Haftka and Yates (Ref. 23, 1974) started the debate on the efficiency of using continuously updated natural modes or using the fixed-mode method. The fixed-mode approach is one in which the primitive natural modes of the original structure are kept unchanged when setting up the generalized equation of motion. This assumption is also maintained whilst generating the unsteady airloads during the whole design process despite the fact that the structure is being constantly resized. Updating the modes requires the systematic adjustment of the natural modes at each structural redesign step. An unexpected conclusion was that "the main computational penalty in using continually updated natural vibration modes in the design process lies in the recalculation of the modes rather than in the recalculation

of the generalized aerodynamic forces". It may be pointed out that this may not be true if inplane degrees of freedom are obviated with a dynamic condensation of the free-vibration problem.

The first and may be the only direct comparison of MP and OC approaches to flutter was performed by Haftka and Starnes in 1974 (Ref. 22). These authors acknowledge that they could not and would not attempt the overwhelming task of evaluating all MP techniques. Rather, they limit their study to a single MP procedure where the design constraints are introduced by means of an interior penalty function in a Sequential Unconstrained Minimization Technique. They employed the same iterative resizing algorithm (Eq. VII.1.1 and VII.1.2) for both a rigorous OC and the intuitive OC of Siegel. But instead of resizing only elements whose strain energies are above the average, they included all design variables in the resizing scheme and imposed the minimum-gauge value on any that violated the minimum side constraints. Their results show an extremely favorable comparison of the rigorous OC with the MP methods. The performance of the rigorous OC is unambiguously quicker: more than twice as fast for a structure with a number of six design variables; more than eleven times as fast for a structure with fifty one design variables. It was also noted that intuitive OC are not consistently reliable in terms of the nearness to the optimum although they proved to be useful in some cases.

In the review and assessment paper of Stroud (Ref. 48, 1974), the work of all its predecessors have been examined. Stroud used a hypothetical two-dimensional space to aid in visualizing the gradient techniques and try to give reasons of the deficiency of convergence of each technique. This paper is recommended for consultation if a deeper and more elaborate discussion is needed.

Rather than dealing with a speed ratio (Eq. VII.1.2) McIntosh and Ashley (Ref. 1) created a very similar iterative scheme but based on the artificial damping (see appendix D, Eq. D.27b). When they compared their resizing technique to two other slightly more complex OC based techniques (Ref.45 and 48), the ratio of CPU times is 1.4 in favor of McIntosh-Ashley's work.

In summary, several major contributions to optimization of structures to attain a required flutter speed have been enumerated to indicate the two traditional facets of solution methods. Attention is now directed towards the current work and its motivation.

2 MOTIVATIONS OF THIS WORK

The paper by Ashley and McIntosh (1978) cited above seems to exhaust the list on flutter synthesis work. From 1978, there appears to be a void in the contributions to flutter synthesis and no current thinking in the area of automated aeroelastic design can be identified. However, it

cannot be said that flutter synthesis has matured and many aspects still need further attention.

The first point is that the assessment of the adequacy and practicality of the techniques has been achieved through discussion rather than by an extensive numerical study. The enormity of the aeroelastic constrained problem have probably hindered numerical comparisons such as that given in Ref. 5 for stress and displacement constrained problems. In this paper, Belegundu and Arora used three evaluation criteria, accuracy, reliability and efficiency, in testing different techniques to different problems so as to reach some kind of global judgment on the "best" method. As the ratio of running times of one technique written by two programmers could be as high as 13/1 (see bibliography on finite element methods, book by Cook, page 401), the task of direct comparisons of flutter optimization techniques would need the programming of all techniques available by the same person and their running on the same machine for the same wide spectrum of structures. This task is obviously considered to be onerous to be undertaken in this modest work. We have in mind a more limited perception in that we shall select the method that is most suitable for our purposes. We shall, then, attempt to give an objective assessment on its validity and applicability and try to identify any possible pitfalls on its implementation as a practical means of optimizing structures to fulfill aeroelastic requirements.

The second point is that so much discussion has centered

on fixed-versus-updated modes in the published literature that we are impelled to single out this specific area as the one deserving further investigation in this treatise. Considering not only the analytical but also the computational difficulties, all the aforementioned publications, apart from those by Haftka, et al., have been contempted with a fixed-mode approach and their algorithms are solely leaning on not updating the modes.

A problem may, however, be encountered with a fixed mode approach to the point where refinements to this matter can be regarded as the necessary requirements to ensure consistently reliable results with automated flutter design.

A fixed mode approach suffers from a major drawback when viewed from a design feasibility angle: it often happens that seemingly optimum designs obtained by such an approach may turn out to be violating the minimum imposed flutter speed. This has been mentioned by different authors and, for instance, as much as a 7% intrusion into the unstable region is reported in Ref. 48. The required flutter speed should be at least 1.2 (for commercial aircrafts) or 1.15 (for military aircrafts) the design speed as imposed by the aviation authorities. With a 7% error, the flutter margins would be reduced to 1.13 and 1.08 respectively. Bearing in mind any possible errors introduced by the theoretical idealization, this violation of the required flutter speed may not be acceptable for safety reasons and might be rejected by any certification test. If this is the case, permanent

remodalization based on the vibration modes of the current configuration should be of paramount necessity. The authors referenced herein made suggestions on two possible ways to may be overcome the flaws of "fixed-mode" method and the computational burdens of "continous-mode-updating" method:

— use of a large number of the original modes to better describe the changing structure.

— occasional recalculation of the mode shapes (called "periodically-updated-mode" hereafter).

Inasmuch as the order of the problem increases with the number of modes, the resources required to execute flutter solutions will be much higher if a large number of original modes is utilized. Moreover, the degree of improvement to the fixed-mode method made possible with an increase in the number of modes has yet to be proven. Anyhow, this formula would not apply if only transverse modes are used, higher than six modes cannot be expected to ameliorate sensibly the idealization of the deformed structure (see chapter VI, tables VI.4 and VI.8).

On the other hand, the "periodically-updated-modes" method has been advocated but so far never applied. Questions which must be addressed are how rarely it must be performed to be attractive in terms of CPU times and how often to reduce to acceptable levels the percentage by which flutter speed drifts into the unfeasible region.

The second step of this research is motivated by the formulation of the dual aeroelastic problem. The progressive estimation of lower bounds on the feasible weight provided by the dual problem is a powerful monitoring tool and a formal convergence test (Ref. 2). In our opinion, as the problem converges, dual monitoring could have other beneficial uses specific to flutter synthesis in particular:

— use of fixed modes until a substantial reduction is achieved in the dual gap where the strategy is changed to mode updating;

— use of a small number of natural vibration modes and increase this number as the dual gap decreases.

If dual bounding can be used to trigger the switching to "mode updating" at minimal computational cost, the solution will be an improvement on what have been accepted in two respects: first, satisfaction of the minimum flutter speed as opposed to a strict fixed-mode approach and second, no computational penalty when compared to a continuous modal analysis.

3 SELECTION OF AN ALGORITHM

A key feature for a selection is that the algorithm should operate in the feasible design space in order to be complemented by a dual monitoring scheme. Another tacit

understanding is that the dual problem should be extracting most if not all of its information from the primal problem so that little extra-computational effort would be needed.

Recalling the short survey of § VII.1, the algorithm of Ref. 1 appears to have the least computing run times amid all other primal algorithms. The reasons for this are not only because it is an OC based algorithm but also because stable flutter modes are pruned down from local informations on the artificial dampings in lieu of full V-g solutions as demanded by some of the other algorithms.

Mcintosh-Ashley redesign factor (see appendix D, Eq. D.27b) reads

$$c_j^{(k)} = \left| \frac{\left(e_v\right)_j^{(k)}}{\left(e_{av}\right)^{(k)}} \right|^{e_1} \left(1 + g^{(k)}\right)^{e_2} \qquad \text{(VII.3.1)}$$

c_j redesign factor

g artificial damping

e_1, e_2 resizing exponents

$\left(e_{av}\right)$ average of all $\left(e_v\right)_j$ for active design variables

The pseudo-energy density terms, $\left(e_v\right)_j$, are required to have, at the optimum, the same value for the active set of design variables

$$\begin{cases} \left(e_v\right)_j = \dfrac{1}{\rho_j l_j} \mathrm{Re}\left(\{\lambda\}^H . \dfrac{\partial [F]}{\partial x_j} . \{\bar{q}\}\right) = -1 \\ \qquad\qquad \text{for bar elements} \\ \text{or} \\ \left(e_v\right)_j = \dfrac{1}{\rho_j A_j} \mathrm{Re}\left(\{\lambda\}^H . \dfrac{\partial [F]}{\partial x_j} . \{\bar{q}\}\right) = -1 \\ \qquad\qquad \text{for quadrilateral or triangular elements} \end{cases} \qquad \text{(VII.3.2)}$$

ρ_j density of the structural material of jth design variable

l_j total length of all the elements composing the jth design variable

A_j total area of all the elements composing the jth design variable

$\{\lambda\}^H$ obtained from adjoint flutter equation, viz., $[F]^T\{\lambda^C\} = \{0\}$

$\{\lambda^C\}$ adjoint aeroelastic eigenvector

With reference to proceeding in the feasible design space, the factor (1+g) in Eq. VII.3.1 ensures that the design variables are raised whenever the artificial damping is positive.

4 DUAL MONITORING

A dual aeroelastic problem designed specifically to bound the primal mass is shown in appendix F (Eq. F.8) to have the following form

$$\left.\begin{array}{l} \text{maximize} \quad m_0 + \sum_{j=1}^{N} m_j x_j + \Lambda g \\ \\ \text{subject to} \begin{cases} m_j + \Lambda \cdot \dfrac{\partial g}{\partial x_j} \leq 0 \qquad \forall\, j \in J_a \\ \\ \text{and to} \\ \\ \Lambda \geq 0 \end{cases} \end{array}\right\} \quad \text{(VII.4.1)}$$

where

Λ Lagrange multiplier

J_a set of indices representing the active design variables

The derivatives of the artificial damping in Eq. VII.4.1 obey the following equation (see appendix E, Eq.43b)

$$\begin{cases} \dfrac{\partial g}{\partial x_j} = \dfrac{1}{D} \cdot \left(\left(\dfrac{2g}{\omega^3} \cdot R_3 + \dfrac{2}{\omega^3} \cdot I_3 + \dfrac{b}{V} \cdot I_{41} - \dfrac{2b}{V\nu} \cdot I_{51} \right) \times \right. \\ \qquad \left. \left(-R_{1_j} + \dfrac{1}{\omega^2} \cdot R_{2_j} - \dfrac{g}{\omega^2} \cdot I_{2_j} \right) \right) \\ \\ \qquad - \dfrac{1}{D} \cdot \left(\left(\dfrac{2}{\omega^3} \cdot R_3 - \dfrac{2g}{\omega^3} \cdot I_3 + \dfrac{b}{V} \cdot R_{41} - \dfrac{2b}{V\nu} \cdot R_{51} \right) \times \right. \\ \qquad \left. \left(-I_{1_j} + \dfrac{g}{\omega^2} \cdot R_{2_j} + \dfrac{1}{\omega^2} \cdot I_{2_j} \right) \right) \end{cases}$$

$$j = 1, \ldots, N \qquad \text{(VII.4.2)}$$

with

ω circular frequency of harmonic oscillation

b reference length of the lifting surface

V flight velocity

ν reduced frequency as defined in Eq. A.26

and

$$\begin{cases} D = \left(\frac{2q}{\omega^3}\cdot R_3 + \frac{2}{\omega^3}\cdot I_3 + \frac{b}{V}\cdot I_{41} - \frac{2b}{V\nu}\cdot I_{51}\right)\cdot\left(\frac{1}{\omega^2}\cdot I_3\right) \\ \qquad + \left(\frac{2}{\omega^3}\cdot R_3 - \frac{2q}{\omega^3}\cdot I_3 + \frac{b}{V}\cdot R_{41} - \frac{2b}{V\nu}\cdot R_{51}\right)\cdot\left(\frac{1}{\omega^2}\cdot R_3\right) \end{cases} \qquad \text{(VII.4.3)}$$

The rest of the terms — R_{1_j}, I_{1_j}, R_{2_j}, I_{2_j}, R_3, I_3, R_{41}, I_{41}, R_{51} and I_{51} — are given respectively by Eq. E.35, E.36, E.37a, E.37b, E.41a, E.41b, E.42a and E.42b. These terms needed for evaluating Eq. VII.4.2 and VII.4.3 and the dual bound may look too complex to be obtained at minimal cost. However, most, if not all, primal flutter algorithms already provide solutions of the aeroelastic eigenvector $\{\bar{q}\}$ and the adjoint aeroelastic eigenvector $\{\lambda^c\}$ which is required in the OC formulation or is necessary to eliminate the troublesome derivatives of $\{\bar{q}\}$ for gradient methods. Therefore, a closer look at these terms shows that the inclusion of the dual bounding involves:

— the extra estimation of the derivatives of the generalized aerodynamic matrix with respect to the reduced frequency;

— few multiplications of small order matrices by the aeroelastic eigenvector $\{\bar{q}\}$ and by the adjoint aeroelastic eigenvector $\{\lambda\}^H$.

A redeeming feature is that [Q] is rendered invariant of the design variables by the fixed-mode method. Therefore, [Q] can be evaluated for few values of ν and estimated by interpolation for any other values during the reduced frequency scanning. The same can be applied to $\frac{\partial[Q]}{\partial\nu}$ to efficiently evaluate $\frac{\partial g}{\partial x_j}$.

Finally, the dual problem expressed above for the purpose of detecting the convergence is not just convenient for our work. It can be used in conjunction with any primal problem operating in the feasible design space.

5 RESULTS

The algorithm was tested for both flutter-free and flutter prone lifting surfaces. The results are summarized in the tables and figures at the end of this chapter.

Beginning with table VII.1, the case of the rectangular-planform wing, we observe that with a required flutter speed of 250 m/s, the program was able to reduce the weight by 64.59 kg. The complete flutter solutions of the

initial design are sketched in Fig. VII.1. The flutter solutions of the final design were also carried out. The flutter mode number two remained the critical branch for the final design and is sketched in Fig. VII.1.

The iteration history (table VII.2) shows the stability of the active-passive set of design variables. In Fig. VII.2, the favorable monotonic weight reduction is enhanced. It can be seen that in the very first two iterations about 40% of the structural weight is removed.

Solutions of the dual mass were obtained with a hand calculator and are also reproduced in Fig. VII.2. The progressive reduction in the duality gap demonstrates the attractiveness of such a technique for augmenting the accuracy of flutter synthesis.

In the case of the swept tailplane, the base design has a slight hump mode, branch 6 in Fig. VII.3, which is greatly exaggerated to highlight the hump. This mode exhibits a positive value of g of 0.00065. This trivial value is assumed not to be critical by certification standards. We, nevertheless, ran the program for the swept tailplane to create freedom from positive artificial damping. The optimization routine succeeded in moving the hump mode within the boundaries of the stable region. The design progress for the swept tailplane is shown in table VII.3.

6 POTENTIAL PROBLEM OF THE ROUTINE

From many other different settings of "design variables" identities, the optimization routine was able to consistently converge to the same final active-passive set. However, one peculiar case which exhibited a non-convergent numerical performance was identified. This is discussed since it illustrates a potential problem of the procedure. Artificial damping at velocities somewhat above the divergence speed is not defined for an unstable mode which exhibits divergence (see Fig. II.1). If the first instability to appear is a divergence rather than flutter, the recursive relation will not be able to extract information on the damping parameter above this speed and will consequently reach a cul-de-sac. This problem will arise for any identical algorithm that works with the damping parameter.

Strangely, this has not been noted elsewhere in the literature, which may suggest that other authors are implicitly accepting that their algorithms are solely for flutter instabilities. It is our opinion that it would be utterly absurd to independently optimize for flutter and for static divergence. These two closely connected aeroelastic phenomena must be embodied in one single aeroelastic optimization process.

As a means of circumventing the numerical impasse, it is proposed that, whenever a design point is identified as having a divergence speed lower than the minimum operational

speed, the recursive relation used in our program (Eq. VII.3.1) is superseded by Eq. VII.1.2. Another solution is to adopt Eq. VII.1.2 from the outset.

		BASE DESIGN	CONSTRAINTS	OPTIMUM DESIGN	
Design variable	Element linkages	Starting dimension	Minimum dimension	Final dimension	
1	1, 7, 16 and 22	2.2×10^{-3} (act.)	1.290×10^{-3}	1.290×10^{-3} (pas.)	m^2
2	2, 8, 17 and 23	2.2×10^{-3} (act.)	1.290×10^{-3}	1.290×10^{-3} (pas.)	
3	3, 9, 18 and 24	2.2×10^{-3} (act.)	1.290×10^{-3}	1.290×10^{-3} (pas.)	
4	4 and 19	3.5×10^{-3} (act.)	2.032×10^{-3}	2.032×10^{-3} (pas.)	m
5	5 and 20	3.5×10^{-3} (act.)	2.032×10^{-3}	2.032×10^{-3} (pas.)	
6	6 and 21	3.5×10^{-3} (act.)	2.032×10^{-3}	2.032×10^{-3} (pas.)	
7	10 and 13	1.9×10^{-3} (act.)	1.016×10^{-3}	1.016×10^{-3} (pas.)	
8	11 and 14	1.9×10^{-3} (act.)	1.016×10^{-3}	1.016×10^{-3} (pas.)	
9	12 and 15	1.9×10^{-3} (act.)	1.016×10^{-3}	1.016×10^{-3} (pas.)	
10	25	1.9×10^{-3} (act.)	1.016×10^{-3}	1.016×10^{-3} (pas.)	
11	26	1.9×10^{-3} (act.)	1.016×10^{-3}	4.757×10^{-3} (act.)	
12	27	1.9×10^{-3} (act.)	1.016×10^{-3}	3.097×10^{-3} (act.)	

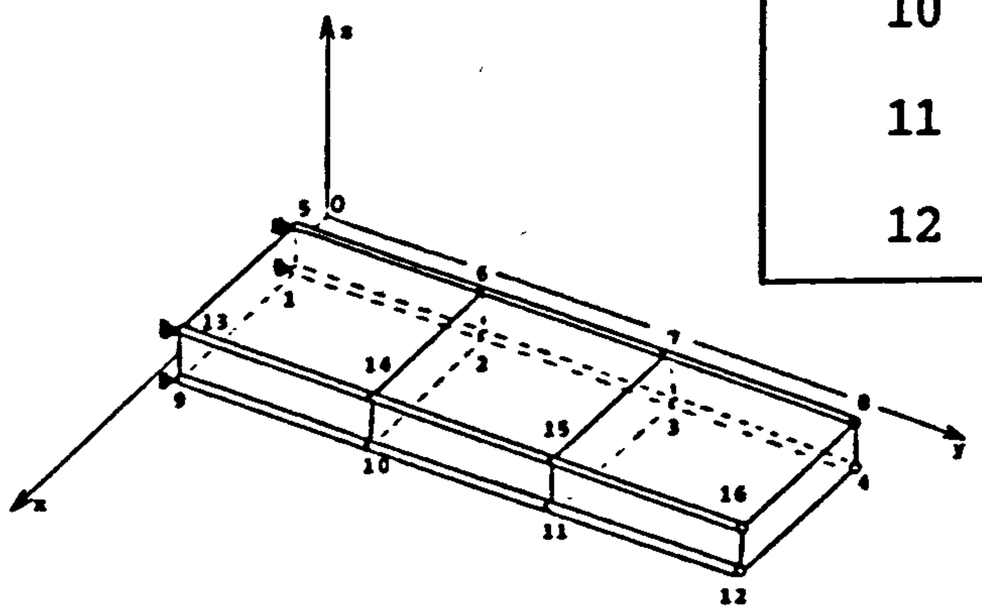

Mass	Required speed	Mass
154.56 kg	250.0 m/s	89.97 kg

Table VII.1 Initial design, constraints and final design for the rectangular-planform wing

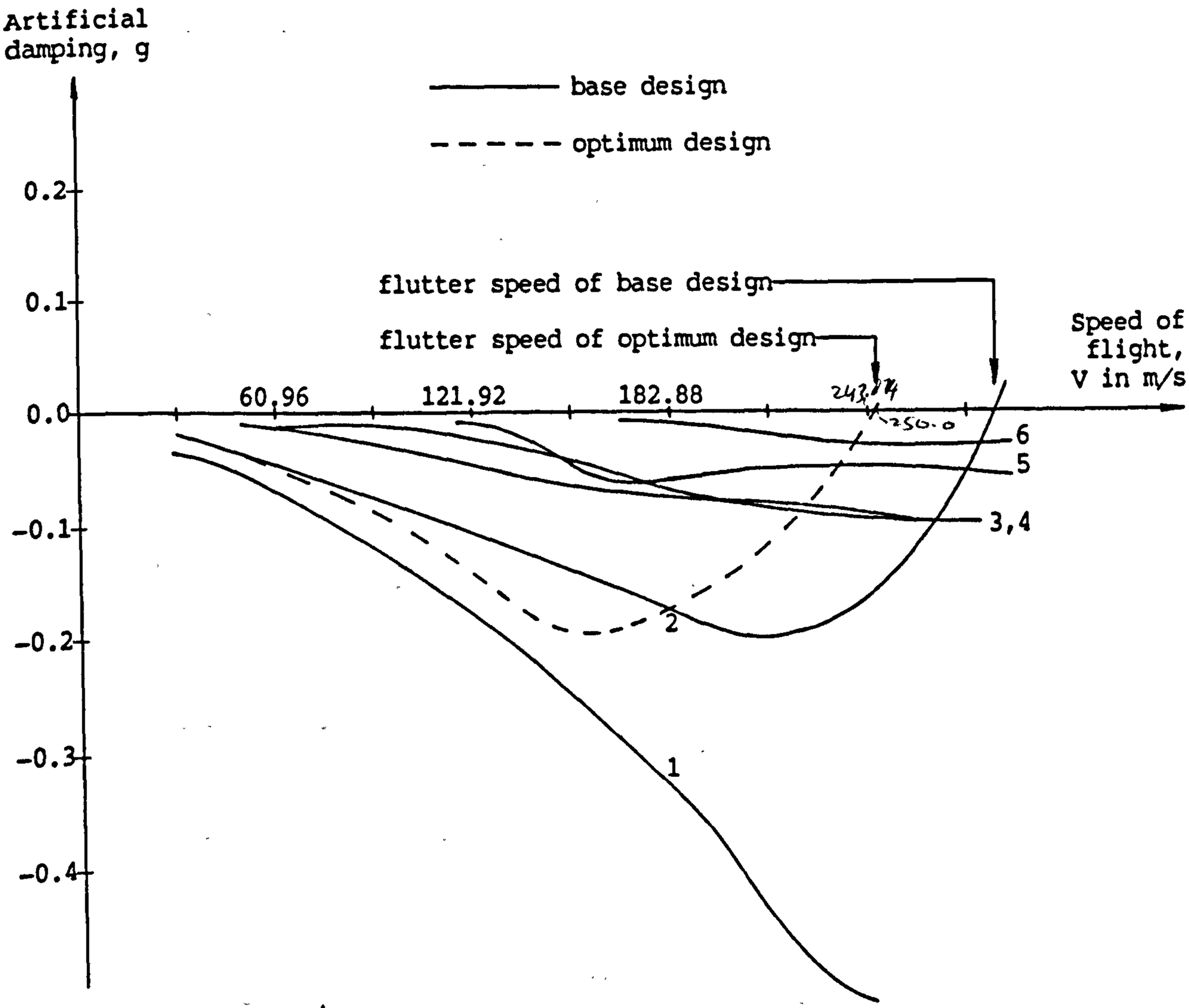

Fig. VII.1 Full "V-g" solutions of the initial design and critical "V-g" branch of the final design

Design variable	BASE DESIGN: Starting dimension	Dimension after the 1st iteration	Dimension after the 2nd iteration	...	Dimension after the 20th iteration	Dimension after the 21st iteration	
1	2.200×10^{-3} (act.)	1.290×10^{-3} (pas.)	1.290×10^{-3} (pas.)		1.290×10^{-3} (pas.)	1.290×10^{-3} (pas.)	m^2
2	2.200×10^{-3} (act.)	1.290×10^{-3} (pas.)	1.290×10^{-3} (pas.)		1.290×10^{-3} (pas.)	1.290×10^{-3} (pas.)	
3	2.200×10^{-3} (act.)	1.290×10^{-3} (pas.)	1.290×10^{-3} (pas.)		1.290×10^{-3} (pas.)	1.290×10^{-3} (pas.)	
4	3.500×10^{-3} (act.)	2.032×10^{-3} (pas.)	2.032×10^{-3} (pas.)		2.032×10^{-3} (pas.)	2.032×10^{-3} (pas.)	m
5	3.500×10^{-3} (act.)	2.397×10^{-3} (act.)	2.032×10^{-3} (pas.)		2.032×10^{-3} (pas.)	2.032×10^{-3} (pas.)	
6	3.500×10^{-3} (act.)	2.718×10^{-3} (act.)	2.032×10^{-3} (pas.)		2.032×10^{-3} (pas.)	2.032×10^{-3} (pas.)	
7	1.900×10^{-3} (act.)	1.016×10^{-3} (pas.)	1.016×10^{-3} (pas.)		1.016×10^{-3} (pas.)	1.016×10^{-3} (pas.)	
8	1.900×10^{-3} (act.)	1.016×10^{-3} (pas.)	1.016×10^{-3} (pas.)		1.016×10^{-3} (pas.)	1.016×10^{-3} (pas.)	
9	1.900×10^{-3} (act.)	1.016×10^{-3} (pas.)	1.016×10^{-3} (pas.)		1.016×10^{-3} (pas.)	1.016×10^{-3} (pas.)	
10	1.900×10^{-3} (act.)	5.954×10^{-3} (act.)	5.461×10^{-3} (act.)		1.022×10^{-3} (act.)	1.016×10^{-3} (pas.)	
11	1.900×10^{-3} (act.)	8.008×10^{-3} (act.)	8.854×10^{-3} (act.)		5.034×10^{-3} (act.)	4.757×10^{-3} (act.)	
12	1.900×10^{-3} (act.)	7.775×10^{-3} (act.)	8.116×10^{-3} (act.)		3.372×10^{-3} (act.)	3.097×10^{-3} (act.)	
Mass	154.56 kg	93.23 kg	92.44 kg		90.08 kg	89.97 kg	

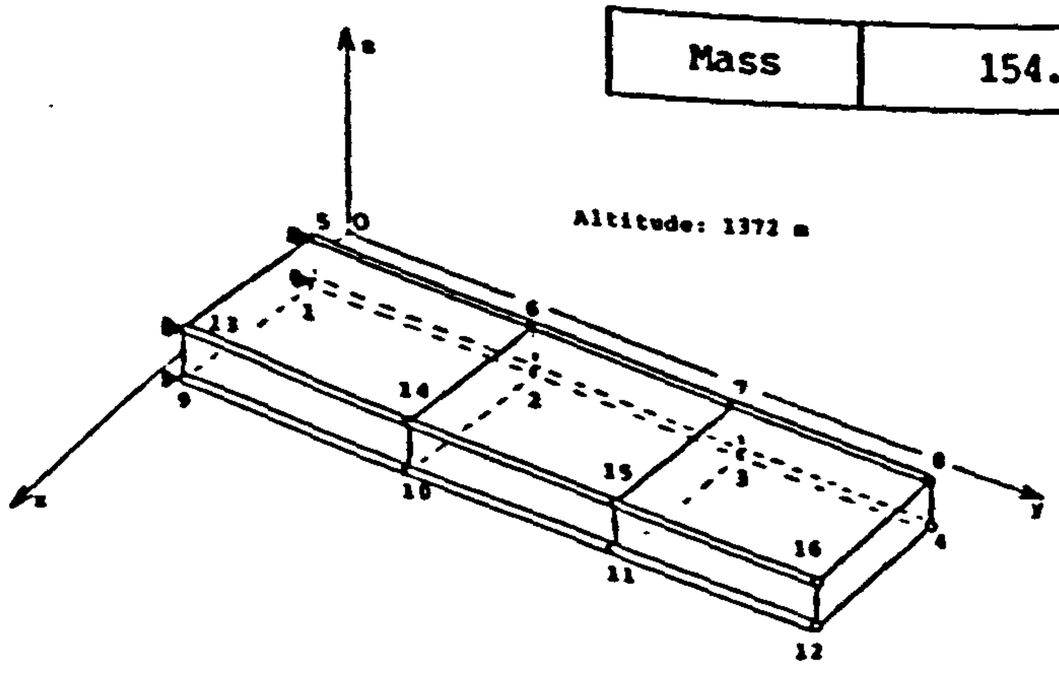

Table VII.2 Iteration history for the rectangular-planform wing

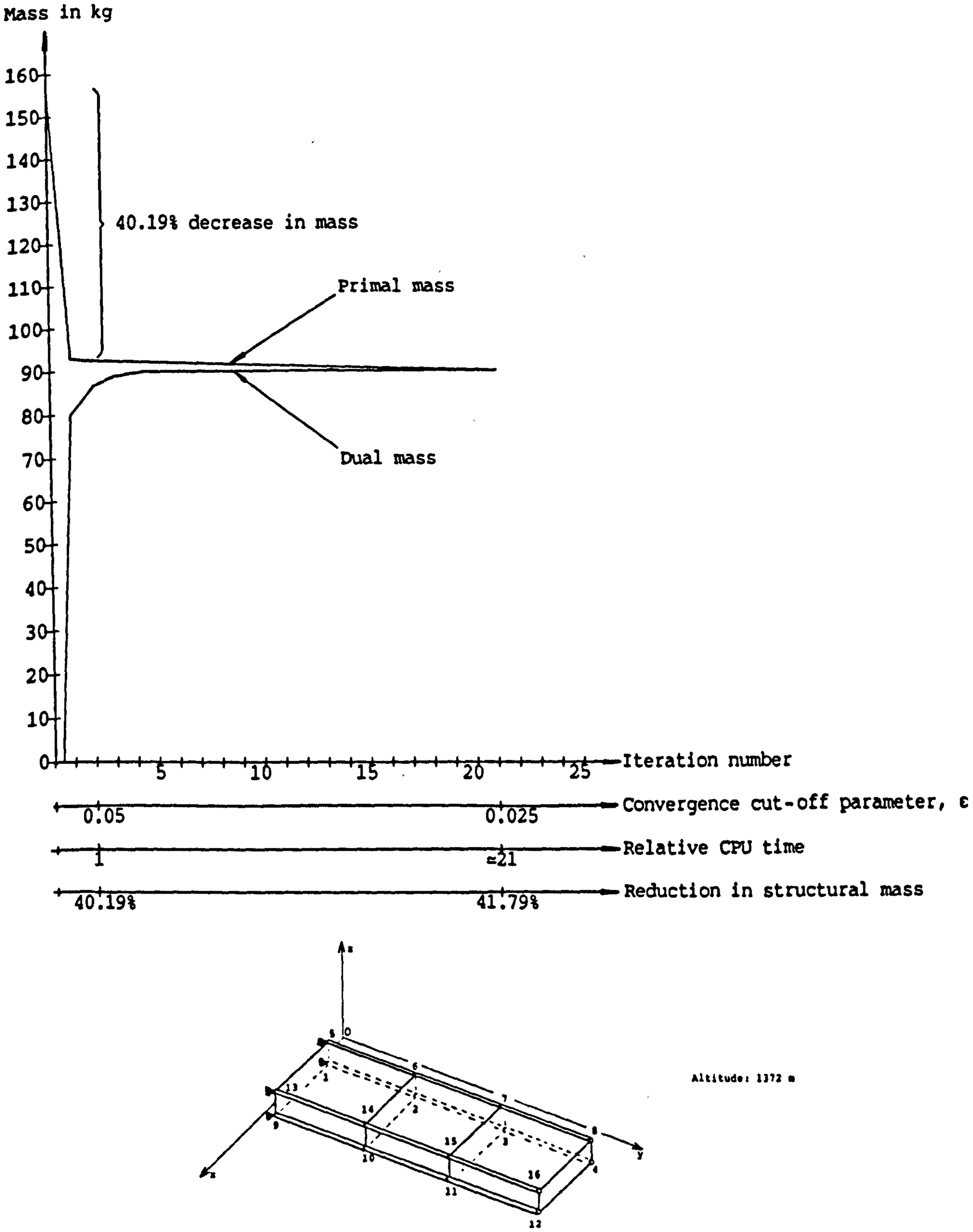

Fig. VII.2 Primal and dual mass (rectangular-planform wing)

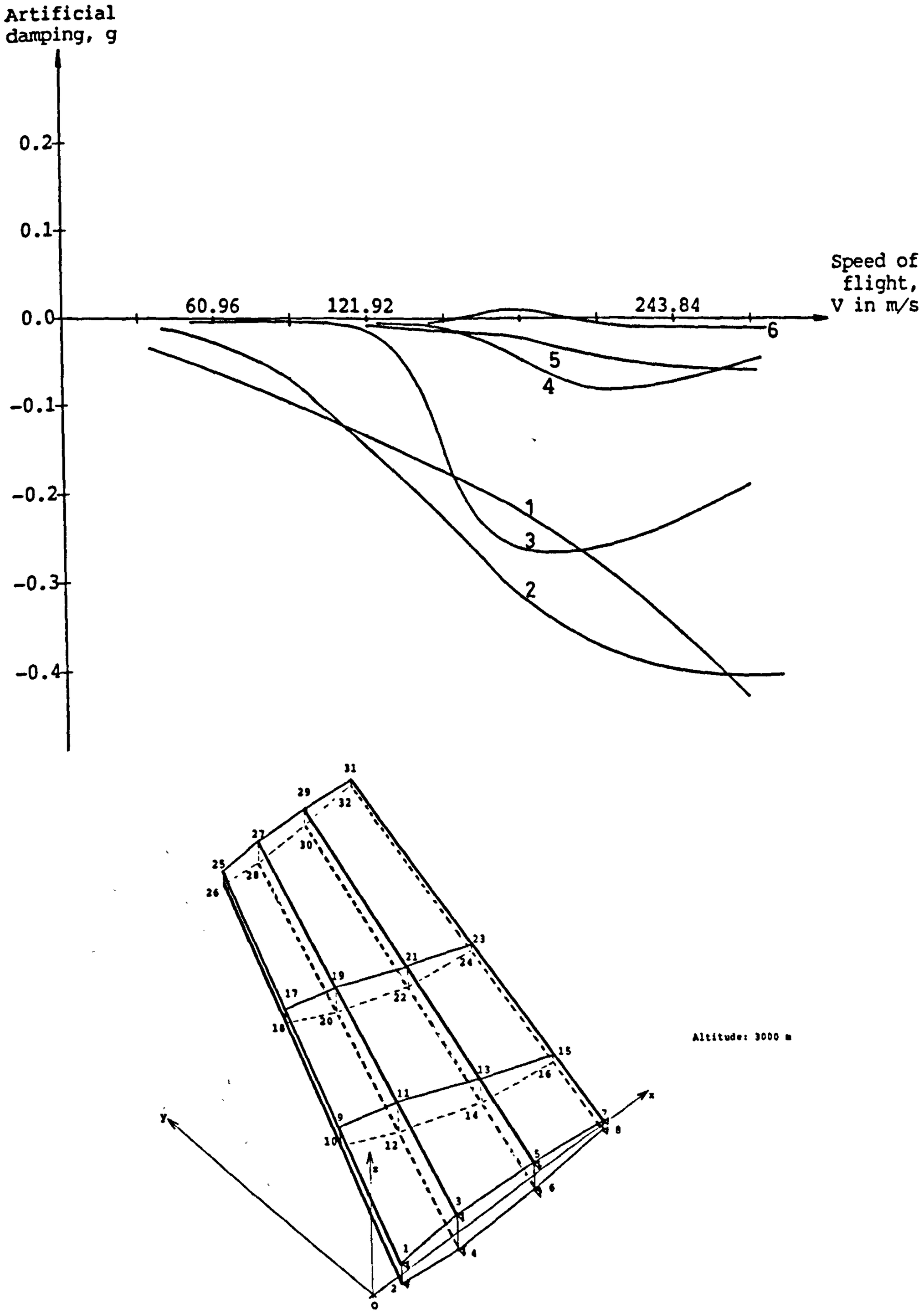

Fig. VII.3 Full "V-g" solutions for the swept tailplane

		BASE DESIGN	CONSTRAINTS	OPTIMUM DESIGN	
Design variable	Element linkages	Starting dimension	Minimum dimension	Final dimension	
1	1	0.90×10^{-3} (pas.)	0.90×10^{-3}	0.90×10^{-3} (pas.)	m
2	2	0.90×10^{-3} (pas.)	0.90×10^{-3}	0.90×10^{-3} (pas.)	
3	3	0.90×10^{-3} (pas.)	0.90×10^{-3}	0.90×10^{-3} (pas.)	
4	4	0.90×10^{-3} (pas.)	0.90×10^{-3}	0.90×10^{-3} (pas.)	
5	5 and 6	0.70×10^{-3} (pas.)	0.70×10^{-3}	0.70×10^{-3} (pas.)	
6	7 and 8	0.70×10^{-3} (pas.)	0.70×10^{-3}	0.70×10^{-3} (pas.)	
7	9 and 10	0.70×10^{-3} (pas.)	0.70×10^{-3}	0.70×10^{-3} (pas.)	
8	11 and 12	34.10×10^{-6} (pas.)	34.10×10^{-6}	34.10×10^{-6} (pas.)	m^2
9	13 and 14	34.10×10^{-6} (pas.)	34.10×10^{-6}	34.10×10^{-6} (pas.)	
10	15 and 16	34.10×10^{-6} (pas.)	34.10×10^{-6}	34.10×10^{-6} (pas.)	
11	17 and 18	34.10×10^{-6} (pas.)	34.10×10^{-6}	34.10×10^{-6} (pas.)	
12	19	0.50×10^{-3} (pas.)	0.50×10^{-3}	0.50×10^{-3} (pas.)	m
13	20	0.50×10^{-3} (pas.)	0.50×10^{-3}	0.50×10^{-3} (pas.)	
14	21	0.50×10^{-3} (pas.)	0.50×10^{-3}	0.50×10^{-3} (pas.)	
15	22	0.50×10^{-3} (pas.)	0.50×10^{-3}	0.50×10^{-3} (pas.)	
16	23	0.50×10^{-3} (pas.)	0.50×10^{-3}	0.50×10^{-3} (pas.)	
17	24	0.50×10^{-3} (pas.)	0.50×10^{-3}	0.50×10^{-3} (pas.)	
18	25	0.50×10^{-3} (pas.)	0.50×10^{-3}	0.50×10^{-3} (pas.)	
19	26 and 27	0.70×10^{-3} (pas.)	0.70×10^{-3}	0.70×10^{-3} (pas.)	
20	28 and 29	0.70×10^{-3} (pas.)	0.70×10^{-3}	0.70×10^{-3} (pas.)	
21	30 and 31	0.70×10^{-3} (pas.)	0.70×10^{-3}	0.70×10^{-3} (pas.)	
22	32 and 33	25.40×10^{-6} (pas.)	25.40×10^{-6}	25.40×10^{-6} (pas.)	m^2
23	34 and 35	25.40×10^{-6} (pas.)	25.40×10^{-6}	25.40×10^{-6} (pas.)	
24	36 and 37	25.40×10^{-6} (pas.)	25.40×10^{-6}	25.40×10^{-6} (pas.)	
25	38 and 39	25.40×10^{-6} (pas.)	25.40×10^{-6}	25.40×10^{-6} (pas.)	
26	40	0.50×10^{-3} (pas.)	0.50×10^{-3}	1.51×10^{-3} (act.)	m
27	41	0.50×10^{-3} (pas.)	0.50×10^{-3}	0.50×10^{-3} (pas.)	
28	42	0.50×10^{-3} (pas.)	0.50×10^{-3}	0.50×10^{-3} (pas.)	
29	43	12.30×10^{-3} (act.)	0.50×10^{-3}	0.50×10^{-3} (pas.)	
30	44	12.30×10^{-3} (act.)	0.50×10^{-3}	0.50×10^{-3} (pas.)	
31	45	12.30×10^{-3} (act.)	0.50×10^{-3}	0.50×10^{-3} (pas.)	
32	46	12.30×10^{-3} (act.)	0.50×10^{-3}	0.50×10^{-3} (pas.)	
33	47 and 48	0.70×10^{-3} (pas.)	0.70×10^{-3}	0.70×10^{-3} (pas.)	
34	49 and 50	0.70×10^{-3} (pas.)	0.70×10^{-3}	0.70×10^{-3} (pas.)	
35	51 and 52	0.70×10^{-3} (pas.)	0.70×10^{-3}	0.70×10^{-3} (pas.)	
36	53 and 54	25.90×10^{-6} (pas.)	25.90×10^{-6}	25.90×10^{-6} (pas.)	m^2
37	55 and 56	25.90×10^{-6} (pas.)	25.90×10^{-6}	25.90×10^{-6} (pas.)	
38	57 and 58	25.90×10^{-6} (pas.)	25.90×10^{-6}	25.90×10^{-6} (pas.)	
39	59 and 60	25.90×10^{-6} (pas.)	25.90×10^{-6}	25.90×10^{-6} (pas.)	
40	61	0.50×10^{-3} (pas.)	0.50×10^{-3}	2.56×10^{-3} (act.)	m
41	62	0.50×10^{-3} (pas.)	0.50×10^{-3}	0.50×10^{-3} (pas.)	
42	63	0.50×10^{-3} (pas.)	0.50×10^{-3}	0.50×10^{-3} (pas.)	
		Mass		Mass	
		44.76 kg		33.12 kg	

Altitude: 3000 m

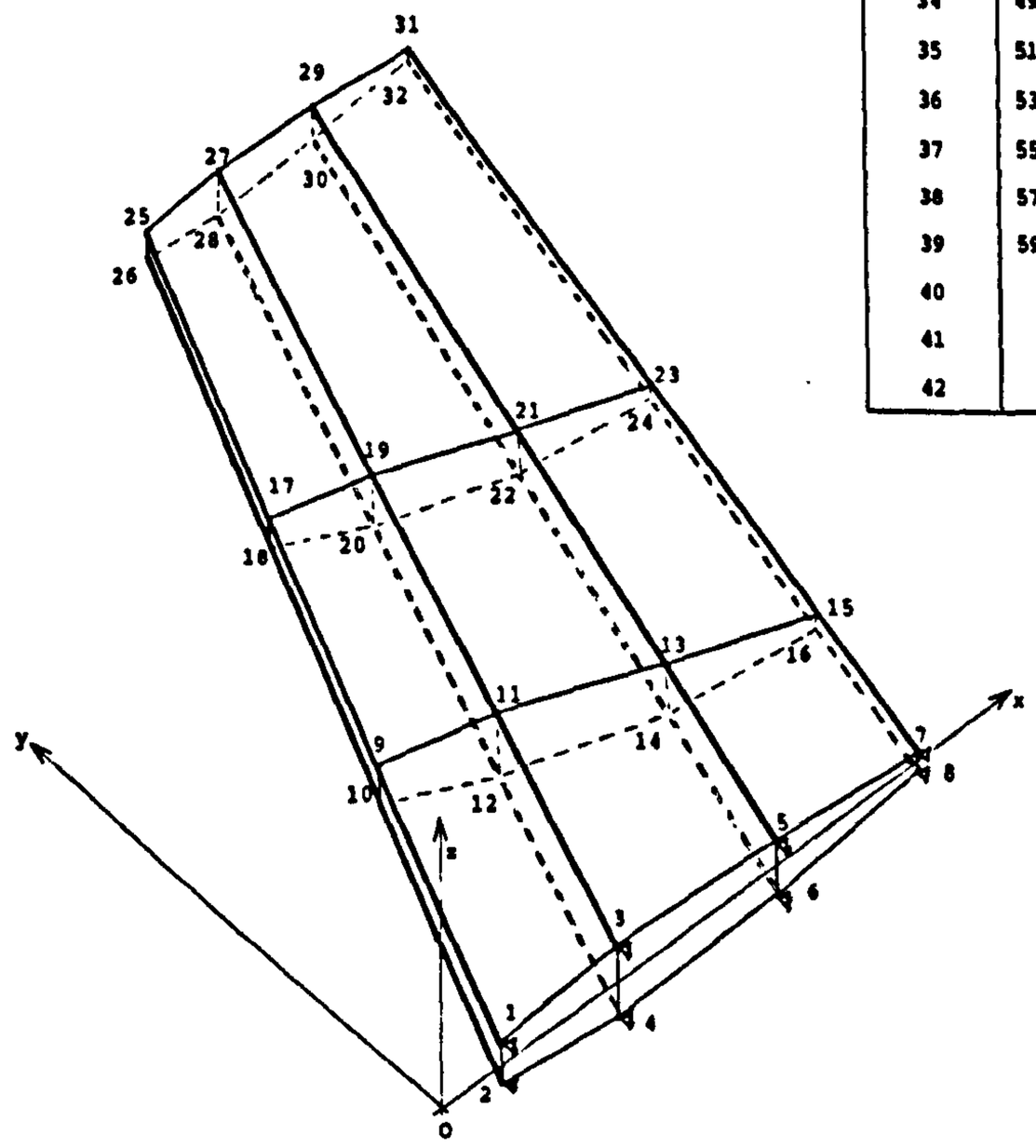

Table VII.3 Design progress of the swept tailplane

CHAPTER VIII

CHECKS AND DEBUGGING

Because the flutter optimization program is extremely complex, a systematic programme of error checking and "debugging" has been followed. This is becoming an essential aspect of developing usable software and it is the author's belief that modern computer-based PhD's should produce this type of software.

1 FINITE ELEMENTS

Mass and stiffness matrices of individual elements and of simple structures were printed and checked with those obtained by a conventional hand calculator.

2 EIGENVALUE ECONOMIZER

Excellent correlation between the reduced and full "free-vibration eigenvalue" problems has been established in chapter VI (see tables VI.1 up to VI.8).

3 SURFACE SPLINES

Satisfactory agreement between plots of mode shapes at points on structural grid and on aerodynamic grids were observed.

4 UNSTEADY AIRLOADS

After the modifications were performed on the "unsteady

aerodynamic" module, the test problems of Ref. 11 were run to verify that no bugs were introduced as a result of our repeated intrusion into the source code.

5 FLUTTER SOLUTIONS

Difficulties arouse in the debugging phase of this analysis as we were unable to duplicate other people's flutter speed predictions apart from that of Ref. 1 because not all parameters about the structural member sizes and flight conditions were produced by the authors to permit comparison.

Fig. VIII.1 displays the "V-g" plots obtained by our program for the rectangular-planform wing for the same flight conditions and structural mass distribution as that of Ref. 1. A flutter point is produced at 237 m/s and a divergence point at 250m/s.

In an attempt to further validate this major analysis module, resort was made to a NASTRAN run which was performed by courtesy of Herr O.Sensburg in MBB at Munich. All the unstable modes of our program, NASTRAN and Ref. 1 are reproduced in one single figure (Fig. VIII.2) in an effort to enhance the comparisons.

In Ref. 1, only the critical flutter mode is given and its speed compares favorably with that obtained here (2.8% error). Whilst there is just a slight difference between

NASTRAN and our divergence mode, it is disturbing to observe a much higher difference of 15.6% on the flutter speeds. This has been a source of consternation and, in seeking for an explanation, it was noted that NASTRAN employs only three modes in the modal analysis. Whilst It is tempting to accept this as an explanation, it seems unlikely that this on its own can justify the large flutter prediction gap. We, therefore, checked also the free-vibration eigensolutions — the only preliminary results provided in the NASTRAN outputs — for consistency with our work. As far as plots of eigenvectors are concerned, the classification and the shape of the modes were the same as the one given by our program. There were, however, unusually large discrepancies in the comparison of the eigenvalues (see table VIII.1). Our eigenvalues have been confirmed by two other finite-element packages, LUSAS and PAFEC, for the rectangular-planform wing, swept tailplane as well as for many other types of structures. The apparent errors of NASTRAN should not remain unexplained and consultation of the NASTRAN theoretical manual (Ref. 32, § 5) suggests that they can be attributed to the non-compatibility of the NASTRAN rod elements and the NASTRAN quadrilateral elements.

6 DERIVATIVES

The results of the derivatives of the artificial damping and of the frequency agree reasonably well with those calculated using a finite-difference scheme.

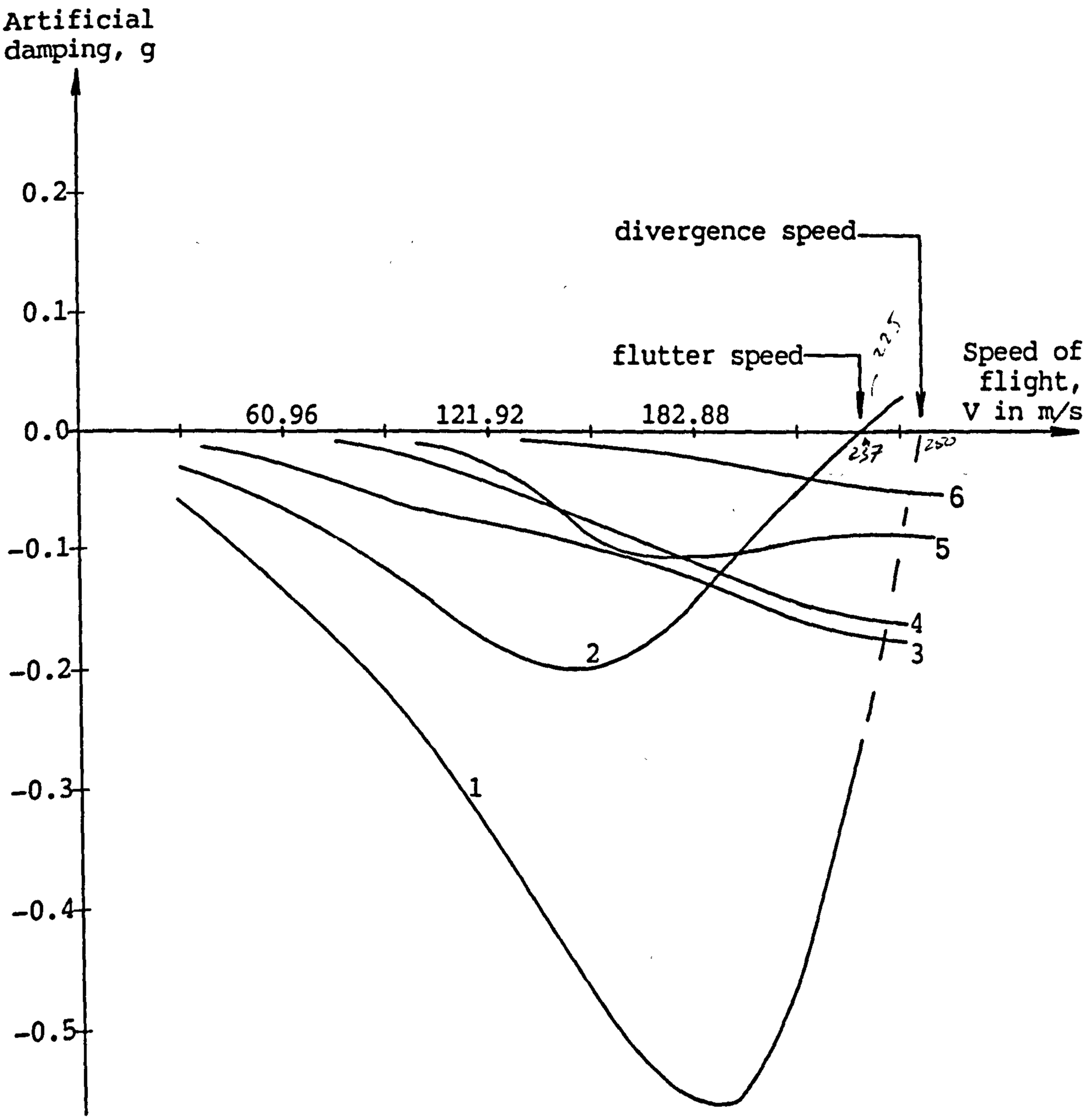

Rectangular-planform wing

Element No.	Element dimensions
1, 2, 3, 7, 8, 9, 16, 17, 18, 22, 23 and 24	1.290×10^{-3} m^2
4, 5, 6, 19, 20 and 21	2.032×10^{-3} m
10, 11, 12, 13, 14, 15, 25, 26 and 27	1.016×10^{-3} m

Altitude: 1372 m

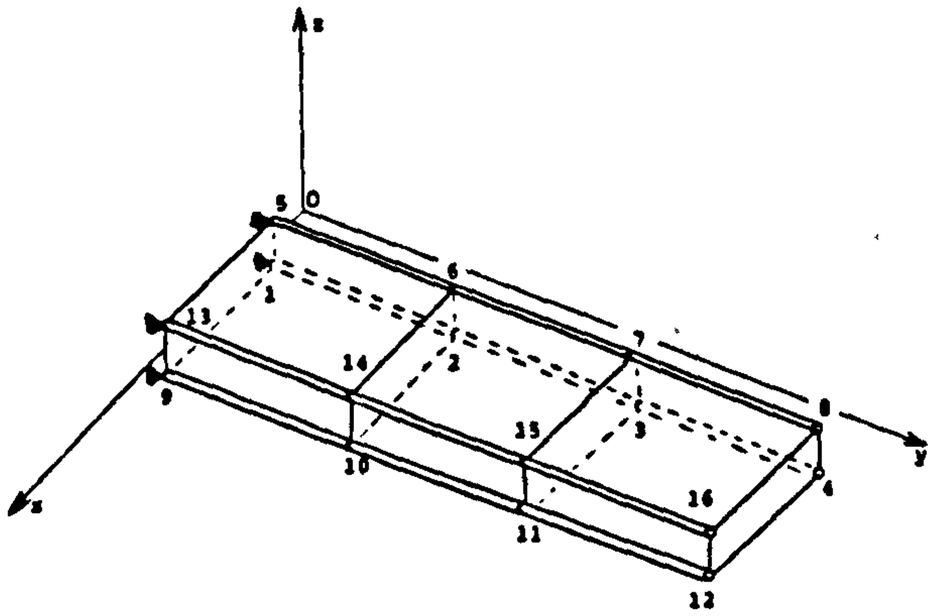

Fig. VIII.1 Full "V-g" plots of the rectangular-planform wing as produced by our program

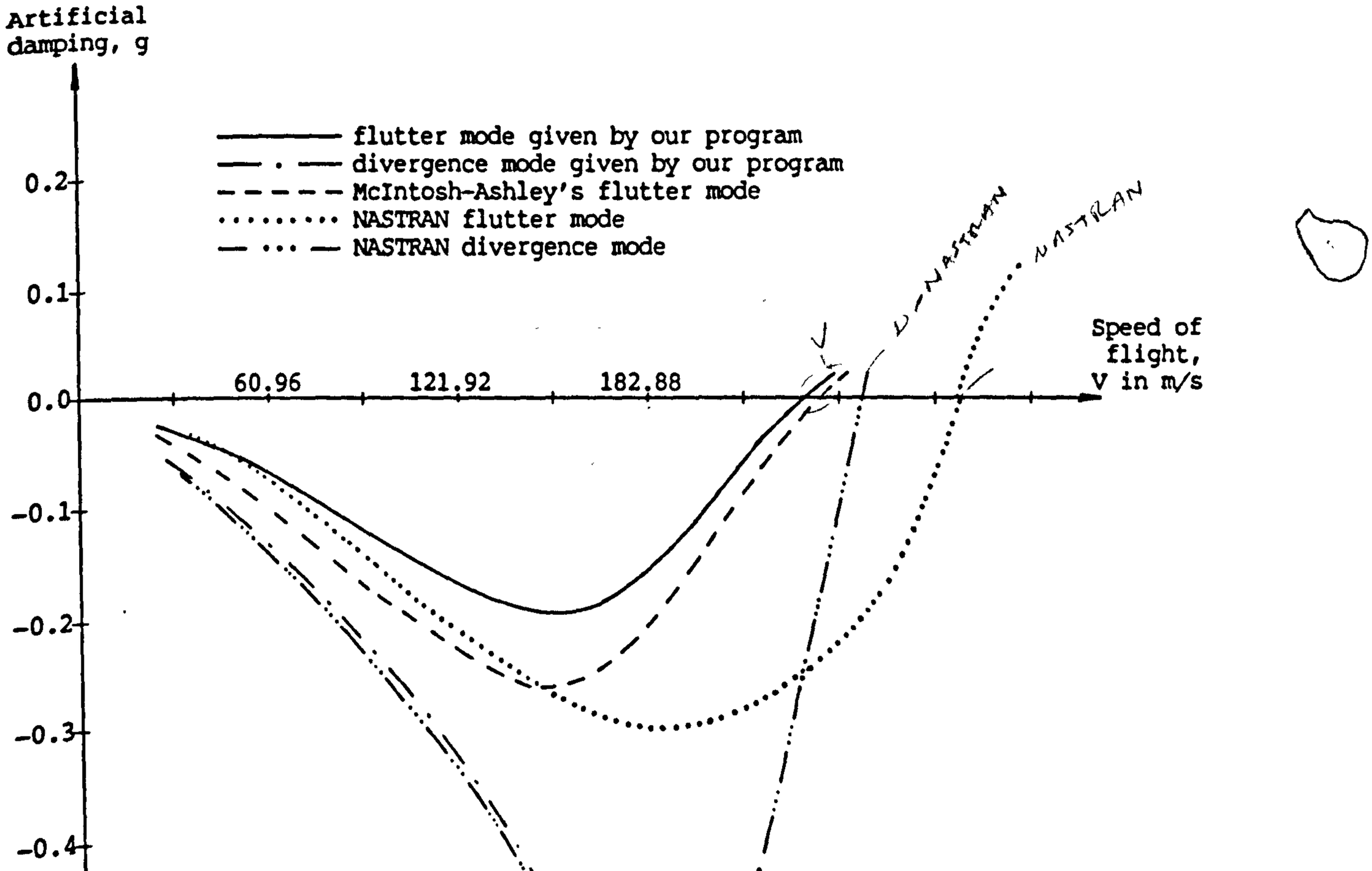

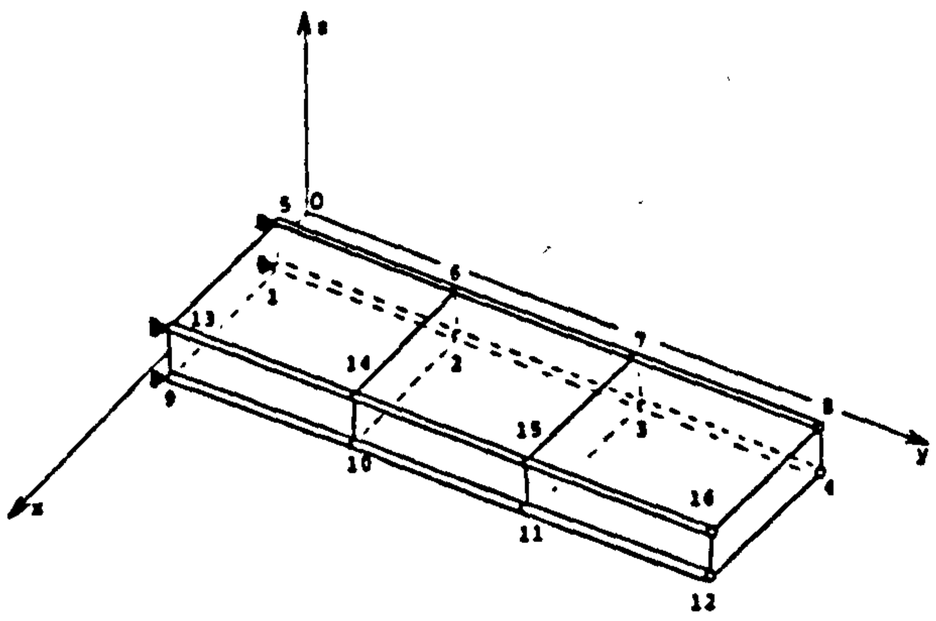

Rectangular-planform wing

Element No.	Element dimensions
1, 2, 3, 7, 8, 9, 16, 17, 18, 22, 23 and 24	1.290×10^{-3} m^2
4, 5, 6, 19, 20 and 21	2.032×10^{-3} m
10, 11, 12, 13, 14, 15, 25, 26 and 27	1.016×10^{-3} m

Altitude: 1372 m

Fig. VIII.2 Critical modes as given by Ref. 1, NASTRAN and our program for the rectangular-planform wing

Table VIII.1 Comparison of natural frequencies as obtained by our program, LUSAS and by NASTRAN

Mode	Natural frequencies in Hz		
	our program	LUSAS+	NASTRAN
1	10.78	10.84	6.42
2	28.67	26.86	25.03
3	37.00*	37.14*	33.78*
4	69.20	71.94	38.31
5	104.20	100.73	———
	⋮	⋮	

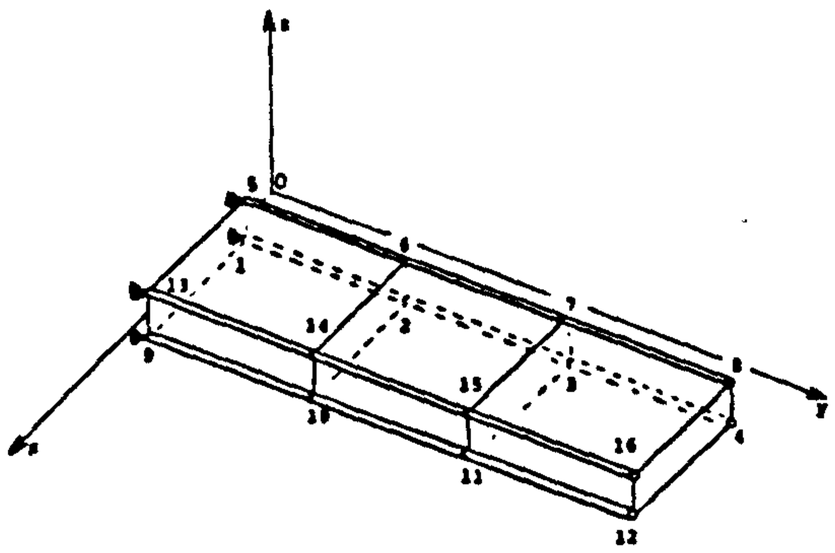

Rectangular-planform wing

Element No.	Element dimensions
1, 2, 3, 7, 8, 9, 16, 17, 18, 22, 23 and 24	1.290×10^{-3} m^2
4, 5, 6, 19, 20 and 21	2.032×10^{-3} m
10, 11, 12, 13, 14, 15, 25, 26 and 27	1.016×10^{-3} m

* Inplane mode
\+ Developed by: Finite Element Analysis Ltd. 25 Holborn Viaduct. London EC1A 2BP. England

CHAPTER IX

CONCLUSIONS AND OUTLOOK

1 PROGRAM UPDATES

The program represents a further step towards the development of a flutter synthesis package. Since the variety of applications and the design environment of this program have been cited elsewhere in the main text, it is appropriate at this stage to indicate its limits. Some guidelines for further extensions or modifications are presented in this section.

The FINEL (finite elements package) version used in the development of our program does not offer a bewildering choice of finite elements. In the course of the work, elementary linear elements such as pin-jointed element (bar), quadrilateral in-plane element (membrane) or triangular in-plane element (membrane) were added to the very limited FINEL element library. Further expansions of the finite-element library are of paramount importance. It is also hoped that FINEL will be extended to the idealization of composite materials thereby leading to the possibility of broadening the aeroelastic capability of the program to static divergence.

As with stress constrained problems, it may be beneficial to augment the program with a feature which allows designing first with an intuitive flutter criterion to within the vicinity of the optimum and then refine the solution with a stricter technique. Although this opportunity has not been

exploited, we would expect it to bring in realistic improvements to the overall program performance.

Finally, in the following, we make passing reference to necessary changes to orient the program towards general use:

— data dumped in the Data Base should be saved so that restarts of jobs could be made possible;

— drastic improvements of the format presentation and arrangement of the input data should be made;

— a more elaborate data pre-processor than the one already built in must be provided to carry out extensive checks of the data so as to diagnose beforehand potential unscheduled program stops.

2 CONCLUSIONS

The time spent in developing the program exacerbated the quantity and diversity of the results we would have hoped to conclusively achieve in the specific field of flutter synthesis. One area of lengthy activity and preparations that we could not fully exploit is the dual bounding technique. The question of how substantial is the contribution of such a method towards the efficiency of flutter optimization should not be left unanswered. To this end, the first subsequent work on the program should be to add a straightforward and simple routine for automatically bounding the weight and

another routine that interpolates [Q] and its derivatives relatively to ν for any values of ν when the fixed-mode method is used. CPU times should be then made available comparing the fixed-mode method with dual bounding and the continuous-mode-updating method.

It has been one of the conclusions of other investigators that CPU times tend to corroborate OC as a technique well suited to flutter constrained problems. Extreme caution should be exercised, however, towards any premature conclusion about their reliability. It must be said that even MP techniques experience non-convergence for certain types of flutter problems (Ref. 48). With all the risks involved in flutter synthesis, it is our point of view that dual bounding must be incorporated regardless whether a fixed-mode or an updated-mode method is employed. On the top of the advantages that are specific to flutter synthesis, dual bounding provides a proper management of the resizing process and deals with the elusive nature of automated flutter design in probably the most satisfactory available way.

BIBLIOGRAPHY AND REFERENCES

BIBLIOGRAPHY ON AEROELASTICITY

BISPLINGHOFF,R.L., ASHLEY,H. and HALFMAN,R.L., "Aeroelasticity". Addison-Wesley Publishing Company, Cambridge, Mass. 1955.

BISPLINGHOFF,R.L. and ASHLEY,H., "Principles of aeroelasticity". John Wiley and Sons, Inc., New York, 1962.

DOWELL,E.H., "Aeroelasticity of plates and shells". Nordhoff International Publishing, Leyden, The netherlands, 1975.

DOWELL,E.H., CURTISS,H.C.,Jr., SCANLAN,R.H. and SISTO,F., "A modern course in aeroelasticity". Sijthoff and Noordhoff, Alphen aan den Rijn, The netherlands, Rockville, Maryland, USA, 1980.

FREBERG,C.R. and KEMLER,E.N., "Aircraft vibration and flutter". John Wiley and Sons, Inc., New York, 1955.

FUNG,Y.C., "An introduction to the theory of aeroelasticity". John Wiley and Sons, Inc., New York, 1955.

SCALAN,R.H. and ROSENBAUM,R., "Aircraft vibration and flutter". Dover Publications, Inc., New York, 1968.

BIBLIOGRAPHY ON FINITE ELEMENT METHODS

COOK,R.D., "Concepts and applications of finite element analysis". John Willey & Sons, New York, 1981, second edition.

DHATT,G. and TOUZOT,G., "Une présentation de la méthode des éléments finis". Maloine S.A éditeur, Paris. Les presses de 1' Univérsite Laval, Quebec. 1981.

PRZEMIENIECKI,J.S., "Theory of matrix structural analysis". McGraw-Hill Book Company, New York, 1968.

RAO,S.S., "The finite element method in engineering". Pergamon Press Ltd, Oxford, England, 1982.

BIBLIOGRAPHY ON OPTIMIZATION

MORRIS,A.J., editor, "Foundations of structural optimization: a unified approach". John Wiley & Sons Ltd, 1982.

REFERENCES

1 ASHLEY,H. and McINTOSH,S.C.,Jr., "On the optimization of discrete structures with aeroelatic constraints". Computer and Structures, Vol. 8, No 3/4, May 1978, pp. 411-419.

2 BARTHOLOMEW,P., "A dual bound used for monitoring structural optimization programs". Engineering Optimization, Vol. 4, No 1, 1979, pp. 45-50.

3 BATHIA,K.G, "An automated method for determining the flutter velocity and the matched point". Journal of aircraft, Vol. 11, No 1, January 1974, pp. 21-27.

4 BELEGUNDU,A.D. and ARORA,J.S., "A study of mathematical programming methods for structural optimization. Part I: theory". International Journal for Numerical Methods in Engineering, Vol. 21, September 1985, pp. 1583-1599.

5 BELEGUNDU,A.D. and ARORA,J.S., "A study of mathematical programming methods for structural optimization. Part II: numerical results". International Journal for Numerical Methods in Engineering, Vol. 21, September 1985, pp. 1601-1623.

6 BELINGER,D., editor, "MSC/NASTRAN, aeroelastic supplement". The MacNeal-Schwendler Corporation, 7442

N.Figueroa Street, Los Angeles, USA, 1980.

7 CAMPUS and MASSONET, "Comportement postcritique des plaques utilisées en construction métallique". Colloque international tenu a l' Univérsite de Liège, mémoires de la Sociéte Royale des Sciences de Liège (in particular the contribution to the discussion by Koiter,W.T. and Skaloud,M. pp. 66-67 and page 103).

8 CARDANI,C. and MANTEGAZZA,P., "Calculation of eigenvalue and eigenvector derivatives for algebraic flutter and divergence eigenproblems". AIAA Journal, Vol. 17, April 1979, pp. 408-412.

9 DAT,R. and MEURZEC,J.L., "Sur les calculs de flottement par la methode dite du balayage en frequence reduite". La Recherche Aerospatiale, No 133, November-December 1969, pp. 41-43.

10 DAVIES,D.E, "Calculation of unsteady generalized airforces on a thin wing oscillating harmonically in subsonic flow". RAE report, A.R.C. R. & M. No. 3049, August 1963.

11 DAVIES,D.E., "On the use of Fortran programs for evaluating the generalized airforces and aerodynamic loading on a flat plate wing oscillating harmonically in subsonic flow". RAE Technical Memorandum Structures 881, January 1976.

12 DAVIES,D.E., "Theoretical determination of subsonic oscillatory airforce coefficients". RAE report, A.R.C. R. & M. No 3804, May 1976.

13 DESMARAIS,R.N. and BENNET,R.M., "An automated procedure for computing flutter eigenvalues". Journal of Aircraft, Vol. 11, February 1974, pp. 75-80.

14 DUNCAN,W.J., "The fundamentals of flutter, part I and part II". Journal of Aircraft Engineering, January 1945, pp. 16-26 and February 1945, pp. 32-38.

15 FLEURY,C., "A unified approach to structural weight minimization". Computer Methods in Applied Mechanics and Engineering, Vol. 20, No 1, 1979, pp. 17-38.

16 FLEURY,C. and SANDER,G., "Relations between optimality criteria and mathematical programming in structural optimization". Proceedings Symposium on Applications of Computer Methods in Engineering. University of Southern California, Los Angeles, August 1977, pp. 507-520.

17 FUNG,Y.C. and SECHLER,E.E., editors, "Thin-shell structures. Theory, experiment and design". pp. 157-201, Prenctice-Hall, Inc., Englewood Cliffs, New Jersey, 1974.

18 GIRARD,R., "Une méthode d' optimisation appliquée aux

structures composites". Note technique No 228, ONÉRA, 1974.

19 GWIN,L.B., "Optimal aeroelastic design of an oblique wing structure". AIAA paper 74-349.

20 GWIN,L.B. and McINTOSH,S.C.,Jr., "A method of minimum-weight synthesis for flutter requirements, part I - Analytical investigation". AFFDL-TR-72-22, June 1972.

21 GWIN,L.B. and TAYLOR,R.F., "A general method for flutter optimization". AIAA paper No 73-391, AIAA/ASME/SAE 14th structures, structural dynamics and material conference, Williamsburg, Virginia, March 1973.

22 HAFTKA,R.T., STARNES,J.H.,Jr. and BARTON,F.W., "A comparison of two types of structural optimization procedures for satisfying flutter requirements". AIAA paper No 74-405, AIAA/ASME/SAE 15th structures, structural dynamics and materials conference, Las Vegas, Nevada, April 1974.

23 HAFTKA,R.T. and YATES,E.C.,Jr., "On repetitive flutter calculations in structural design". AIAA paper No 74-141, AIAA 12th aerospace sciences meeting, Washington, D.C, January-February 1974.

24 HITCHINGS,D., "FINEL introduction manual". Imperial

College of Science and Technology, Dept. of Aeronautics.

25 HITCHINGS,D., "FINEL programming manual". Imperial College of Science and Technology, Dept. of Aeronautics.

26 HITCHINGS,D., "FINEL user's manual". Imperial College of Science and Technology, Dept. of Aeronautics.

27 JOHNSON,W., "Application of unsteady airfoil theory to rotary wings". Journal of Aircraft, Vol. 17, April 1980, pp. 285-286.

28 KAZA,K.R.V., "Application of unsteady airfoil theory to rotary wings". Journal of Aircraft, Vol. 18, July 1981, pp. 604-605.

29 KOTTAPALLI,S.B.R., "Unsteady aerodynamics of oscillating airfoils with inplane motions". Journal of the American Helicopter Society, Vol. 30, January 1985, pp. 62-63.

30 LANSING.W., LERNER,E. and TAYLOR,R.F., "Applications of structural optimization for strength and aeroelastic design requirements". AGARD Report No. 664, paper presented at the 45th structures and material panel meeting, Voss, Norway, September 1977.

31 LAWRENCE,A.J. and JACKSON.P., "Comparison of different methods of assessing the free oscillatory characteristics of aeroelastic systems". RAE report,

A.R.C. C.P. No. 1084, December 1968.

32 MACNEAL,R.H., editor, "The NASTRAN theoretical manual". The MacNeal-Schwendler Corporation, 7442 N.Figueroa Street, Los Angeles, USA, 1972.

33 MEIROVITCH,L., "Computational methods in structural dynamics". Sijthoff and Noordhoff, Alphen aan den Rijn, The netherlands, Rockville, Maryland, USA, 1980.

34 MORRIS,A.J., BARTHOLOMEW,P. and DENNIS,J., "A computer based system for structural design, analysis and optimization". Paper presented at the Flight Mechanics Panel Symposium on "the use of computers as a design tool", Germany, 3-6 September 1979; AGARD conference proceedings No 280,

35 NGUYEN,D.T, ARORA,J.S. and BELEGUNDU,A.D, "Design optimization codes for structures: DOCS computer program". Journal of Aircraft, Vol. 20, September 1983, pp. 817-824.

36 O'CONNELL,R.F., "Incremented flutter analysis". Journal of Aircraft, Vol. 11, April 1974, pp. 236-240.

37 O'CONNELL,R.F., RADOVCICH,N.A. and HASSIG,H.J., "Structural optimization with flutter speed constraints using maximized step size". Journal of Aircraft, Vol. 14, January 1977, pp. 85-89.

38 PINES,S., "An elementary explanation of the flutter mechanism". Proceedings National Specialists Meeting on Dynamics and Aeroelasticity. Institute of the Aeronautical sciences, Ft. Worth, Texas, November 1958. pp. 52-58.

39 PINES,S. and NEWMAN,M., "Structural optimization for aeroelastic requirements". AIAA paper No 73-389, AIAA/ASME/SAE 14th structures, structural dynamics and materials conference, Williamsburg, Virginia, March 1973.

40 RAO,S.S., "Rates of change of flutter Mach number and flutter frequency". AIAA Journal, Vol. 10, December 1972, pp. 1526-1528.

41 ROGERS,C.L., "Derivatives of eigenvalues and eigenvectors". AIAA Journal, Vol. 8, May 1970, pp. 943-944.

42 RUDISILL,C.S. and BHATIA,K.G., "Optimization of complex structures to satisfy flutter requirements". AIAA Journal, Vol. 9, August 1971, pp. 1487-1491.

43 RUDISILL,C.S. and BHATIA,K.G., "Second derivatives of the flutter velocity and the optimization of aircraft structures". AIAA Journal, Vol. 10, December 1972, pp. 1569-1572.

44 SCHMIT,L.A. "Structural design by systematic synthesis". Proceedings of the 2nd conference on electronic computation. ASCE, New York, 1960, pp. 105-122.

45 SEGENREICH,S.A. and McINTOSH,S.C.,Jr., "Weight minimization of structures for fixed flutter speed via an optimality criterion". AIAA paper No 75-779, AIAA/ASME/SAE 16th structures, structural dynamics and materials conference, Denver, Colorado, USA, May 1975.

46 SIEGEL,S., "A flutter optimization program for aircraft structural design". AIAA paper No 72-795, AIAA 4th aircraft design, flight test and operations meeting, Los Angeles, California, USA, August 1972.

47 SOBIESZCZANSKI,J. and LOENDORF,D., "A mixed optimization method for automated design of fuselage structures". Journal of Aircraft, Vol. 9, December 1972, pp. 805-811.

48 STROUD,W.J., "Automated structural design with aeroelastic constraints: a review and assessment of the state of the art". Structural optimization symposium, AMD Vol. 7, pp. 77-118, ASME, New York, 1974.

49 STROUD,W.J., DEXTER,C.B. and STEIN,M., "Automated preliminary design of simplified wing structures to satisfy strength and flutter requirements". NASA TN D-6534, December 1971.

50 SYMODYNES,E.E., "Gradient optimization of structural weight for specified flutter speed". Journal of Aircraft, Vol. 11, March 1974, pp. 143-147.

51 THOMPSON,G.O. and KASS,G.J., "Active flutter suppression, an emerging technology". Journal of Aircraft, Vol. 9, January 1972, pp. 230-235.

52 THOMSON,W.T., "Theory of vibration with applications". Prenctice-Hall, Inc., Englewood Cliffs, 1981.

53 TURNER,M.J., "Optimization of structures to satisfy flutter requirements". AIAA Journal, Vol. 7, May 1969, pp. 945-951.

54 WILKINSON,K., MARKOWITZ,J., LERNER,E., GEORGE,D. and BATILL,S.M., "FASTOP: a flutter and strength optimization program for lifting-surface structures". Journal of Aircraft, Vol.14, June 1977, pp. 581-587.

55 WYKES,J.H., MILLER,G.D. and BROSNAN,M.J., "Rigid-body structural mode coupling on a forward swept wing aircraft and an active control solution". Proceedings of the International Conference on Forward Swept Wing Aircraft, University of Bristol, UK, 24-26 March 1982.

APPENDIX A

GENERALIZED EQUATION OF MOTION

The flutter equation which is used throughout the main text and appendices differs slightly in its form from those used by others. Therefore, a decision was taken to proceed in this appendix by showing how this generalized equation of motion is derived so that any further work on this equation does not require elaborate explanation. The terms utilized in this equation are unequivocally defined in this appendix.

In formulating the flutter equation of a system, the extraordinarly valuable principle of Lagrange's equation and concept of generalized coordinates are often used. A detailed description of these is left to classical books in mechanics. It is, however, of interest to recall that the Lagrangian function is given by

$$L = T - \Pi_p \tag{A.1}$$

where T is the system kinetic energy and Π_p is the system potential energy. We are concerned here with the case where elastic stiffness is predominant and we will refer to Π_p as strain energy.

For a non-conservative discrete system of order n, the Lagrangian differential equations of motion take the form

$$\frac{d}{dt}\left(\frac{\partial L}{\partial \dot{q}_i}\right) - \left(\frac{\partial L}{\partial q_i}\right) + \left(\frac{\partial R}{\partial \dot{q}_i}\right) = Q_i \qquad i = 1,\ldots,n \tag{A.2}$$

q_i ith generalized coordinate

$\dot{}$ time differentiation, $\dot{q}_i \equiv \frac{\partial q_i}{\partial t}$

Q_i ith generalized aerodynamic force

R dissipation energy (structural damping)

For structures modelled by finite elements with a finite number of degrees of freedom, the different energy terms can be expressed as follows

$$\left.\begin{aligned} T &= \frac{1}{2}\{\dot{U}\}^T[M]\{\dot{U}\} \\ \Pi_p &= \frac{1}{2}\{U\}^T[K]\{U\} \end{aligned}\right\} \quad (A.3a)$$

$$R = \frac{1}{2}\{\dot{U}\}^T[C]\{\dot{U}\} \quad (A.3b)$$

[M] mass or inertia matrix of order r×r

[K] stiffness matrix of order r×r

[C] structural damping matrix of order r×r

$\{U\} \equiv \{U(x,y,z,t)\}$

{U} is the vector of nodal displacements and depends on the spatial cartesian coordinates x,y and z of the nodes of the finite element mesh and on the time t. {U} describes the r discret freedoms of the system.

The dissipation through structural damping can be rewritten by entering the expression of the damping matrix [C] (see appendix B, Eq. B.1) into Eq. A.3b. Hence,

$$R = \frac{1}{2}\,\frac{g}{\omega}\,\{\dot{U}\}^T[K]\{\dot{U}\} \quad (A.3c)$$

We now proceed to the special case of flutter of aircraft lifting surfaces. If the x- and y-axis define the

plane of the lifting surface and the z-axis is the out-of-plane axis, the structure can be reasonably assumed to vibrate principally in the direction of the z-axis. This is tantamount to retaining only transverse degrees of freedom (displacement parallel to the z-axis). The static force-displacement equations, $[K]\{U\}=\{P\}$, can be used to derive the relationship between the out-of-plane and in-plane degrees of freedom. After assuming that no loads are applied to the in-plane degrees of freedom and after a proper separation and rearrangement of the degrees of freedom, these equations become

$$\left[\begin{array}{c|c} [K_{mm}] & [K_{ms}] \\ \hline [K_{sm}] & [K_{ss}] \end{array}\right] \left\{\begin{array}{c} \{w\} \\ \hline \left\{\begin{array}{c}\{u\}\\\{v\}\end{array}\right\} \end{array}\right\} = \left\{\begin{array}{c} \{P\} \\ \hline \{0\} \end{array}\right\} \qquad (A.4)$$

$[K_{mm}]$ order p×p

$[K_{sm}]$ order q×p

$[K_{ms}]$ order p×q; $[K_{ms}] = [K_{sm}]^T$

$[K_{ss}]$ order q×q

$\{w\}$ vector of p nodal displacements in the z-direction; out-of-plane or transverse displacements of the nodes of the structure

$\left\{\begin{array}{c}\{u\}\\\{v\}\end{array}\right\}$ vector of q nodal displacements in the x- and y-direction (not necessarily separated); in-plane displacements of the nodes of the structure

$\{P\}$ load vector; order p

$r = p + q$

p number of out-of-plane degrees of freedom

q number of in-plane degrees of freedom (not related to and not to be confused with the generalized coordinate q_i)

q should be twice p; however, this is not always valid as the ratio of m and p is dependent on the number and directions of the restraints imposed on the structure.

From the lower partition of Eq. A.4, we find

$$\left[K_{sm} \right]\{w\} + \left[K_{ss} \right]\begin{Bmatrix}\{u\}\\ \{v\}\end{Bmatrix} = \{0\} \qquad (A.5)$$

leading to

$$\begin{Bmatrix}\{u\}\\ \{v\}\end{Bmatrix} = -\left[K_{ss} \right]^{-1}\left[K_{sm} \right]\{w\} \qquad (A.6)$$

Eq. A.6 can be used to yield the following equation giving a coordinate transformation relationship

$$\{U\} \equiv \begin{Bmatrix}\{w\}\\ - - -\\ \begin{Bmatrix}\{u\}\\ \{v\}\end{Bmatrix}\end{Bmatrix} = \begin{bmatrix}\ulcorner 1 \lrcorner\\ - - - - - - - - - - -\\ -\left[K_{ss} \right]^{-1}\left[K_{sm} \right]\end{bmatrix}\{w\} \equiv [T]\{w\} \qquad (A.7)$$

$\ulcorner 1 \lrcorner$ identity matrix of order pxp

[T] transformation matrix; order rxp

With the transformation matrix shown in Eq. A.7, the energy terms (Eq. A.3a and A.3c) can be restated as

$$\left.\begin{aligned} T &= \frac{1}{2}\{\dot{w}\}^T[T]^T[M][T]\{\dot{w}\} \\ \Pi_p &= \frac{1}{2}\{w\}^T[T]^T[K][T]\{w\} \\ R &= \frac{1}{2}\,\frac{g}{\omega}\,\{\dot{w}\}^T[T]^T[K][T]\{\dot{w}\} \end{aligned}\right\} \quad (A.8)$$

Let

$$\left.\begin{aligned} \left[\ M_r\ \right] &= [T]^T[M][T] \\ \left[\ K_r\ \right] &= [T]^T[K][T] \end{aligned}\right\} \quad (A.9)$$

$\left[\ K_r\ \right]$, $\left[\ M_r\ \right]$ reduced stiffness and reduced mass matrices; order pxp

The new equations for the system kinetic, potential and dissipation energies are therefore

$$\left.\begin{aligned} T &= \frac{1}{2}\{\dot{w}\}^T\left[\ M_r\ \right]\{\dot{w}\} \\ \Pi_p &= \frac{1}{2}\{w\}^T\left[\ K_r\ \right]\{w\} \\ R &= \frac{1}{2}\,\frac{g}{\omega}\,\{\dot{w}\}^T\left[\ K_r\ \right]\{\dot{w}\} \end{aligned}\right\} \quad (A.10)$$

Any general vibratory motion of an elastic system having small deflections from an equilibrium configuration can be expressed as a linear combination of the various mode shapes (natural modes of undamped free vibrations). This is the familiar procedure of modal superposition. Thus, the transverse displacement field of the structure can be given

by the following

$$\begin{Bmatrix} w_1 \\ w_2 \\ \vdots \\ w_p \end{Bmatrix} = b \left[\begin{Bmatrix} \zeta_1 \\ \zeta_2 \\ \vdots \\ \zeta_p \end{Bmatrix}_{m_1}, \begin{Bmatrix} \zeta_1 \\ \zeta_2 \\ \vdots \\ \zeta_p \end{Bmatrix}_{m_2} \ldots, \begin{Bmatrix} \zeta_1 \\ \zeta_2 \\ \vdots \\ \zeta_p \end{Bmatrix}_{m_p} \right] \begin{Bmatrix} q_1 \\ q_2 \\ \vdots \\ q_p \end{Bmatrix} \qquad \text{(A.11)}$$

$$\{w\} = b \sum_{i=1}^{p} \{\zeta\}_{m_i} q_i = b\left[\zeta_m \right]\{q\}$$

$$\{w(x,y,z,t)\} = b.\left[\zeta_m(x,y,z)\right].\{q(t)\}$$

b typical (reference) length of the lifting planform

$\{\zeta\}_{m_i}$ shape of ith out-of-plane mode of oscillation of the structure (ith out-of-plane mode shape)

$\left[\zeta_m \right]$ pxp modal matrix whose columns are the out-of-plane mode shapes

{q} weighting vector of order p or vector of modal amplitudes

The typical length by which the second member of Eq. A.11 is multiplied is there simply to render the weighting vector {q} non-dimensional. It may not be superfluous as well to note that the amplitudes of the components of the weighting vector express how each natural mode is contributing in appropriate proportion in the vibration motion.

The basic concept behind the use of mode superposition

is to create a new set of uncoupled equations. For the specific case of flutter, this concept of transforming the problem into a set of uncoupled single-degree-of-freedom systems cannot be easily applied because of the aerodynamic matrix. However, the benefit we will gain for carrying out this linear transformation is to artificially reduce the size of physical degrees of freedom and hence the number of the equations.

For high-order systems such as aircraft structures, it is not necessary nor practical to retain all the mode shapes. The modal matrix can be truncated and the resulting limited number of eigenvectors — corresponding with the lowest natural frequencies — can approximate the vibrating structure with sufficient precision. This leads to reformulating Eq. A.11 into

$$\begin{Bmatrix} w_1 \\ w_2 \\ w_3 \\ \vdots \\ w_p \end{Bmatrix} = b \left[\begin{Bmatrix} \zeta_1 \\ \zeta_2 \\ \zeta_3 \\ \vdots \\ \zeta_p \end{Bmatrix}_{m_1} , \begin{Bmatrix} \zeta_1 \\ \zeta_2 \\ \zeta_3 \\ \vdots \\ \zeta_p \end{Bmatrix}_{m_2} , \ldots , \begin{Bmatrix} \zeta_1 \\ \zeta_2 \\ \zeta_3 \\ \vdots \\ \zeta_p \end{Bmatrix}_{m_n} \right] \begin{Bmatrix} q_1 \\ q_2 \\ \vdots \\ q_n \end{Bmatrix}$$

with $p >> n$

$$\{w\} = b \sum_{i=1}^{n} \{\zeta\}_{m_i} q_i = b\left[\zeta_m \right]\{q\} \qquad (A.12)$$

where in this case $\left[\zeta_m \right]$ and $\{q\}$ are respectively of order pxn and n because only n mode shapes are kept.

Unlike the components of {U} and {w} which have physical meanings such as rotations or translations, the components of {q} are abstract quantities and hence are called generalized displacements or coordinates.

The expression for the Lagrangian function becomes (see Eq. A.1, A10 and A.12)

$$L = \frac{1}{2}b^2\{\dot{q}\}^T\left[\ \zeta_m\ \right]^T\left[\ M_r\ \right]\left[\ \zeta_m\ \right]\{\dot{q}\} - \frac{1}{2}b^2\{q\}^T\left[\ \zeta_m\ \right]^T\left[\ K_r\ \right]\left[\ \zeta_m\ \right]\{q\} \tag{A.13}$$

In a similar way, the dissipation through structural damping can be found

$$\left.\begin{array}{l}\text{Eq. A.10}\\ \text{Eq. A.12}\end{array}\right\} \Rightarrow\ R = \frac{1}{2}\,\frac{g}{\omega}\,b^2\{\dot{q}\}^T\left[\ \zeta_m\ \right]^T\left[\ K_r\ \right]\left[\ \zeta_m\ \right]\{\dot{q}\} \tag{A.14}$$

Because of the assumption of out-of-plane vibrations, the mode shapes are obtained by solving the reduced free vibration problem as stated below

$$\left[\left[\ K_r\ \right] - \left(\omega_N\right)^2\left[\ M_r\ \right]\right]\{\zeta\}_m = \{0\} \tag{A.15}$$

$\left(\omega_N\right)^2$ eigenvalue

ω_N circular natural frequency

$\left[\ K_r\ \right]$ and $\left[\ M_r\ \right]$ as above

$\{\zeta\}_m$ out-of-plane mode shape of the structure

The eigenvectors $\{\zeta\}_m$ are orthogonal with respect to the real symmetric reduced stiffness and inertia matrices. They can be normalized with respect to the inertia matrix so that

$$\{\zeta\}_{m_i}^T \left[M_r \right] \{\zeta\}_{m_j} = \delta_{ij} \qquad i,j = 1,\ldots,p \tag{A.16}$$

where

$$\delta_{ij} = \begin{cases} 1 \text{ if } i=j \\ 0 \text{ if } i \neq j \end{cases} \tag{A.17}$$

δ_{ij} Kronecker delta

It is also evident from Eq. A.15 that as a consequence of Eq. A.16

$$\{\zeta\}_{m_i}^T \left[K_r \right] \{\zeta\}_{m_j} = \left(\omega_{Ni}\right)^2 \delta_{ij} \qquad i,j = 1,\ldots,p \tag{A.18}$$

$\left(\omega_{Ni}\right)^2$ ith eigenvalue corresponding to ith out-of-plane mode shape

With the use of the modal matrix instead of the mode shapes, Eq. A.16 and A.18 appear as

$$\left.\begin{array}{l} \text{Eq. A.16} \\ \text{Eq. A.17} \\ \text{Eq. A.18} \end{array}\right\} \Leftrightarrow \left\{\begin{array}{l} \left[\zeta_m \right]^T \left[M_r \right] \left[\zeta_m \right] = \left[1 \right] \\ \left[\zeta_m \right]^T \left[K_r \right] \left[\zeta_m \right] = \left[\omega_N^2 \right] \end{array}\right\} \tag{A.19}$$

$\left[\ 1\ \right]$ identity matrix; in this context, it is of order nxn if [ζ] is of order pxn

$\left[\ \omega_N^2\ \right]$ spectral matrix; Diagonal matrix of squared natural frequencies or eigenvalues; order nxn

The final expression of the Lagrangian function would show

$$\left.\begin{matrix}\text{Eq. A.13}\\ \text{Eq. A.19}\end{matrix}\right\} \Leftrightarrow L = \frac{1}{2}b^2\{\dot{q}\}^T\left[\ 1\ \right]\{\dot{q}\} - \frac{1}{2}b^2\{q\}^T\left[\ \omega_N^2\ \right]\{q\} \tag{A.20}$$

Similarly, for the dissipation energy

$$\left.\begin{matrix}\text{Eq. A.14}\\ \text{Eq. A.19}\end{matrix}\right\} \Rightarrow R = \frac{1}{2}\frac{g}{\omega}b^2\{\dot{q}\}^T\left[\ \omega_N^2\ \right]\{\dot{q}\} \tag{A.21}$$

Finally, differentiations of Eq. A.20 and A.21 according to Eq. A.2 yields

$$\left(\left[\ 1\ \right]\{\ddot{q}\} + \left[\ \omega_N^2\ \right]\{q\} + \frac{g}{\omega}\left[\ \omega_N^2\ \right]\{\dot{q}\}\right)b^2 = \{Q\} \tag{A.22}$$

with {Q} being the vector that groups all n generalized aerodynamic forces (Eq. A.2).

Next, we turn our attention to the Q_i terms in Eq. A.2 or {Q} in Eq. A.22 which are forces of aerodynamic origin caused by the perturbation of the flow surrounding the fluttering structure. Altogether, these forces are the source of inertia, damping and stiffness airloads. Inertia forces

are significant only for incompressible flow, otherwise they are generally negligibly small, and hence, are ignored. Unlike mass and stiffness matrices that possess properties of symmetry, sparseness and "bandiness", aerodynamic matrices are complex — due to phase lags between motions and forces —, non-symmetric and fully populated. Owing to this fact, pre- and post-multiplication by the mode shapes to perform modal analysis (referred to above as mode superposition) is rather cumbersome in terms of computer storage and handling. These forces are, therefore, obtained directly as generalized airloads which, by definition, can be evaluated from the expression of virtual work (appendix C).

For motion other than steady-state harmonic, there is as yet no satisfactory formulation on unsteady aerodynamics. The generalized aerodynamic vector {Q} is, as tacitly agreed in appendix C, correct only when the motion is sinusoidal. For this reason, we seek solutions to Eq. A.22 of the form

$$\{q\} = \{\bar{q}\}e^{i\omega t} \tag{A.23}$$

$\{\bar{q}\}$ vector of complex amplitudes or quantities defining amount of harmonic constituents in {q}

ω circular frequency of harmonic oscillation (real)

Differentiating the vector {q} relatively to time gives

$$\left.\begin{aligned} \{\dot{q}\} &= i\omega\{\bar{q}\}e^{i\omega t} \\ \{\ddot{q}\} &= -\omega^2\{\bar{q}\}e^{i\omega t} \end{aligned}\right\} \tag{A.24}$$

In virtue of Eq. A.23, A.24 and C.14a, Eq. A.22 can be updated to

$$\left[-\omega^2\left[\,1\,\right] + \left[\,\omega_N^2\,\right] + ig\left[\,\omega_N^2\,\right]\right]\{\bar{q}\} = \rho_\infty V^2 b[Q]\{\bar{q}\} \tag{A.25}$$

If we let

$$\nu = \frac{\omega b}{V} \tag{A.26}$$

and

$$\Omega = \frac{1+ig}{\omega^2} \tag{A.27}$$

Eq. A.25 can be further manipulated into the desired form of the generalized equation of motion governing the aeroelastic behavior

$$\left[\,\left[\,1\,\right] - \Omega\left[\,\omega_N^2\,\right] + \rho_\infty \frac{b^3}{\nu^2}[Q]\,\right]\{\bar{q}\} = \{0\} \tag{A.28a}$$

$\left[\,1\,\right]$ generalized inertia matrix; order nxn

$\left[\,\omega_N^2\,\right]$ generalized stiffness matrix; order nxn

[Q] matrix of generalized airforce coefficients; order nxn

Ω complex eigenvalue (aeroelastic eigenvalue) as defined by Eq. A.27

g structural damping factor or artificial damping

ω circular frequency of harmonic oscillation

ρ_∞ air density in the uniform flow far upstream of the lifting planform

b reference length of the lifting surface

ν reduced frequency as defined by Eq. A.26

V flight velocity

If the original modes of the base design are used throughout the optimization process, the generalized inertia and stiffness matrices in Eq. A.28a take the more general form as shown below

$$\left[\left[M_G \right] - \Omega \left[K_G \right] + \rho_\infty \frac{b^3}{\nu^2} [Q] \right] \{\bar{q}\} = \{0\} \qquad \text{(A.28b)}$$

$\left[M_G \right]$ generalized inertia matrix; order nxn

$\left[K_G \right]$ generalized stiffness matrix; order nxn

It is gratifying to observe that by assuming transverse oscillations, the large number of degrees of freedom necessary to model practical lifting structures has been roughly divided by three. Then by cleverly using modal analysis, this number has been further reduced to a much lesser and more reasonable number of n degrees of freedom representing the order of the complex eigenvalue problem (Eq. A.28a and A.28b).

By way of conclusion, it may be worthwhile to make some

general comments on why g is referred to as artificial damping. The conventional approach to flutter analysis — dictated by the limited knowledge on unsteady aerodynamic loads — consists of assuming neutral stability from the outset. The validity of the flutter equation derived in this appendix is for airfoils oscillating with steady amplitudes (pure sinusoidal motions), e.g, any of the n equations forming Eq. A.28a or A.28b is correct at a critical flutter speed. Hence, the structural damping factor g have a physical significance only at critical flutter points, that is, at neutral stability between converging and diverging oscillations. At other points, the perturbed airfoil motions will decay or diverge and in such circumstances g is no more than a mathematical artifice. When constructing plots of g by varying the speed, g can be interpreted as a qualitative measure of stability; in a stable system, g is a negative number and can be seen as representing the amount of negative fictious damping that must be applied to the system to force it to undergo neutrally stable oscillations; likewise, in an unstable system, g is a positive number that can be thought as the amount of positive fictious damping that must be applied to the system to bring it into neutral stability.

APPENDIX B

STRUCTURAL DAMPING

Damping in flutter calculations plays a substantial part in the accuracy of the results. The two main sources of damping are:

— aerodynamic damping caused by the flapping of the structure through the air (see appendix C).

— structural damping arising from hysteresis in the material and from frictions at joints and connections between the different aircraft components.

While natural damping inherent in a material is relatively small, the energy dissipation in a structure due to joint interface slip can give rise to relatively appreciable dampings. Analyzing the damping of a structural assembly is not an easy task. It is important to consider not only the material composing the structure but also the way the structure is constructed. Riveted and bolted structures possess more damping than one which uses largely integrally machined components. Moreover, with age the loosening of bolts and joints may well change the damping propriety of the structure.

This latter trait gives some insight into the difficulty of any attempt to derive an expression to model dissipation through structural damping. Thus certain simplistic assumptions must be made regarding these energy-loss mechanisms. One popular scheme is the complex stiffness

concept which consists of introducing the loss as a fraction of the stiffness and which permits the damping to be orthogonal and the modes to decouple in the equations governing the motion.

The following is excerpted from Ref. 33 (page 212) but with slight variations in the notation to ensure consistency throughout this work:

> "Another type of damping results from internal friction in deformable bodies and is associated with the so-called hysteresis loop during cyclic stress. Such damping is commonly referred to as structural damping. It turns out that in the case of harmonic external excitation one can devise an analogy whereby structural damping can be treated as if it were viscous (...). Indeed, if the excitation... is of the form
>
> $$\{q(t)\} = \{\bar{q}\}e^{i\omega t}$$
>
> where $\{\bar{q}\}$ is a constant vector and ω is the frequency of excitation and if the system is known to possess structural damping, then... the damping matrix has the form
>
> $$[C] = \frac{1}{\pi.\omega}[D]$$
>
> so that structural damping is inversely proportional to the excitation frequency. The matrix $(1/\pi\omega)[D]$ is known as the hysteretic damping matrix.
>
> It is customary to assume that the hysteretic damping matrix is proportional to the stiffness matrix, or
>
> $$[D] = \pi g[K]$$
>
> where g is a structural damping factor."

This will result in a structural damping matrix of the form

$$[C] = \frac{g}{\omega} [K] \qquad (B.1)$$

APPENDIX C

GENERALIZED AERODYNAMIC FORCES

To begin with, we recall that the structure has been already assumed to displace in a linear combination of a limited number of mode shapes (see Eq. A.12). The displacement Z(X,Y,t) of a point (X,Y) on the lifting surface at time t is therefore given by the relation

$$Z(X,Y,t) = b \sum_{i=1}^{n} \xi_i(X,Y) q_i(t) \qquad (C.1)$$

Z(X,Y,t) out-of-plane displacement of a point (X,Y) on the aerodynamic planform

b typical or reference length of the planform

$\xi_i(X,Y)$ deflection of the aerodynamic planform at a point (X,Y) due to ith structural mode shape

n number of mode shapes considered

$q_i(t)$ ith generalized coordinate

The difference between $\{\zeta\}_{m_i}$ as introduced in appendix A and $\xi_i(X,Y)$ used above is that $\{\zeta\}_{m_i}$ denotes a mode shape of the structure defined at structural grid nodes whereas ξ_i denotes a deflection at a point (X,Y) in the aerodynamic planform caused by that same mode shape. Obviously, some kind of interpolation scheme is necessary to derive deflection shapes at the aerodynamic grid points from deflection shapes at structural grid points.

The form in which theoretical unsteady aerodynamic forces can be evaluated accounts only for flow phenomena around airfoils with steady-state harmonic oscillations as

imposed by means of the following formulae

$$q_i(t) = \bar{q}_i(\omega)e^{i\omega t} \qquad i = 1,\ldots,n \tag{C.2}$$

$\bar{q}_i(\omega)$ ith complex amplitude or quantity defining amount of harmonic constituent in $q_i(t)$

ω circular frequency of harmonic oscillation (real)

If at time t the lifting surface goes through an incremental virtual displacement δZ, the variation δW or virtual work done by the applied airforces is given as

$$\delta W = \iint_S L(x,y,t).\delta Z(x,y).dxdy \tag{C.3}$$

δW virtual work

$\iint_S$ integration over the aerodynamic planform of area S

$L(x,y,t)$ net aerodynamic pressure acting at time t at a point (x,y) on an element of the planform with area dxdy; aerodynamic loading distribution

$\delta Z(x,y)$ virtual displacement

dxdy differential area

From Eq. C.1, the virtual displacement can be expanded as follows

$$\delta Z(x,y) = b \sum_{i=1}^{n} \xi_i(x,y)\delta q_i \tag{C.4}$$

$$\left.\begin{matrix}\text{Eq. C.3}\\ \text{Eq. C.4}\end{matrix}\right\} \Leftrightarrow \delta W = b \sum_{i=1}^{n} \delta q_i \iint_S L(x,y,t)\xi_i(x,y)dxdy \tag{C.5}$$

In an infinitesimal virtual displacement, the virtual work can be alternatively expressed in terms of generalized forces and displacements

$$\delta W = \sum_{i=1}^{n} Q_i(t)\delta q_i \qquad (C.6)$$

$Q_i(t)$ generalized aerodynamic force in the ith mode of oscillation at time t

From Eq. C.5 and C.6 and through mere identification, we may establish the relation giving the generalized force

$$Q_i(t) \equiv b \iint_S L(x,y,t)\xi_i(x,y)dxdy \qquad i = 1,\ldots,n \qquad (C.7)$$

Next, we follow Ref. 10 and 11 in which the normal pressure force per unit area, called the aerodynamic loading, at the point (x,y) of the planform at time t in the jth harmonic oscillation $b\xi_j(x,y)e^{i\omega t}$ is defined as

$$L_j(x,y,t) = \rho_\infty V^2 \ell_j(x,y;\nu,M_\infty)e^{i\omega t} \qquad (C.8)$$

$L_j(x,y,t)$ aerodynamic loading in the jth harmonic oscillation

ρ_∞ air density in the uniform flow far upstream of the lifting surface

V speed of the main airstream (flight speed); it is in the positive x-direction

$\ell_j(x,y;\nu,M_\infty)$ loading function corresponding to the jth harmonic oscillation

ν reduced frequency; $\nu = \frac{\omega b}{V}$

M_∞ free-stream Mach number; $M_\infty = \frac{V}{a}$

a speed of sound in the uniform flow far upstream of the lifting surface

For our weighted modes of oscillation $b\xi_j(x,y)\bar{q}_j(\omega)e^{i\omega t}$ $(j = 1,\ldots,n)$, the aerodynamic loadings take the form

$$L_j(x,y,t) = \rho_\infty V^2 \ell_j(x,y;\nu,M_\infty)\bar{q}_j(\omega)e^{i\omega t} \qquad j = 1,\ldots,n \tag{C.9}$$

Assumption of small amplitude of oscillations permits the linearisation of the governing equation of the flow about the lifting surface. Accordingly, the principle of superposition holds and the total aerodynamic loading $L(x,y,t)$ can be assumed to consist of a sum of contributions from each mode

$$L(x,y,t) = \rho_\infty V^2 \sum_{j=1}^{n} \ell_j(x,y;\nu,M_\infty)\bar{q}_j(\omega)e^{i\omega t} \tag{C.10}$$

Substitution of Eq. C.10 back into Eq. C.7 leads to

$$Q_i(t) = \rho_\infty V^2 b \sum_{j=1}^{n} \bar{q}_j(\omega)e^{i\omega t} \iint_S \xi_i(x,y)\ell_j(x,y;\nu,M_\infty)dxdy \qquad i = 1,\ldots,n \tag{C.11}$$

Following Ref. 10, we use the dimensionless quantity Q_{ij} to denote a generalized airforce coefficient and rewrite the above expression into the alternative form

$$\left.\begin{aligned} Q_i(t) &= \rho_\infty V^2 b^3 \sum_{j=1}^{n} Q_{ij}(\nu, M_\infty)\bar{q}_j(\omega)e^{i\omega t} \\ & \qquad\qquad i = 1,\ldots,n \qquad (C.12) \end{aligned}\right\} \Leftrightarrow \text{Eq. C.11}$$

where

$$Q_{ij}(\nu, M_\infty) = \frac{1}{b^2}\iint_S \xi_i(x,y)\ell_j(x,y;\nu,M_\infty)dxdy \qquad i,j = 1,\ldots,n \qquad (C.13)$$

$Q_{ij}(\nu, M_\infty)$ generalized airforce coefficient as computed by the program of Ref. 11

In matrix notation

$$\text{Eq. C.12} \Leftrightarrow \{Q(t)\} = \rho_\infty V^2 b^3 \left[Q(\nu, M_\infty)\right] \{\bar{q}(\omega)\}e^{i\omega t} \qquad (C.14a)$$

or

$$\left.\begin{matrix} \text{Eq. C.2} \\ \text{Eq. C.12} \end{matrix}\right\} \Leftrightarrow \{Q(t)\} = \rho_\infty V^2 b^3 \left[Q(\nu, M_\infty)\right] \{q(t)\} \qquad (C.14b)$$

{Q} vector of n generalized aerodynamic forces

[Q] matrix of generalized airforce coefficients; order n×n

{q} vector of n generalized coordinate

In the literature, it is commonly considered that the

generalized airforce coefficients are functions of the reduced frequency and of the Mach number because only these two parameters need to be varied in order to perform flutter solutions. By virtue of the optimization process where the structure is constantly resized and, obviously, its oscillatory behavior modified, the generalized aiforce coefficients are dependent on the mode shapes as well

$$Q_{ij}(\nu, M_\infty) \equiv Q_{ij}(\nu, M_\infty, \{\xi\}) \tag{C.15}$$

APPENDIX D

OPTIMALITY CRITERION

Consider that the structure is idealized by bar, triangular and quadrilateral elements. The total structural mass is the sum of non-variable and variable structural items

$$m = m_0 + \sum_{j=1}^{N} m_j x_j \qquad (D.1)$$

m total mass of the structure

m_0 mass of fixed structural items

m_j mass per unit length (for bar elements) or per unit area (for quadrilateral or triangular elements) of jth variable element

x_j jth design variable

N number of design variables

If ρ_j designates the density of the structural material of the jth variable element, then

$$m_j = \rho_j . l_j \qquad \text{for bar elements} \qquad (D.2a)$$

$$m_j = \rho_j . A_j \qquad \text{for quadr. or triang. elements} \qquad (D.2b)$$

l_j length along the bar element

A_j surface of the quadrilateral or triangular element

For bar elements, x_j is the cross-sectional area of the jth element and for quadrilateral or triangular elements, x_j is the thickness of the jth element.

The structural optimization problem with a constraint on the flutter speed and constraints on manufacturing gauges is to

$$\left.\begin{aligned} &\text{minimize} \quad m = m_0 + \sum_{j=1}^{N} m_j x_j \\ &\text{subject to} \quad V_f \geq V_r \\ &\text{and to} \quad x_j \geq \underline{x}_j \qquad j = 1,\ldots,N \end{aligned}\right\} \quad (D.3)$$

V_f flutter speed

V_r required speed

$\underline{x}_j$ jth minimum gauge constraints; minimum value imposed on jth design variable

Rewriting the flutter equation (Eq. A.28a or A.28b) into the condensed form

$$[F]\{\bar{q}\} = \{0\} \quad (D.4a)$$

$[F]$ flutter matrix

When the modes are updated during the resizing process, the flutter matrix is obtained from

$$[F] = \left[\ 1\ \right] - \Omega\left[\ \omega_N^2\ \right] + \rho_\infty \frac{b^3}{\nu^2}[Q] \quad (D.4b)$$

and when the modes of the original structure are used throughout the design process, it is obtained from

$$[F] = \left[\ M_G\ \right] - \Omega\left[\ K_G\ \right] + \rho_\infty \frac{b^3}{\nu^2}[Q] \quad (D.4c)$$

Introducing Eq. D.4a at the critical flutter mode to replace the constraint on the flutter speed in the

optimization problem (Eq. D.3) yields

$$\left.\begin{aligned} &\text{minimize} \quad m = m_0 + \sum_{j=1}^{N} m_j x_j \\ &\text{subject to} \quad [F]\{\bar{q}\} = \{0\} \\ &\text{and to} \quad x_j \geq \underline{x}_j \qquad j = 1,\ldots,N \end{aligned}\right\} \quad (D.5)$$

But, if we let superscripts ′ and " identify the real part and imaginary part of a complex quantity, then

$$\text{Eq. D.4a} \Leftrightarrow \left[[F'] + i[F"]\right]\left\{\{\bar{q}'\} + i\{\bar{q}"\}\right\} = \{0\} \quad (D.6)$$

The matrix of generalized airforce coefficients is complex and is computed by WLST1 (Ref. 10, 11 and 12) as

$$[Q] = [Q'] + i\nu[Q"] \quad (D.7)$$

$[Q']$ real part of $[Q]$

$\nu[Q"]$ imaginary part of $[Q]$

The real and imaginary part of the flutter matrix are given by the following relations when the modes are updated

$$\left.\begin{aligned} &\text{Eq. A.27} \\ &\text{Eq. D.4b} \\ &\text{Eq. D.7} \end{aligned}\right\} \Leftrightarrow \left\{\begin{aligned} &[F'] \equiv \left\lceil 1 \right\rfloor - \frac{1}{\omega^2}\left\lceil \omega_N^2 \right\rfloor + \rho_\infty \frac{b^3}{\nu^2}[Q'] \\ &\text{and} \\ &[F"] \equiv -\frac{g}{\omega^2}\left\lceil \omega_N^2 \right\rfloor + \rho_\infty \frac{b^3}{\nu}[Q"] \end{aligned}\right. \quad (D.8a)$$

and by the following relations when the modes are not updated

$$\left.\begin{array}{l}\text{Eq. A.27}\\ \text{Eq. D.4c}\\ \text{Eq. D.7}\end{array}\right\} \Leftrightarrow \left\{\begin{array}{l}[F'] \equiv \left[M_G \right] - \dfrac{1}{\omega^2}\left[K_G \right] + \rho_\infty \dfrac{b^3}{\nu^2}[Q'] \\ \\ \text{and} \\ \\ [F''] \equiv - \dfrac{g}{\omega^2}\left[K_G \right] + \rho_\infty \dfrac{b^3}{\nu}[Q'']\end{array}\right. \tag{D.8b}$$

The single complex equality constraint in Eq. D.5 represents therefore two constraints. Thus, the constrained minimization problem above (Eq. D.5) is equivalent to

$$\left.\begin{array}{l}\text{minimize} \quad m = m_0 + \sum_{j=1}^{N} m_j x_j \\ \\ \text{subject to} \quad \left\{\begin{array}{l}[F']\{\bar{q}'\} - [F'']\{\bar{q}''\} = \{0\} \\ \\ \text{and} \\ \\ [F'']\{\bar{q}'\} + [F']\{\bar{q}''\} = \{0\}\end{array}\right. \\ \\ \text{and to} \quad x_j \geq \underline{x}_j \qquad j = 1,\ldots,N\end{array}\right\} \tag{D.9}$$

Considering that the side constraints can be treated separately on a trial-and-error basis, let X be the set of the primal points satisfying the constraints on the gauges

$$X = \left\{ \{x\} \;:\; \{x\} \in E^N;\; x_j \geq \underline{x}_j,\; j = 1,\ldots,N \right\} \tag{D.10}$$

$\{x\}$ vector grouping all design variables

E^N N dimensional euclidean space

In summary, then, our structural optimization problem is

$$\left.\begin{array}{l} \text{minimize} \quad m = m_0 + \sum_{j=1}^{N} m_j x_j \equiv m(\{x\}) \\ \qquad\qquad\qquad\qquad\qquad\qquad \forall\ \{x\} \in X \\ \text{subject to} \begin{cases} [F']\{\bar{q}'\} - [F'']\{\bar{q}''\} = \{0\} \\ \text{and} \\ [F'']\{\bar{q}'\} + [F']\{\bar{q}''\} = \{0\} \end{cases} \end{array}\right\} \quad (D.11)$$

In developing optimality criteria, the normally adopted approach is to seek a stationary point of the Lagrangian. As indicated before it is not necessary to enforce Lagrangian multipliers with the side constraints and the Lagrangian function takes the form

$$\mathfrak{L} = m + \{\lambda'\}^T\left\{[F']\{\bar{q}'\} - [F'']\{\bar{q}''\}\right\} + \{\lambda''\}^T\left\{[F'']\{\bar{q}'\} + [F']\{\bar{q}''\}\right\} \quad (D.12a)$$

or

$$\mathfrak{L} = m + \{\lambda'\}^T[F']\{\bar{q}'\} - \{\lambda'\}^T[F'']\{\bar{q}''\} + \{\lambda''\}^T[F'']\{\bar{q}'\} + \{\lambda''\}^T[F']\{\bar{q}''\} \quad (D.12b)$$

in which $\{\lambda'\}$ and $\{\lambda''\}$ are vectors of Lagrangian multipliers (vector of dual variables) associated with the behavior constraint on flutter.

Let

$$\{\lambda\} = \{\lambda'\} + i\{\lambda''\} \tag{D.13}$$

$$\left.\begin{array}{l}\text{Eq. D.12b}\\ \text{Eq. D.13}\end{array}\right\} \Rightarrow \mathfrak{L} \equiv \mathfrak{L}(\Omega, \{\lambda\}, \{\bar{q}\}, \{x\})$$

$$= m + \text{Re}\left(\{\lambda\}^H [F] \{\bar{q}\}\right) \tag{D.14}$$

where superscript H denotes the hermitian transpose, e.g,

$$\{\lambda\}^H \equiv \{\lambda^c\}^T \equiv \{\lambda'\}^T - i\{\lambda''\}^T \tag{D.15}$$

and superscript c denotes the complex conjugate.

Following McIntosh and Ashley (Ref. 1), the necessary conditions that a point is an optimal solution are the vanishing of the partial derivatives of the Lagrangian relatively to the parameter Ω and to the elements of the vector parameters $\{\lambda'\}$, $\{\lambda''\}$, $\{q'\}$, $\{q''\}$ and $\{x\}$

$$\frac{\partial \mathfrak{L}}{\partial \Omega} = \text{Re}\left(\{\lambda\}^H \cdot \frac{\partial [F]}{\partial \Omega} \cdot \{\bar{q}\}\right) = 0 \tag{D.16a}$$

$$[F]\{\bar{q}\} = \{0\} \tag{D.16b}$$

$$\left\{\{\lambda\}^H [F]\right\}^T \equiv [F]^T \left\{\{\lambda\}^H\right\}^T \equiv [F]^T \{\lambda^c\} = \{0\} \tag{D.16c}$$

$$\frac{\partial \mathfrak{L}}{\partial x_j} = m_j + \mathrm{Re}\left(\{\lambda\}^H \cdot \frac{\partial [F]}{\partial x_j} \cdot \{\bar{q}\}\right) = 0 \qquad j = 1,\ldots,N \tag{D.16d}$$

Predecessors to McIntosh and Ashley (Haftka and Starnes, Ref. 22, and Pines and Newman, Ref. 39) derived Eq. D.16a but relatively to the flutter frequency ω. However, McIntosh and Ashley take their derivates relative to Ω as equivalent to the vanishing of the variation of the Lagrangian with respect to ω at the constraint boundary where $g = 0$.

Eq. D.16b represents the original flutter constraint whereas Eq. D.16c identifies $\left\{\{\lambda'\} - i\{\lambda''\}\right\}$ as the adjoint flutter eigenvector and represents the adjoint flutter equation. Very similar forms to Eq. D.16d have been used by all these authors as the optimality criterion (the difference reside in that we used the definition of the hermitian of a complex matrix to present the Lagrangian and the optimality criterion in much more elegant mathematical forms). We are going to follow most of the references and adopt a fixed mode approach in which the mode shapes of the original structure are kept unchanged throughout the redesign cycle. This renders the generalized aerodynamic forces independent of the modes shapes and hence not dependent on the elements of the vector of design variables $\{x\}$. Therefore

$$\frac{\partial [F]}{\partial x_j} = \frac{\partial [M]}{\partial x_j} - \Omega \cdot \frac{\partial [K]}{\partial x_j} \qquad j = 1,\ldots,N \tag{D.17}$$

The use of linear elements implies the linear dependence of stiffness and inertia properties on the design variables.

$$[M] = \left[M_0 \right] + \sum_{j=1}^{N} \left[M_j \right] x_j \qquad \text{(D.18a)}$$

$$[K] = \left[K_0 \right] + \sum_{j=1}^{N} \left[K_j \right] x_j \qquad \text{(D.18b)}$$

$\left[M_0 \right]$ contributions of fixed structural items to the inertia matrix

$\left[K_0 \right]$ contributions of fixed structural items to the stiffness matrix

$\left[M_j \right]$ jth elemental inertia matrix or changes in inertia per unit length or area of the jth variable element

$\left[K_j \right]$ jth elemental stiffness matrix or changes in stiffness per unit length or area of the jth variable element

If nodal displacements (like in Ref. 22) are used in the flutter equation the partial derivatives of [F] with respect to x_j are

Eq. D.17, Eq. D.18a, Eq. D.18b $\Rightarrow$

$$\frac{\partial [F]}{\partial x_j} = \left[M_j \right] - \Omega \left[K_j \right] \qquad j = 1,\ldots,N \qquad \text{(D.19a)}$$

McIntosh and Ashley (Ref. 1), although using modal amplitudes as generalized coordinates, take the derivatives of [F] with respect to x_j as below

$$\frac{\partial[F]}{\partial x_j} = \left[M_j \right] - \Omega\left[K_j \right] \qquad j = 1,\ldots,N \tag{D.19b}$$

The second expression (Eq. D.19b) looks very much similar to Eq. D.19a although modal analysis has been performed on the flutter equation. We need to clarify this point not only for McIntosh-Ashley's work but for ours because we are also using the "modal superposition". Moreover, our adoption of the "eigenvalue economizer" technique will need a further step of explanation. The derivatives of [F] are not as straightforward as when nodal displacements are utilized and we should start with the formulation of the generalized inertia and stiffness matrices

$$\left[M_G \right] = \left[\zeta^{(0)} \right]^T \left[\left[M_0 \right] + \sum_{j=1}^{N} \left[M_j \right] x_j \right] \left[\zeta^{(0)} \right] \tag{D.20a}$$

$$\left[K_G \right] = \left[\zeta^{(0)} \right]^T \left[\left[K_0 \right] + \sum_{j=1}^{N} \left[K_j \right] x_j \right] \left[\zeta^{(0)} \right] \tag{D.20b}$$

$\left[\zeta^{(0)} \right]$ modal matrix of the original structure; matrix whose columns are the full mode shapes of the original structure

When modal amplitudes are utilized as generalized

coordinates, Eq. D.17 should read

$$\frac{\partial[F]}{\partial x_j} = \frac{\partial}{\partial x_j}\left[M_G \right] - \Omega\cdot\frac{\partial}{\partial x_j}\left[K_G \right] \qquad j = 1,\ldots,N \tag{D.21a}$$

with

$$\frac{\partial}{\partial x_j}\left[M_G \right] = \left[\zeta^{(0)} \right]^T \left[M_j \right] \left[\zeta^{(0)} \right] \qquad j = 1,\ldots,N \tag{D.21b}$$

$$\frac{\partial}{\partial x_j}\left[K_G \right] = \left[\zeta^{(0)} \right]^T \left[K_j \right] \left[\zeta^{(0)} \right] \qquad j = 1,\ldots,N \tag{D.21c}$$

Unless the terms in Eq. D.19b, $\left[M_j \right]$ and $\left[K_j \right]$, are implicitly assumed by McIntosh and Ashley to be generalized matrices as shown in Eq. D.21b and D.21c, Eq. D.19b does not hold if modal analysis is performed on the equation of motion. It is worth noting that Eq. D.21b and D.21c are constant expressions throughout the design process.

Utilizing master degrees of freedom only (refer back to appendix A), Eq. D.21b and Eq. D.21c should be reformulated as

$$\begin{aligned} \frac{\partial}{\partial x_j}\left[M_G \right] &= \left[\zeta_m^{(0)} \right]^T [T]^T \left[M_j \right] [T] \left[\zeta_m^{(0)} \right] \\ &\simeq \left[\zeta^{(0)} \right]^T \left[M_j \right] \left[\zeta^{(0)} \right] \end{aligned} \qquad j = 1,\ldots,N \tag{D.22a}$$

$$\frac{\partial}{\partial x_j}\left[K_G \right] = \left[\zeta_m^{(0)} \right]^T [T]^T \left[K_j \right] [T] \left[\zeta_m^{(0)} \right]$$

$$\simeq \left[\zeta^{(0)} \right]^T \left[K_j \right] \left[\zeta^{(0)} \right] \qquad j = 1,\ldots,N \qquad \text{(D.22b)}$$

$\left[\zeta_m^{(0)} \right]$ modal matrix whose columns are the master mode shapes of the original structure

In view of the fact that $\left[M_j \right]$ and $\left[K_j \right]$ are very sparse matrices, the program stores in the data base only the few non-zero terms. Because of this dominance of zero terms and because the full eigenvector consists of a master eigenvector and relatively negligible terms composing the slave parts of the eigenvector (§ VI.2), the derivatives of the generalized inertia and stiffness matrices can be, without noticeable errors, assumed to be

$$\frac{\partial}{\partial x_j}\left[M_G \right] \simeq \left[\zeta_m^{(0)} \right]^T \left[\bar{M}_j \right] \left[\zeta_m^{(0)} \right] \qquad j = 1,\ldots,N \qquad \text{(D.23a)}$$

$$\frac{\partial}{\partial x_j}\left[K_G \right] \simeq \left[\zeta_m^{(0)} \right]^T \left[\bar{K}_j \right] \left[\zeta_m^{(0)} \right] \qquad j = 1,\ldots,N \qquad \text{(D.23b)}$$

$\left[\bar{M}_j \right]$ and $\left[\bar{K}_j \right]$ are the same as $\left[M_j \right]$ and $\left[K_j \right]$ but the terms in the x- and y-directions are deleted by simply removing complete lines and columns.

Eq. D.23a and D.23b are evaluated only once at the start of the program run before the optimization routine. A special subroutine that performs pre- and post-multiplication of the elemental inertia and stiffness matrices with the "master" modal matrix was written taking into account that these matrices are still full of zero terms despite the elimination of lines in the x- and y-directions.

During the resizing process some design variables may become passive, i.e, equal to the specified lower limits on the design variables that reflects fabrication considerations. Eq. D.16d in such a case is valid only for the active set of design variables. Therefore, we introduce the set of indices defined below

$$J_a = \left\{ j = 1,\ldots,N \ : \ x_j > \underline{x}_j \right\} \tag{D.24}$$

J_a set of indices representing the active design variables only

The optimality criterion in Eq. D.16d can be rewritten in a slightly different form as follows

$$\left(e_v\right)_j = \frac{1}{m_j} \, \mathrm{Re}\left(\{\lambda\}^H . \frac{\partial [F]}{\partial x_j} . \{\bar{q}\} \right) = -1 \qquad \forall \ j \in J_a \tag{D.25}$$

Of interest, but of lesser rigor is the intuitive OC of Ref. 46 which assumes that the most efficient distribution of structural mass is the one which exhibits a uniform strain energy per volume throughout the structure when it is

deformed in the critical flutter mode. Eq. D.25 resembles somewhat that intuitive OC and, hence, can be regarded as a form of "energy density" terms.

Taking into account that some design variables are bar elements and some are quadrilateral or triangular elements, the final form of these "energy density" terms is

Eq. D.25, Eq. D.2a, Eq. D.2b $\Rightarrow$

$$\begin{cases} \forall\, j \in J_a, \\ \\ \left(e_v\right)_j = \dfrac{1}{\rho_j l_j} \mathrm{Re}\left(\{\lambda\}^H . \dfrac{\partial [F]}{\partial x_j} . \{\bar{q}\}\right) = -1 \\ \\ \text{for bar elements} \\ \\ \text{and} \\ \\ \left(e_v\right)_j = \dfrac{1}{\rho_j A_j} \mathrm{Re}\left(\{\lambda\}^H . \dfrac{\partial [F]}{\partial x_j} . \{\bar{q}\}\right) = -1 \\ \\ \text{for quadrilateral or} \\ \text{triangular elements} \end{cases} \tag{D.26}$$

with any design variable linking, l_j and A_j would represent the total length or area of all the elements composing the design variable.

A recurrence relation proposed by Ref. 1 and based on this criterion is

$$x_j^{(k+1)} = C_j^{(k)} . x_j^{(k)} \tag{D.27a}$$

with

$$C_j^{(k)} = \left(\left| \frac{\left(e_v\right)_j^{(k)}}{\left(e_{av}\right)^{(k)}} \right|^{e_1} \left(1 + g^{(k)}\right)^{e_2} \right) \qquad \text{(D.27b)}$$

where

C_j redesign factor

$\left(e_{av}\right)$ average of all $\left(e_v\right)_j$ $\forall$ $j \in J_a$ (all active design variables)

k iteration counter

e_1, e_2 resizing exponents

g artificial damping

APPENDIX E

BEHAVIORAL RESPONSE SENSITIVITY

Analytical equations of the partial derivatives of the flutter velocity and of the frequency with respect to a set design variables were first derived by Rudisill and Bathia (Ref. 42; see also Ref. 45). In this appendix, we follow similar methods to give expressions for the partial derivatives of artificial damping and frequency. Moreover, we will extend the derivations to the design procedure with a continuous mode updating.

To aid assimilation and avoid repetitive reference to previous appendices, we reproduce the simplified form of the equation of motion (Eq. D.4a)

$$[F]\{\bar{q}\} = \{0\} \tag{E.1a}$$

Some of the equations associated with the flutter equation are also reproduced below (see Eq. D.4b, D.4c, D.7, A.26, A.27, D.6, D.13, D.16c, D.19a, D.23a, D.23b and C.15)

$$\left.[F] \equiv \left[\ 1\ \right] - \Omega\left[\ \omega_N^2\ \right] + \rho_\infty \frac{b^3}{\nu^2}[Q]\right\} \text{ when the modes are updated} \tag{E.1b}$$

$$\left.[F] \equiv \left[\ M_G\ \right] - \Omega\left[\ K_G\ \right] + \rho_\infty \frac{b^3}{\nu^2}[Q]\right\} \text{ when the modes are not updated} \tag{E.1c}$$

$$[Q] = [Q'] + i\nu[Q''] \tag{E.2}$$

$$\nu = \frac{\omega b}{V} \tag{E.3}$$

$$\Omega = \frac{1+ig}{\omega^2} \tag{E.4}$$

$$\{q\} = \{\bar{q}'\} + i\{\bar{q}''\} \tag{E.5}$$

$$\{\lambda\} = \{\lambda'\} + i\{\lambda''\} \tag{E.6}$$

$$\{\lambda\}^H[F] = \{0\}^T \tag{E.7}$$

$$\frac{\partial[M]}{\partial x_j} = \left[M_j \right] \qquad j = 1,\ldots,N \tag{E.8}$$

$$\frac{\partial[K]}{\partial x_j} = \left[K_j \right] \qquad j = 1,\ldots,N \tag{E.9}$$

$$\frac{\partial}{\partial x_j}\left[M_G \right] \simeq \left[\zeta_m^{(0)} \right]^T \left[\bar{M}_j \right] \left[\zeta_m^{(0)} \right] \qquad j = 1,\ldots,N \tag{E.10}$$

$$\frac{\partial}{\partial x_j}\left[K_G \right] \simeq \left[\zeta_m^{(0)} \right]^T \left[\bar{K}_j \right] \left[\zeta_m^{(0)} \right] \qquad j = 1,\ldots,N \tag{E.11}$$

$$[M] \equiv [M(\{x\})] \tag{E.12}$$

$$[K] \equiv [K(\{x\})] \tag{E.13}$$

The optimization process is carried out at a fixed altitude and at a fixed speed, hence ρ and M_∞ are constant and

$$[Q] \equiv [Q(\nu,\{\xi\})] \tag{E.14}$$

The full free-vibration problem for each eigen-pair

$\left(\omega_{Ni}\right)^2$ and $\{\zeta\}_i$ is

$$\left[[K] - \left(\omega_{Ni}\right)^2[M]\right]\{\zeta\}_i = \{0\} \qquad i = 1,\ldots,r \qquad \text{(E.15)}$$

and the normalization equation is

$$\{\zeta\}_i^T[M]\{\zeta\}_i = 1 \qquad i = 1,\ldots,r \qquad \text{(E.16)}$$

It is useful to start with the differentiation of the full free-vibration eigenvalue problem that is expressed above (Eq. E.15)

$$\frac{d}{dx_j}\left(\left[[K] - \left(\omega_{Ni}\right)^2[M]\right]\{\zeta\}_i\right) = \{0\}$$

$$i = 1,\ldots,r \qquad \text{and} \qquad j = 1,\ldots,N \qquad \text{(E.17a)}$$

$$\Rightarrow \left(\left[\frac{d[K]}{dx_j} - \frac{d\left(\omega_{Ni}\right)^2}{dx_j}\cdot[M] - \left(\omega_{Ni}\right)^2\cdot\frac{d[M]}{dx_j}\right]\{\zeta\}_i + \left[[K] - \left(\omega_{Ni}\right)^2[M]\right]\cdot\frac{d\{\zeta\}_i}{dx_j} \right) = \{0\}$$

$$i = 1,\ldots,r \qquad \text{and} \qquad j = 1,\ldots,N \qquad \text{(E.17b)}$$

Premultiplication of Eq. E.17b by the transpose of the eigenvector, $\{\zeta\}_i^T$, yields

$$\left(\{\zeta\}_i^T \left[\frac{d[K]}{dx_j} - \frac{d\left(\omega_{Ni}\right)^2}{dx_j} \cdot [M] - \left(\omega_{Ni}\right)^2 \cdot \frac{d[M]}{dx_j} \right] \{\zeta\}_i \right.$$

$$\left. + \{\zeta\}_i^T \left[[K] - \left(\omega_{Ni}\right)^2 [M] \right] \cdot \frac{d\{\zeta\}_i}{dx_j} \right) = \{0\}$$

$$i = 1,\ldots,r \qquad \text{and} \qquad j = 1,\ldots,N \qquad \text{(E.17c)}$$

$$\Leftrightarrow \quad \{\zeta\}_i^T \frac{d\left(\omega_{Ni}\right)^2}{dx_j} \cdot [M]\{\zeta\}_i = \{\zeta\}_i^T \left[\frac{d[K]}{dx_j} - \left(\omega_{Ni}\right)^2 \cdot \frac{d[M]}{dx_j} \right] \{\zeta\}_i$$

$$+ \{\zeta\}_i^T \left[[K] - \left(\omega_{Ni}\right)^2 [M] \right] \cdot \frac{d\{\zeta\}_i}{dx_j}$$

$$i = 1,\ldots,r \qquad \text{and} \qquad j = 1,\ldots,N \qquad \text{(E.17d)}$$

Because [K] and [M] are symmetric matrices

$$\left(\{\zeta\}_i^T \left[[K] - \left(\omega_{Ni}\right)^2 [M] \right] \right)^T = \left[[K]^T - \left(\omega_{Ni}\right)^2 [M]^T \right] \{\zeta\}_i$$

$$= \left[[K] - \left(\omega_{Ni}\right)^2 [M] \right] \{\zeta\}_i = \{0\}$$

$$i = 1,\ldots,r \qquad \text{(E.17e)}$$

$$\Rightarrow \quad \{\zeta\}_i^T \left[[K] - \left(\omega_{Ni}\right)^2 [M] \right] = \{0\}^T \qquad i = 1,\ldots,r \qquad \text{(E.17f)}$$

Taking into account Eq. E.17f, we rewrite Eq. E.17d as

$$\frac{d\left(\omega_{Ni}\right)^2}{dx_j} = \frac{\{\zeta\}_i^T \left[\frac{d[K]}{dx_j} - \left(\omega_{Ni}\right)^2 . \frac{d[M]}{dx_j}\right] \{\zeta\}_i}{\{\zeta\}_i^T [M] \{\zeta\}_i}$$

$$i = 1,\ldots,r \qquad \text{and} \qquad j = 1,\ldots,N \qquad \text{(E.17g)}$$

Eq. E.17g
Eq. E.16
Eq. E.8
Eq. E.9
$\Leftrightarrow$

$$\begin{cases} \dfrac{d\left(\omega_{Ni}\right)^2}{dx_j} = \{\zeta\}_i^T \left[\left[M_j \right] - \left(\omega_{Ni}\right)^2 . \left[K_j \right] \right] \{\zeta\}_i \\ i = 1,\ldots,r \qquad \text{and} \qquad j = 1,\ldots,N \end{cases} \qquad \text{(E.17h)}$$

Knowing that $\left[M_j \right]$ and $\left[K_j \right]$ are very sparse matrices and that $\{\zeta\}_i$ consists of master terms and relatively negligible terms composing the slave part of the eigenvector, we can assume that

$$\frac{d\left(\omega_{Ni}\right)^2}{dx_j} \simeq \{\zeta\}_{m_i}^T \left[\left[\overline{M}_j \right] - \left(\omega_{Ni}\right)^2 . \left[\overline{K}_j \right] \right] \{\zeta\}_{m_i}$$

$$i = 1,\ldots,p \qquad \text{and} \qquad j = 1,\ldots,N \qquad \text{(E.17i)}$$

where $\left[\bar{M}_j \right]$ and $\left[\bar{K}_j \right]$ are the matrices $\left[M_j \right]$ and $\left[K_j \right]$ with lines and columns deleted in x- and y-directions.

Differentiating the complex eigenvalue (Eq. E.4), we obtain

$$\frac{\partial \Omega}{\partial x_j} = \frac{\partial\left(\frac{1+ig}{\omega^2}\right)}{\partial x_j} = \frac{\partial\left(\frac{1}{\omega^2}\right)}{\partial x_j} + i\cdot\frac{\partial\left(\frac{g}{\omega^2}\right)}{\partial x_j} \qquad j = 1,\ldots,N \tag{E.18a}$$

$$\frac{\partial \Omega}{\partial x_j} = -\frac{2\omega\cdot\frac{\partial \omega}{\partial x_j}}{\omega^4} + i\cdot\frac{\omega^2\cdot\frac{\partial g}{\partial x_j} - 2\omega g\cdot\frac{\partial \omega}{\partial x_j}}{\omega^4}$$

$$= -\frac{2}{\omega^3}\cdot\frac{\partial \omega}{\partial x_j} + i\cdot\frac{1}{\omega^3}\cdot\left(\omega\cdot\frac{\partial g}{\partial x_j} - 2g\cdot\frac{\partial \omega}{\partial x_j}\right) \qquad j = 1,\ldots,N \tag{E.18b}$$

or

$$-\frac{\partial \Omega}{\partial x_j} = \frac{2}{\omega^3}\cdot\frac{\partial \omega}{\partial x_j} + i\cdot\frac{1}{\omega^3}\left(2g\frac{\partial \omega}{\partial x_j} - \omega\frac{\partial g}{\partial x_j}\right) \qquad j = 1,\ldots,N \tag{E.18c}$$

Differentiating other expressions useful for future derivations

$$\frac{\partial}{\partial x_j}\left(\rho_\infty \frac{b^3}{\nu^2}\right) = \rho_\infty b^3\cdot\frac{\partial\left(\nu^{-2}\right)}{\partial x_j} = -\frac{2\rho_\infty b^3}{\nu^3}\cdot\frac{\partial \nu}{\partial x_j} \qquad j = 1,\ldots,N \tag{E.19a}$$

But, from the definition of ν (Eq. E.3), the partial

derivatives of ν with respect to x_j are

$$\frac{\partial \nu}{\partial x_j} = \frac{\partial \nu}{\partial \omega} \cdot \frac{\partial \omega}{\partial x_j} = \frac{b}{V} \cdot \frac{\partial \omega}{\partial x_j} \qquad j = 1,\ldots,N \tag{E.19b}$$

$$\left.\begin{array}{l} \text{Eq. E.19a} \\ \text{Eq. E.19b} \end{array}\right\} \Rightarrow \left\{ \frac{\partial}{\partial x_j}\left(\rho_\infty \frac{b^3}{\nu^2}\right) = -\frac{2\rho_\infty b^4}{V\nu^3} \cdot \frac{\partial \omega}{\partial x_j} \right. \qquad j = 1,\ldots,N \tag{E.19c}$$

When the modes shapes of the original structure are kept unchanged, the partial derivative expressions of the generalized airforce coefficients [Q] with respect to x_j can only take the following form

$$\frac{\partial [Q]}{\partial x_j} = \frac{\partial [Q]}{\partial \nu} \cdot \frac{\partial \nu}{\partial x_j} \qquad j = 1,\ldots,N \tag{E.20a}$$

$$\left.\begin{array}{l} \text{Eq. E.20a} \\ \text{Eq. E.19b} \end{array}\right\} \Rightarrow \left\{ \frac{\partial [Q]}{\partial x_j} = \frac{b}{V} \cdot \frac{\partial [Q]}{\partial \nu} \cdot \frac{\partial \omega}{\partial x_j} \right. \qquad j = 1,\ldots,N \tag{E.20b}$$

$$\text{Eq. E.20b} \Rightarrow \rho_\infty \frac{b^3}{\nu^2} \cdot \frac{\partial [Q]}{\partial x_j} = \frac{\rho_\infty b^4}{V\nu^2} \cdot \frac{\partial [Q]}{\partial \nu} \cdot \frac{\partial \omega}{\partial x_j} \qquad j = 1,\ldots,N \tag{E.20c}$$

Now, we turn our attention to the differentiation of the flutter equation (Eq. E.1a)

$$\frac{\partial}{\partial x_j}\left([F]\{\bar{q}\}\right) = \frac{\partial [F]}{\partial x_j} \cdot \{\bar{q}\} + [F] \cdot \frac{\partial \{\bar{q}\}}{\partial x_j} = \{0\} \qquad j = 1,\ldots,N \tag{E.21}$$

To remove the terms that involve the partial derivatives of the aeroelastic eigenvector $\{\bar{q}\}$, we pre-multiply Eq. E.21 by the adjoint aeroelastic eigenvector $\{\lambda\}^H$

$$\{\lambda\}^H \cdot \left(\frac{\partial [F]}{\partial x_j} \cdot \{\bar{q}\} + [F] \cdot \frac{\partial \{\bar{q}\}}{\partial x_j} \right) = 0 \qquad j = 1,\ldots,N \tag{E.22}$$

$$\left.\begin{matrix} \text{Eq. E.22} \\ \text{Eq. E.7} \end{matrix}\right\} \Leftrightarrow \{\lambda\}^H \cdot \left(\frac{\partial [F]}{\partial x_j} \cdot \{\bar{q}\} \right) = 0 \qquad j = 1,\ldots,N \tag{E.23}$$

Continuing with the assumption of fixed-mode approach in which the mode shapes of the original structure are utilized despite the structure being continuously resized. Then, the flutter matrix is given by the expression in Eq. E.1c. and its partial derivatives — with respect to the design variables x_j, $j = 1,\ldots,N$ — will take the following form

$$\frac{\partial [F]}{\partial x_j} = \frac{\partial \left[M_G \right]}{\partial x_j} - \frac{\partial \Omega}{\partial x_j} \cdot \left[K_G \right] - \Omega \cdot \frac{\partial \left[K_G \right]}{\partial x_j}$$

$$+ \left(\frac{\partial}{\partial x_j} \left(\rho_\infty \frac{b^3}{\nu^2} \right) \right) \cdot [Q] + \rho_\infty \frac{b^3}{\nu^2} \cdot \frac{\partial [Q]}{\partial x_j}$$

$$j = 1,\ldots,N \tag{E.24}$$

When all the terms composing Eq. E.24 are replaced by

their definitions or by expressions evaluated previously, the partial derivatives of the flutter matrix [F] are given by

Eq. E.24
Eq. E.4
Eq. E.18c
Eq. E.19c
Eq. E.20c
$\Rightarrow$

$$\left\{ \begin{aligned} \frac{\partial [F]}{\partial x_j} = \frac{\partial \left[M_G \right]}{\partial x_j} + \left(\frac{2}{\omega^3} \cdot \frac{\partial \omega}{\partial x_j} + i \cdot \frac{1}{\omega^3} \left(2g \frac{\partial \omega}{\partial x_j} - \omega \frac{\partial g}{\partial x_j} \right) \right) \cdot \left[K_G \right] \\ - \frac{1+ig}{\omega^2} \cdot \frac{\partial \left[K_G \right]}{\partial x_j} - \left(\frac{2\rho_\infty b^4}{V\nu^3} \cdot \frac{\partial \omega}{\partial x_j} \right) \cdot [Q] \\ + \frac{\rho_\infty b^4}{V\nu^2} \cdot \frac{\partial [Q]}{\partial \nu} \cdot \frac{\partial \omega}{\partial x_j} \end{aligned} \right.$$

$$j = 1, \ldots, N \qquad (E.25)$$

where $\frac{\partial \left[M_G \right]}{\partial x_j}$ and $\frac{\partial \left[K_G \right]}{\partial x_j}$ are respectively given by Eq. E.10 and E.11.

In order to cast Eq. E.23 in a much more presentable form, let us define

$$R_{1_j} = \mathrm{Re}\left(\{\lambda\}^H \cdot \frac{\partial \left[M_G \right]}{\partial x_j} \cdot \{\bar{q}\} \right) \qquad j = 1, \ldots, N \qquad (E.26a)$$

$$I_{1_j} = Im\left(\{\lambda\}^H \cdot \frac{\partial\left[M_G \right]}{\partial x_j} \cdot \{\bar{q}\}\right) \qquad j = 1,\ldots,N \qquad \text{(E.26b)}$$

$$R_{2_j} = Re\left(\{\lambda\}^H \cdot \frac{\partial\left[K_G \right]}{\partial x_j} \cdot \{\bar{q}\}\right) \qquad j = 1,\ldots,N \qquad \text{(E.27a)}$$

$$I_{2_j} = Im\left(\{\lambda\}^H \cdot \frac{\partial\left[K_G \right]}{\partial x_j} \cdot \{\bar{q}\}\right) \qquad j = 1,\ldots,N \qquad \text{(E.27b)}$$

$$R_3 = Re\left(\{\lambda\}^H \cdot \left[K_G \right] \cdot \{\bar{q}\}\right) \qquad \text{(E.28a)}$$

$$I_3 = Im\left(\{\lambda\}^H \cdot \left[K_G \right] \cdot \{\bar{q}\}\right) \qquad \text{(E.28b)}$$

$$R_4 = Re\left(\{\lambda\}^H \cdot \frac{\partial[Q]}{\partial \nu} \cdot \{\bar{q}\}\right) \qquad \text{(E.29a)}$$

$$I_4 = Im\left(\{\lambda\}^H \cdot \frac{\partial[Q]}{\partial \nu} \cdot \{\bar{q}\}\right) \qquad \text{(E.29b)}$$

$$R_5 = Re\left(\{\lambda\}^H \cdot [Q] \cdot \{\bar{q}\}\right) \qquad \text{(E.30a)}$$

$$I_5 = Im\left(\{\lambda\}^H \cdot [Q] \cdot \{\bar{q}\}\right) \qquad \text{(E.30b)}$$

Replacing the derivatives of the flutter matrix [F] (Eq. E.25) back into Eq. E.23 and using the last 10 relations

(Eq. E.26a through to E.30b), we obtain

$$\left(R_{1_j} + iI_{1_j}\right) + \left(\frac{2}{\omega^3}\cdot\frac{\partial\omega}{\partial x_j} + i\cdot\frac{1}{\omega^3}\left(2g\frac{\partial\omega}{\partial x_j} - \omega\frac{\partial g}{\partial x_j}\right)\right)\cdot\left(R_3 + iI_3\right)$$

$$- \frac{1+ig}{\omega^2}\cdot\left(R_{2_j} + iI_{2_j}\right) - \left(\frac{2\rho_\infty b^4}{V\nu^3}\cdot\frac{\partial\omega}{\partial x_j}\right)\cdot\left(R_5 + iI_5\right)$$

$$+ \frac{\rho_\infty b^4}{V\nu^2}\cdot\left(R_4 + iI_4\right)\cdot\frac{\partial\omega}{\partial x_j} = 0$$

$$j = 1,\ldots,N$$

(E.31)

Eq. E.31 $\Leftrightarrow$

$$\left\{\begin{array}{l} R_{1_j} + iI_{1_j} + \frac{2}{\omega^3}\cdot R_3\cdot\frac{\partial\omega}{\partial x_j} + i\cdot\frac{2g}{\omega^3}\cdot R_3\cdot\frac{\partial\omega}{\partial x_j} - i\cdot\frac{1}{\omega^2}\cdot R_3\cdot\frac{\partial g}{\partial x_j} \\ \quad + i\cdot\frac{2}{\omega^3}\cdot I_3\cdot\frac{\partial\omega}{\partial x_j} - \frac{2g}{\omega^3}\cdot I_3\cdot\frac{\partial\omega}{\partial x_j} + \frac{1}{\omega^2}\cdot I_3\cdot\frac{\partial g}{\partial x_j} - \frac{1}{\omega^2}\cdot R_{2_j} \\ \quad - i\cdot\frac{g}{\omega^2}\cdot R_{2_j} - i\cdot\frac{1}{\omega^2}\cdot I_{2_j} + \frac{g}{\omega^2}\cdot I_{2_j} - \frac{2\rho_\infty b^4}{V\nu^3}\cdot R_5\cdot\frac{\partial\omega}{\partial x_j} \\ - i\cdot\frac{2\rho_\infty b^4}{V\nu^3}\cdot I_5\cdot\frac{\partial\omega}{\partial x_j} + \frac{\rho_\infty b^4}{V\nu^2}\cdot R_4\cdot\frac{\partial\omega}{\partial x_j} + i\cdot\frac{\rho_\infty b^4}{V\nu^2}\cdot I_4\cdot\frac{\partial\omega}{\partial x_j} = 0 \\ \qquad\qquad j = 1,\ldots,N \end{array}\right.$$

(E.32)

This last single complex scalar equation can be decomposed into two real scalar equations with the two unknowns $\frac{\partial\omega}{\partial x_j}$ and $\frac{\partial g}{\partial x_j}$.

$$
\begin{cases}
\left(\frac{2g}{\omega^3}\cdot R_3 + \frac{2}{\omega^3}\cdot I_3 + \frac{\rho_\infty b^4}{V\nu^2}\cdot I_4 - \frac{2\rho_\infty b^4}{V\nu^3}\cdot I_5\right)\cdot\frac{\partial\omega}{\partial x_j} \\
\qquad - \left(\frac{1}{\omega^2}\cdot R_3\right)\cdot\frac{\partial g}{\partial x_j} \\
\qquad = -I_{1_j} + \frac{g}{\omega^2}\cdot R_{2_j} + \frac{1}{\omega^2}\cdot I_{2_j} \\
\qquad j = 1,\ldots,N
\end{cases}
$$

and

$$
\begin{cases}
\left(\frac{2}{\omega^3}\cdot R_3 - \frac{2g}{\omega^3}\cdot I_3 + \frac{\rho_\infty b^4}{V\nu^2}\cdot R_4 - \frac{2\rho_\infty b^4}{V\nu^3}\cdot R_5\right)\cdot\frac{\partial\omega}{\partial x_j} \\
\qquad + \left(\frac{1}{\omega^2}\cdot I_3\right)\cdot\frac{\partial g}{\partial x_j} \\
\qquad = -R_{1_j} + \frac{1}{\omega^2}\cdot R_{2_j} - \frac{g}{\omega^2}\cdot I_{2_j} \\
\qquad j = 1,\ldots,N
\end{cases}
\qquad (E.33)
$$

The determinant D of the above system can be found from the following

$$
D = \left(\frac{2g}{\omega^3}\cdot R_3 + \frac{2}{\omega^3}\cdot I_3 + \frac{\rho_\infty b^4}{V\nu^2}\cdot I_4 - \frac{2\rho_\infty b^4}{V\nu^3}\cdot I_5\right)\cdot\left(\frac{1}{\omega^2}\cdot I_3\right)
$$

$$
+ \left(\frac{2}{\omega^3}\cdot R_3 - \frac{2g}{\omega^3}\cdot I_3 + \frac{\rho_\infty b^4}{V\nu^2}\cdot R_4 - \frac{2\rho_\infty b^4}{V\nu^3}\cdot R_5\right)\cdot\left(\frac{1}{\omega^2}\cdot R_3\right)
\qquad (E.34a)
$$

The solutions $\frac{\partial \omega}{\partial x_j}$ and $\frac{\partial g}{\partial x_j}$ to the system represented in Eq. E.33 take the form

$$\frac{\partial \omega}{\partial x_j} = \frac{1}{D}\cdot\left(\left(-R_{1_j} + \frac{1}{\omega^2}\cdot R_{2_j} - \frac{g}{\omega^2}\cdot I_{2_j}\right)\cdot\left(\frac{1}{\omega^2}\cdot R_3\right)\right)$$

$$+ \frac{1}{D}\cdot\left(\left(-I_{1_j} + \frac{g}{\omega^2}\cdot R_{2_j} + \frac{1}{\omega^2}\cdot I_{2_j}\right)\cdot\left(\frac{1}{\omega^2}\cdot I_3\right)\right)$$

$$j = 1,\ldots,N \qquad \text{(E.34b)}$$

$$\frac{\partial g}{\partial x_j} = -\frac{1}{D}\cdot\left(\left(\frac{2}{\omega^3}\cdot R_3 - \frac{2g}{\omega^3}\cdot I_3 + \frac{\rho_\infty b^4}{V\nu^2}\cdot R_4 - \frac{2\rho_\infty b^4}{V\nu^3}\cdot R_5\right)\times\right.$$

$$\left.\left(-I_{1_j} + \frac{g}{\omega^2}\cdot R_{2_j} + \frac{1}{\omega^2}\cdot I_{2_j}\right)\right)$$

$$+ \frac{1}{D}\cdot\left(\left(\frac{2g}{\omega^3}\cdot R_3 + \frac{2}{\omega^3}\cdot I_3 + \frac{\rho_\infty b^4}{V\nu^2}\cdot I_4 - \frac{2\rho_\infty b^4}{V\nu^3}\cdot I_5\right)\times\right.$$

$$\left.\left(-R_{1_j} + \frac{1}{\omega^2}\cdot R_{2_j} - \frac{g}{\omega^2}\cdot I_{2_j}\right)\right)$$

$$j = 1,\ldots,N \qquad \text{(E.34c)}$$

To complete the derivatives evaluations, Eq. E.34b and

E.34c can be further elucidated by expanding the terms R_{1_j}, I_{1_j}, R_{2_j}, I_{2_j}, R_3, I_3, R_4, I_4, R_5 and I_5 by using the definiting equations. Starting with R_{1_j} and I_{1_j}

Eq. E.26a
Eq. E.26b
Eq. E.5
Eq. E.6
Eq. E.10

$\Rightarrow$

$$R_{1_j} = \{\lambda'\}^T \cdot \frac{\partial \left[M_G \right]}{\partial x_j} \cdot \{\bar{q}'\} + \{\lambda''\}^T \cdot \frac{\partial \left[M_G \right]}{\partial x_j} \cdot \{\bar{q}''\}$$

$$j = 1,\ldots,N \qquad \text{(E.35a)}$$

and

$$I_{1_j} = \{\lambda'\}^T \cdot \frac{\partial \left[M_G \right]}{\partial x_j} \cdot \{\bar{q}''\} - \{\lambda''\}^T \cdot \frac{\partial \left[M_G \right]}{\partial x_j} \cdot \{\bar{q}'\}$$

$$j = 1,\ldots,N \qquad \text{(E.35b)}$$

with

$$\frac{\partial}{\partial x_j}\left[M_G \right] \simeq \left[\zeta_m^{(0)} \right]^T \left[\bar{M}_j \right] \left[\zeta_m^{(0)} \right]$$

$$j = 1,\ldots,N \qquad \text{(E.35c)}$$

(E.35)

Eq. E.27a
Eq. E.27b
Eq. E.5
Eq. E.6
Eq. E.11
} ⇒

$$R_{2_j} = \{\lambda'\}^T \cdot \frac{\partial \left[K_G \right]}{\partial x_j} \cdot \{\bar{q}'\} + \{\lambda''\}^T \cdot \frac{\partial \left[K_G \right]}{\partial x_j} \cdot \{\bar{q}''\}$$

$$j = 1,\ldots,N \qquad \text{(E.36a)}$$

and

$$I_{2_j} = \{\lambda'\}^T \cdot \frac{\partial \left[K_G \right]}{\partial x_j} \cdot \{\bar{q}''\} - \{\lambda''\}^T \cdot \frac{\partial \left[K_G \right]}{\partial x_j} \cdot \{\bar{q}'\}$$

$$j = 1,\ldots,N \qquad \text{(E.36b)}$$

with

$$\frac{\partial}{\partial x_j}\left[K_G \right] \simeq \left[\zeta_m^{(0)} \right]^T \left[\bar{K}_j \right] \left[\zeta_m^{(0)} \right]$$

$$j = 1,\ldots,N \qquad \text{(E.36c)}$$

(E.36)

Eq. E.28a
Eq. E.5
Eq. E.6
} ⇒

$$R_3 = \{\lambda'\}^T \cdot \left[K_G \right] \cdot \{\bar{q}'\} + \{\lambda''\}^T \cdot \left[K_G \right] \cdot \{\bar{q}''\} \qquad \text{(E.37a)}$$

Eq. E.28b
Eq. E.5
Eq. E.6
} ⇒

$$I_3 = \{\lambda'\}^T \cdot \left[K_G \right] \cdot \{\bar{q}''\} - \{\lambda''\}^T \cdot \left[K_G \right] \cdot \{\bar{q}'\} \qquad \text{(E.37b)}$$

The program stores in the Data Base the matrices related to the aerodynamic forces as $\rho_\infty \frac{b^3}{\nu^2}[Q']$ and $\rho_\infty \frac{b^3}{\nu}[Q'']$. In order to facilitate the numerical evaluation of $\frac{\partial \omega}{\partial x_j}$ and $\frac{\partial q}{\partial x_j}$, we let

$$R_{41} = \rho_\infty \frac{b^3}{\nu^2} \cdot R_4 \qquad \text{(E.38a)}$$

$$I_{41} = \rho_\infty \frac{b^3}{\nu^2} \cdot I_4 \qquad \text{(E.38b)}$$

$$R_{51} = \rho_\infty \frac{b^3}{\nu^2} \cdot R_5 \qquad \text{(E.39a)}$$

$$I_{51} = \rho_\infty \frac{b^3}{\nu^2} \cdot I_5 \qquad \text{(E.39b)}$$

As will become clear in a moment, these last four expressions — defining R_{41}, I_{41}, R_{51} and I_{51} — permit the direct use of some elements involving the aerodynamic matrices immediately after retrieval from the Data Base without further manipulations.

We can now exploit Eq. E.2 to note that

$$\frac{\partial[Q]}{\partial\nu} = \frac{\partial[Q']}{\partial\nu} + i\cdot\left([Q''] + \nu\cdot\frac{\partial[Q'']}{\partial\nu}\right) \tag{E.40}$$

Eq. E.29a
Eq. E.38a
Eq. E.40
Eq. E.5
Eq. E.6
$\Rightarrow$

$$\left\{\begin{aligned}
R_{41} = {} & \left(\{\lambda'\}^T\cdot\left[\rho_\infty\frac{b^3}{\nu^2}\cdot\frac{\partial[Q']}{\partial\nu}\right]\cdot\{\bar{q}'\}\right) \\
& + \frac{1}{\nu}\cdot\left(\{\lambda''\}^T\cdot\left[\rho_\infty\frac{b^3}{\nu}\cdot[Q'']\right]\cdot\{\bar{q}'\}\right) \\
& + \left(\{\lambda''\}^T\cdot\left[\rho_\infty\frac{b^3}{\nu}\cdot\frac{\partial[Q'']}{\partial\nu}\right]\cdot\{\bar{q}'\}\right) \\
& - \frac{1}{\nu}\cdot\left(\{\lambda'\}^T\cdot\left[\rho_\infty\frac{b^3}{\nu}\cdot[Q'']\right]\cdot\{\bar{q}''\}\right) \\
& - \left(\{\lambda'\}^T\cdot\left[\rho_\infty\frac{b^3}{\nu}\cdot\frac{\partial[Q'']}{\partial\nu}\right]\cdot\{\bar{q}''\}\right) \\
& + \left(\{\lambda''\}^T\cdot\left[\rho_\infty\frac{b^3}{\nu^2}\cdot\frac{\partial[Q']}{\partial\nu}\right]\cdot\{\bar{q}''\}\right)
\end{aligned}\right. \tag{E.41a}$$

Eq. E.29b
Eq. E.38b
Eq. E.40
Eq. E.5
Eq. E.6
} ⇒

$$
\left\{
\begin{aligned}
I_{41} = & \left(\{\lambda'\}^T \cdot \left[\rho_\infty \frac{b^3}{\nu^2} \cdot \frac{\partial [Q']}{\partial \nu} \right] \cdot \{\bar{q}''\} \right) \\
& + \frac{1}{\nu} \cdot \left(\{\lambda''\}^T \cdot \left[\rho_\infty \frac{b^3}{\nu} \cdot [Q''] \right] \cdot \{\bar{q}''\} \right) \\
& + \left(\{\lambda''\}^T \cdot \left[\rho_\infty \frac{b^3}{\nu} \cdot \frac{\partial [Q'']}{\partial \nu} \right] \cdot \{\bar{q}''\} \right) \\
& + \frac{1}{\nu} \cdot \left(\{\lambda'\}^T \cdot \left[\rho_\infty \frac{b^3}{\nu} \cdot [Q''] \right] \cdot \{\bar{q}'\} \right) \\
& + \left(\{\lambda'\}^T \cdot \left[\rho_\infty \frac{b^3}{\nu} \cdot \frac{\partial [Q'']}{\partial \nu} \right] \cdot \{\bar{q}'\} \right) \\
& - \left(\{\lambda''\}^T \cdot \left[\rho_\infty \frac{b^3}{\nu^2} \cdot \frac{\partial [Q']}{\partial \nu} \right] \cdot \{\bar{q}'\} \right)
\end{aligned}
\right.
$$

(E.41b)

In Eq. E.41a and E.41b, all the terms between the big square brackets are matrices related to the unsteady aerodynamic in forms as stored in the Data Base. This is also true for the ensuing two equations which display how R_{51} and

I_{51} are obtained

Eq. E.30a
Eq. E.39a
Eq. E.2
Eq. E.5
Eq. E.6
$\Rightarrow$

$$\left\{ R_{51} = \left(\{\lambda'\}^T \cdot \left[\rho_\infty \frac{b^3}{\nu^2} \cdot [Q'] \right] \cdot \{\bar{q}'\} \right) \right.$$

$$+ \left(\{\lambda''\}^T \cdot \left[\rho_\infty \frac{b^3}{\nu} \cdot [Q''] \right] \cdot \{\bar{q}'\} \right)$$

$$- \left(\{\lambda'\}^T \cdot \left[\rho_\infty \frac{b^3}{\nu} \cdot [Q''] \right] \cdot \{\bar{q}''\} \right)$$

$$\left. + \left(\{\lambda''\}^T \cdot \left[\rho_\infty \frac{b^3}{\nu^2} \cdot [Q'] \right] \cdot \{\bar{q}''\} \right) \right.$$

(E.42a)

Eq. E.30b
Eq. E.39b
Eq. E.2
Eq. E.5
Eq. E.6
$\Rightarrow$

$$\left\{ I_{51} = \left(\{\lambda'\}^T \cdot \left[\rho_\infty \frac{b^3}{\nu^2} \cdot [Q'] \right] \cdot \{\bar{q}''\} \right) \right.$$

$$+ \left(\{\lambda''\}^T \cdot \left[\rho_\infty \frac{b^3}{\nu} \cdot [Q''] \right] \cdot \{\bar{q}''\} \right)$$

$$+ \left(\{\lambda'\}^T \cdot \left[\rho_\infty \frac{b^3}{\nu} \cdot [Q''] \right] \cdot \{\bar{q}'\} \right)$$

$$\left. - \left(\{\lambda''\}^T \cdot \left[\rho_\infty \frac{b^3}{\nu^2} \cdot [Q'] \right] \cdot \{\bar{q}'\} \right) \right.$$

(E.42b)

Let us recapitulate and write the final form of the partial derivatives of the artificial damping g and the frequency ω with respect to any design variables

<u>for a fixed-mode approach</u>

$$\frac{\partial \omega}{\partial x_j} = \frac{1}{D}\cdot\left(\left(-R1_j + \frac{1}{\omega^2}\cdot R2_j - \frac{g}{\omega^2}\cdot I2_j\right)\cdot\left(\frac{1}{\omega^2}\cdot R3\right)\right)$$

$$+ \frac{1}{D}\cdot\left(\left(-I1_j + \frac{g}{\omega^2}\cdot R2_j + \frac{1}{\omega^2}\cdot I2_j\right)\cdot\left(\frac{1}{\omega^2}\cdot I3\right)\right)$$

$$j = 1,\ldots,N \qquad \text{(E.43a)}$$

$$\frac{\partial g}{\partial x_j} = \frac{1}{D}\cdot\left(\left(\frac{2g}{\omega^3}\cdot R3 + \frac{2}{\omega^3}\cdot I3 + \frac{b}{V}\cdot I41 - \frac{2b}{V\nu}\cdot I51\right)\times\right.$$

$$\left.\left(-R1_j + \frac{1}{\omega^2}\cdot R2_j - \frac{g}{\omega^2}\cdot I2_j\right)\right)$$

$$- \frac{1}{D}\cdot\left(\left(\frac{2}{\omega^3}\cdot R3 - \frac{2g}{\omega^3}\cdot I3 + \frac{b}{V}\cdot R41 - \frac{2b}{V\nu}\cdot R51\right)\times\right.$$

$$\left.\left(-I1_j + \frac{g}{\omega^2}\cdot R2_j + \frac{1}{\omega^2}\cdot I2_j\right)\right)$$

$$j = 1,\ldots,N \qquad \text{(E.43b)}$$

(E.43)

where R_{1_j} and I_{1_j} are given by Eq. E.35; R_{2_j} and I_{2_j} by Eq. E.36; R_3, I_3, R_{41}, I_{41}, R_{51} and I_{51} respectively by Eq. E.37a, E.37b, E.41a, E.41b, E.42a and E.42b; the determinant D by

$$D = \left(\frac{2g}{\omega^3}\cdot R_3 + \frac{2}{\omega^3}\cdot I_3 + \frac{b}{V}\cdot I_{41} - \frac{2b}{V\nu}\cdot I_{51}\right)\cdot\left(\frac{1}{\omega^2}\cdot I_3\right)$$

$$+ \left(\frac{2}{\omega^3}\cdot R_3 - \frac{2g}{\omega^3}\cdot I_3 + \frac{b}{V}\cdot R_{41} - \frac{2b}{V\nu}\cdot R_{51}\right)\cdot\left(\frac{1}{\omega^2}\cdot R_3\right) \qquad (E.44)$$

We have hitherto made the assumption that, in setting up the flutter equation and in generating the unsteady aerodynamic forces, the mode shapes of the base design are kept the same at each step of the synthesis process. If the modes are updated with structural design changes, the expressions for the derivatives of g and ω are the same apart from the following three remarks which stem from a direct comparison of Eq. E.1b and E.1c and from a reformulation of the differential of the aerodynamic matrix of generalized airforce coefficients.

<u>1st remark</u>

$$\text{Because } \frac{\partial\left[\begin{smallmatrix}\nwarrow & 1 & \nearrow\\ \swarrow & & \searrow\end{smallmatrix}\right]}{\partial x_j} = [0] \qquad j = 1,\ldots,N$$

$$R_{1_j} = I_{1_j} = 0 \qquad j = 1,\ldots,N \qquad (E.45)$$

2nd remark

$$R_{2_j} = \{\lambda'\}^T \cdot \frac{\partial \left[\omega_N^2\right]}{\partial x_j} \cdot \{\bar{q}'\} + \{\lambda''\}^T \cdot \frac{\partial \left[\omega_N^2\right]}{\partial x_j} \cdot \{\bar{q}''\}$$

$$= \{\lambda'\}^T \left[\frac{\partial \left(\omega_{Ni}\right)^2}{\partial x_j}\right] \cdot \{\bar{q}'\} + \{\lambda''\}^T \left[\frac{\partial \left(\omega_{Ni}\right)^2}{\partial x_j}\right] \cdot \{\bar{q}''\}$$

$$j = 1,\ldots,N \qquad \text{(E.46a)}$$

$$I_{2_j} = \{\lambda'\}^T \cdot \frac{\partial \left[\omega_N^2\right]}{\partial x_j} \cdot \{\bar{q}''\} - \{\lambda''\}^T \cdot \frac{\partial \left[\omega_N^2\right]}{\partial x_j} \cdot \{\bar{q}'\}$$

$$= \{\lambda'\}^T \left[\frac{\partial \left(\omega_{Ni}\right)^2}{\partial x_j}\right] \cdot \{\bar{q}''\} - \{\lambda''\}^T \left[\frac{\partial \left(\omega_{Ni}\right)^2}{\partial x_j}\right] \cdot \{\bar{q}'\}$$

$$j = 1,\ldots,N \qquad \text{(E.46b)}$$

The diagonal terms $\frac{\partial \left(\omega_{Ni}\right)^2}{\partial x_j}$, i = 1,...,p, are found by using Eq. E.17i.

3rd remark

Because the simplified assumption of constant mode shapes is lifted, an extra term must be added to the variations of [Q] to account for changes in the design

variables. The total differentiation of [Q] yields

$$d[Q] = \frac{\partial[Q]}{\partial x_j} \cdot dx_j + \frac{\partial[Q]}{\partial \nu} \cdot d\nu \qquad j = 1,\ldots,N \qquad \text{(E.47a)}$$

dividing by dx_j

$$\frac{d[Q]}{dx_j} = \frac{\partial[Q]}{\partial x_j} + \frac{\partial[Q]}{\partial \nu} \cdot \frac{d\nu}{dx_j} \qquad j = 1,\ldots,N \qquad \text{(E.47b)}$$

Then, the definitions of R_4 and I_4 (Eq. E.29a and E.29b) now become

$$R_4 = Re\left(\frac{V}{b} \cdot \{\lambda\}^H \cdot \frac{\partial[Q]}{\partial x_j} \cdot \{\bar{q}\} + \{\lambda\}^H \cdot \frac{\partial[Q]}{\partial \nu} \cdot \{\bar{q}\}\right) \qquad \text{(E.47c)}$$

$$I_4 = Im\left(\frac{V}{b} \cdot \{\lambda\}^H \cdot \frac{\partial[Q]}{\partial x_j} \cdot \{\bar{q}\} + \{\lambda\}^H \cdot \frac{\partial[Q]}{\partial \nu} \cdot \{\bar{q}\}\right) \qquad \text{(E.47d)}$$

If we separate the expression of the generalized matrix into mode-dependent and mode-independent matrices (Ref. 23), $\frac{\partial[Q]}{\partial x_j}$ in Eq. E.47c and E.47d would have terms that are constant or null and terms related to the derivatives of the mode shapes, $\frac{\partial \xi}{\partial x_j}$, and to the derivatives of the slopes, $\frac{\partial}{\partial x_j}\left(\frac{\partial \xi}{\partial x}\right)$.

Since the deflections and slopes at the aerodynamic panels are related to the values of the mode shapes at the structural grid by interpolation, finding the derivatives of

ξ and $\partial\xi/\partial x$ with respect to the design variables x_j is equivalent to applying interpolation formulas to the derivatives of $\{\zeta\}_m$ with respect to the design variables. The standard technique to find the derivatives of the mode shapes at the structural grid (Ref. 8 and 41) is to differentiate the free-vibration problem (Eq. E.17b) and the equation that shows the normalization of its eigenvector solutions (for instance Eq. E.16).

To sum up, the values of $\frac{\partial g}{\partial x_j}$ and $\frac{\partial \omega}{\partial x_j}$, $j = 1,\ldots,N$, are evaluated for both fixed-mode and updated-mode approaches by the program developed. There is just one term missing in the "updated-mode" derivatives and it is the one represented by $\frac{\partial [Q]}{\partial x_j}$ in Eq. E.47c and E.47d. With regard to this term, it should be noted that time did not permit its computation which would require drastic changes to the unsteady aerodynamic program, WLST1 (Ref. 10).

As we shall see in appendix F, it is only the derivatives of the artificial damping g which are of primary interest to this research. The derivatives of the frequency ω are, however, evaluated for the simple reason that they may be required for any further investigations on the field of flutter synthesis. Because they are composed of terms already calculated for $\frac{\partial g}{\partial x_j}$, the derivatives of ω do not put any CPU penalty on the program apart from a single FORTRAN equation

inserted within the loop on the design variables.

APPENDIX F

DUAL PROBLEM

Employing the artificial damping parameter as the behavior constraint instead of the flutter speed, the primal problem (Eq. D.3) can be re-cast into the following alternative form

$$\left.\begin{aligned} &\text{minimize} \quad m = m_0 + \sum_{j=1}^{N} m_j x_j \\ &\text{subject to} \quad g \leq 0 \\ &\text{and to} \quad x_j \geq \underline{x}_j \qquad j = 1,\ldots,N \end{aligned}\right\} \quad (F.1)$$

or into

$$\left.\begin{aligned} &\text{minimize} \quad m = m_0 + \sum_{j=1}^{N} m_j x_j \\ &\text{subject to} \quad -g \geq 0 \\ &\text{and to} \quad x_j \geq \underline{x}_j \qquad j = 1,\ldots,N \end{aligned}\right\} \quad (F.2)$$

In order to bound the primal mass, we introduce upper limit gauge constraints in lieu of the lower limit gauge constraints (infinite values may be imposed on the upper limits to force active design variables on the lower limits to be active on the upper limits). Eq. F.2 is re-written as

$$\left.\begin{aligned} &\text{minimize} \quad m = m_0 + \sum_{j=1}^{N} m_j x_j \\ &\text{subject to} \quad -g \geq 0 \\ &\text{and to} \quad x_j \leq \overline{x}_j \qquad j = 1,\ldots,N \end{aligned}\right\} \quad (F.3)$$

or into

$$\left.\begin{aligned} &\text{minimize} \quad m = m_0 + \sum_{j=1}^{N} m_j x_j \\ &\text{subject to} \quad -g \geq 0 \\ &\text{and to} \quad \bar{x}_j - x_j \geq 0 \qquad j = 1,\ldots,N \end{aligned}\right\} \quad (F.4)$$

The Lagrangian function takes the form

$$\mathcal{L} = m_0 + \sum_{j=1}^{N} m_j x_j + \Lambda g - \sum_{j=1}^{N} \mu_j \left(\bar{x}_j - x_j\right) \quad (F.5)$$

Λ Lagrange multiplier associated with the behavior constraint

μ_j $(j = 1,\ldots,N)$ Lagrange multiplier associated with the side constraints

The well-known kuhn-tucker conditions are represented by the following equations

$$\left.\begin{aligned} &m_j + \Lambda \cdot \frac{\partial g}{\partial x_j} + \mu_j = 0 \\ &\Lambda \geq 0 \\ &\mu_j \geq 0 \\ &\forall\ j \in J_a \quad \text{(active design variables)} \end{aligned}\right\} \quad (F.6)$$

Corresponding to the primal problem (Eq. F.4), the aeroelastic dual problem (used for bounding the mass) is defined as

$$\left\{ \begin{array}{l} \text{maximize} \quad \mathfrak{L} = m_0 + \sum_{j=1}^{N} m_j x_j + \Lambda g - \sum_{j=1}^{N} \mu_j \left(\bar{x}_j - x_j \right) \\ \\ \text{subject to} \left\{ \begin{array}{l} m_j + \Lambda \cdot \dfrac{\partial g}{\partial x_j} + \mu_j = 0 \\ \text{and to} \\ \Lambda \geq 0, \qquad \mu_j \geq 0; \\ \forall\, j \in J_a \end{array} \right. \end{array} \right. \tag{F.7}$$

A better formulation of Eq. F.7 and a better bound of the mass can be obtained by taking into account that μ_j and $\left(\bar{x}_j - x_j \right)$ are always positive or at least equal to zero for all j. Therefore, Eq. F.7 becomes

$$\left. \begin{array}{l} \text{maximize} \quad m_0 + \sum_{j=1}^{N} m_j x_j + \Lambda g \\ \\ \text{subject to} \left\{ \begin{array}{ll} m_j + \Lambda \cdot \dfrac{\partial g}{\partial x_j} \leq 0 & \forall\, j \in J_a \\ \text{and to} & \\ \Lambda \geq 0 & \end{array} \right. \end{array} \right\} \tag{F.8}$$